MEMBRANE LIPIDS AND SYNAPTIC VESICLE TRAFFICKING IN THE CNS

APPROVED BY SUPERVISORY COMMITTEE

Ege T. Kavalali, Ph.D. Advisor _____

Kimberly Huber, Ph.D. Committee Chair _____

Joseph Peter Albanesi, Ph.D. _____

Joachim Herz, M.D. _____

DEDICATION

For my Mom

MEMBRANE LIPIDS AND SYNAPTIC VESICLE TRAFFICKING IN THE CNS

by

CATHERINE REBECCA WASSER

DISSERTATION

Presented to the Faculty of the Graduate School of Biomedical Sciences
The University of Texas Southwestern Medical Center at Dallas
In Partial Fulfillment of the Requirements
for the Degree of

DOCTOR OF PHILOSOPHY

The University of Texas Southwestern Medical Center at Dallas
Dallas, Texas
August 2008

MEMBRANE LIPIDS AND SYNAPTIC VESICLE TRAFFICKING IN THE CNS

CATHERINE REBECCA WASSER, PH.D.

The University of Texas Southwestern Medical Center at Dallas, 2008

EGE T. KAVALALI, PH.D.

Most vesicles within a synapse are dormant. The rest participate in synaptic neurotransmission, with a portion of these preferentially fusing first. Moreover, all synapses experience spontaneous neurotransmitter release which may originate from the random exocytosis of vesicles prepared to fuse immediately upon calcium influx; however, spontaneously fusing vesicles may be independent because they preferentially recycle spontaneously. These functional separations argue that the synaptic vesicle membrane composition could be unique between pools.

The first three chapters explore the role of cholesterol in synaptic transmission. We treated hippocampal cultures with methyl-beta-cyclodextrin, which reversibly binds cholesterol, or mevastatin, an inhibitor of cholesterol biosynthesis, to deplete cholesterol. We also used hippocampal cultures from Niemann-Pick type C1-deficient mice defective in intracellular cholesterol trafficking. These conditions revealed augmented spontaneous neurotransmission. In contrast, the same treatments severely impaired responses evoked by action potentials and hypertonicity. These results suggest that synaptic cholesterol balances evoked and spontaneous neurotransmission by hindering spontaneous synaptic vesicle turnover and sustaining evoked exo-endocytosis.

Chapter five examines the role of sphingosine on neurotransmitter release. By adding sphingosine to hippocampal cultures, we found that sphingosine enhances neurotransmission in a synaptobrevin-2-dependent manner.

Chapter six investigates the stability of actively recycling synaptic vesicles. We employed several approaches (fluorescent and ultrastructural imaging) to monitor not only the fate recycling vesicles, but also the origin and reuse of spontaneously fusing vesicles. We conclude that at rest, the total recycling pool remains active and resists spontaneous fusion up to at least six hours; while spontaneous fusion of spontaneously fusing vesicles is much faster. This argues that vesicles fusing spontaneously do not originate from the recycling pool.

In chapter seven, we observe how modifying synaptic vesicle membranes might affect neurotransmitter release. By the uptake of horseradish peroxidase into vesicles followed by hydrogen peroxide perfusion, we induced free radical modification of vesicle membranes and found that modifying recycling pool vesicles increased spontaneous fusion and attenuated evoked release.

Taken together, the results of each chapter appear to suggest that the fusion of action potential-dependent and-independent vesicles are regulated by different mechanisms, supporting the theory that some vesicles may be unique within a synapse.

ACKNOWLEDGEMENTS

I would first like to thank Ege T. Kavalali for taking me under his wing and revealing the inner workings of the synapse. His support, guidance and friendship are priceless.

I would also like to thank my committee, Joseph Peter Albanesi, Joachim Herz, and especially Kimberly Huber. I appreciate the time the time they took to help shape my research;
I truly enjoyed each committee meeting.

To the members of the lab, past and present, thank you for your friendship, advice and support.

Finally, I cannot forget to acknowledge my family. Through good times and bad they supported me and I am forever grateful.

TABLE OF CONTENTS

PRIOR PUBLICATIONS

Wasser C.R., Ertunc M., Liu X., Kavalali E.T., Cholesterol-dependent balance between evoked and spontaneous synaptic vesicle recycling. *J Physiol* **2007; 579**(Pt 2): 413-29.

Wasser C.R. and Kavalali E.T., Leaky Synapses: Regulation of spontaneous neurotransmission in central synapses. *Neuroscience* 2008

LIST OF FIGURES

LIST OF ABBREVIATIONS

AICAR: 5-aminoimidazole-4-carboxamide riboside
AMP: adenosine monophosphate
AMPK: AMP-activated kinase
AP5: dl-2-amino-5-phosphonovaleric acid
ChOx: cholesterol oxidase
CNQX: 6-cyano-7-nitroquinoxaline-2,3-dione
CNS: central nervous system
DAB: 3,3'-diaminobenzidine
DMSO: Dimethyl sulfoxide
d-MAPP: d-*erythro*-MAPP
EPSC: excitatory postsynaptic current
EtOH ethanol
H_2O_2: Hydrogen peroxide
HMG-CoA reductase: β-hydroxy-β-methylglutaryl-coenzyme A
HRP: horseradish peroxidase
IPSC: inhibitory postsynaptic current
mEPSC: miniature excitatory postsynaptic current
MCD: methyl-β-cyclodextrin
mIPSC: miniature inhibitory postsynaptic current
NBQX: 2,3-dioxo-6-nitro-1,2,3,4-tetrahydrobenzo[f]quinoxaline-7-sulphonamide
NPC1: Niemann-Pick type C1
PTX: picrotoxin
sAP: spontaneous action potentials
SNAREs (soluble-N-ethylmaleimide sensitive factor attachment protein receptors)
Syb2 +/–: synaptobrevin-2 heterozygous
Syb2 –/–: synaptobrevin-2-deficient
TTX: tetrodotoxin
WT: wild-type

CHAPTER 1: INTRODUCTION

1.1 Vesicles residing in the synapse

Vesicles in a CNS nerve terminal can be divided into two pools. The first pool contains a relatively small fraction (5–10%) of vesicles close to release sites. These vesicles are generally thought to be ready for release since they can be fused by rapid uncaging of intrasynaptic Ca^{2+} (Schneggenburger et al., 1999), a 10-ms Ca^{2+}-current pulse (Wu and Borst, 1999), a brief high-frequency train of action potentials (Murthy and Stevens, 1999) or by hypertonic stimulation (Rosenmund and Stevens, 1996). This release-ready pool of vesicles is referred to as the immediately releasable pool or the readily releasable pool (RRP). RRP vesicles are usually considered to be in a morphologically docked state, although not all morphologically docked vesicles are necessarily release competent at any given time (Schikorski and Stevens, 2001). In addition to the morphological docking, a "priming" step is required to make vesicles fully release competent (Jahn et al., 2003). A secondary pool of vesicles, the reserve pool (RP), is thought to be spatially distant from the release sites and replenishes the vesicles in the RRP that have exocytosed. The number of vesicles contained in the RRP is a critical parameter that regulates the probability of release, which is defined as the probability that a presynaptic action potential can result in an exocytotic event. In addition, several lines of evidence support the presence of a non-recycling pool of vesicles in the synapse. Mechanisms that can render this "resting" (or "dormant")

pool functional remain to be determined (Sudhof, 2000, Harata et al., 2001).This functional allocation of synaptic vesicles into pools aims to account for the properties of evoked neurotransmitter release during activity. On the other hand, studies examining spontaneous neurotransmission typically rely on three assumptions with respect to the pool organization of the vesicles giving rise to spontaneous release. First, it is generally assumed that in a nerve terminal, vesicles that fuse spontaneously originate from the same RRP as the vesicles that fuse in response to stimulation. This is a key assumption used to justify the analysis of spontaneous release kinetics as a reporter of the number and fusion propensity of vesicles in the RRP. Second, the priming mechanisms that prepare synaptic vesicles for fusion are believed to be the same for both spontaneous and evoked fusion. In addition, the fusion machinery leading to spontaneous and evoked release is thought to be identical and subject to similar types of regulation aside from evoked release's steep Ca^{2+}-dependence and reliance on Ca^{2+} influx (Lou et al., 2005). Finally, the analysis of spontaneous neurotransmission relies on the assumption that evoked fusion events and spontaneous fusion events in a given synapse activate the same set of postsynaptic receptors. Although only a small number of studies have questioned the validity of the last assumption [(Colmeus et al., 1982); but see (Van der Kloot and Naves, 1996), recent studies have addressed the first two assumptions and provided further insight to the complex relationship between evoked and spontaneous release.

For instance, a recent study from our group proposed that a large fraction of vesicles that fuse spontaneously do not originate from the RRP, which gives rise to evoked release in response to action potential firing and Ca^{2+} influx into nerve terminals (Sara et al., 2005). In this study, synaptic vesicle recycling at rest was detected by the uptake and re-availability of an antibody against the lumenal domain of synaptic vesicle protein synatotagmin-1 as well as the internalization and release of styryl dye FM2-10. Results of these experiments indicated that vesicles recycling spontaneously were more likely to re-fuse spontaneously. Vesicles that took up dye during spontaneous exo-endocytosis were swiftly mobilized in the absence of activity compared with vesicles that recycle during activity. Moreover, spontaneous dye release after spontaneous dye uptake closely followed the kinetics of spontaneous neurotransmission as estimated by previous work (Murthy and Stevens, 1999). In contrast, vesicles that fuse in response to action potentials were not as readily available for release in the absence of stimulation. Taken together, this study proposed that spontaneously endocytosed vesicles preferentially populate a reluctant/reserve pool, which has limited crosstalk with vesicles in the activity-dependent recycling pool. However, a later study using simultaneous multicolor imaging of spontaneous and evoked uptake of FM1-43 (a green dye) and FM5-95 (a red dye) argued that vesicles that fuse and endocytose spontaneously populate the same pool as vesicles that fuse in response to action potentials (Groemer and Klingauf, 2007), corroborating an

earlier study (Prange and Murphy, 1999). Although, this elegant study disagreed with the proposal that spontaneously endocytosed vesicles recycled independently of the RRP vesicles, it did not examine the resistance of RRP vesicles to spontaneous fusion. To better understand this potential mechanism, I investigated the role of synaptic cholesterol levels in the regulation of spontaneous fusion propensity and found that synaptic vesicle cholesterol is a major factor impeding spontaneous fusion, while enhancing evoked vesicle fusion. Also, experiments performed by myself and lab mate ChiHye Chung show that after activity-dependent dye uptake, stained synapses were resistant to spontaneous dye loss up to 6 h, consistent with the resilience of RRP vesicles to spontaneous fusion. Sustained resistance of RRP vesicles to spontaneous fusion implies that most synaptic vesicles are actively prevented from fusing spontaneously by an unknown mechanism. Taken together, currently there are multiple scenarios that can account for the origin of spontaneous release, which do not necessarily constitute mutually exclusive possibilities.

1.2 Synaptic vesicle recycling

1.2.1 Action potential-dependent vesicle recycling

After docking at the active zone, synaptic vesicles undergo a series of priming reactions to mature to a fusion-competent state. Recent evidence suggests that docking and priming reactions can occur within 300 ms (Zenisek et al.,

2000). At this point, the influx of Ca^{2+} ions through voltage-gated Ca^{2+}-channels in response to action potentials triggers rapid exocytosis of fusion-competent vesicles. The initial release of vesicles from the RRP or docked-primed pool, and subsequent replenishment and release from the reserve pool, results in biphasic release kinetics, with a rapidly depressing release phase corresponding to release from the RRP and a slow depressing release phase due to the mobilization and release of vesicles from the reserve pool. The underlying cause of this depression is thought to be limitations in the number of functional vesicles present in a synapse, although the potential role of an active process that limits the rate of synaptic vesicle fusion at high frequencies cannot be excluded. In support of the limitation of vesicle number hypothesis, several studies have shown that central synapses have a small number of functional synaptic vesicles especially during early stages of maturation after synaptogenesis (Mozhayeva et al., 2002).

1.2.2 Recycling of spontaneously fusing vesicles

The absence of spontaneous signaling may compromise neuronal survival and structural stability of synaptic connections (Verhage et al., 2000) in the brain; however, unregulated enhanced release of excitatory neurotransmitters can lead to neuronal damage and death. This excitotoxic neuronal death induced by increased synaptic glutamate is implicated in the pathology of multiple neurodegenerative diseases including Alzheimer's and Huntington's diseases along with ischemia

and epilepsy (Nishizawa, 2001, Lo et al., 2003, Hynd et al., 2004). In addition, excess spontaneous fusion may cause presynaptic vesicle depletion and impair synaptic function in the long term. As excess or diminished spontaneous neurotransmitter release may lead to adverse consequences, regulatory mechanisms are necessary to fine-tune this type of fusion. The modulation of spontaneous neurotransmitter release occurs through several signaling pathways (reviewed in (Bouron, 2001). Many neuromodulators decrease evoked release through inhibition of voltage-gated Ca^{2+} channels (Gβγ- mediated), but some can also exert inhibition on spontaneous release. For example, adenosine acts through A1 receptors and unlike other neuromodulators attenuates both evoked and spontaneous neurotransmission (Fredholm et al., 2005). To suppress evoked neurotransmission, A1 receptors act through P-type Ca^{2+} channels to inhibit neurotransmission (Dittman and Regehr, 1996). The mechanism underlying inhibition of spontaneous neurotransmission is unclear but it may be shared with the action of glutamate through presynaptic group II metabotropic glutamate receptors to inhibit spontaneous vesicle fusion (Glitsch, 2006).

1.3 Role of lipids in synaptic neurotransmission

In addition to neuromodulators, membrane lipids such as cholesterol, sphingolipids and phosphoinositides have a strong impact on the propensity of synaptic vesicle fusion (Cremona et al., 1999, Wenk and De Camilli, 2004, Rohrbough and Broadie, 2005). In fact, enrichment and colocalization of these

lipids are common at the synapse. Implicated in almost every aspect of the synaptic vesicle cycle, phosphoinosides and their metabolites are integral to the fidelity of synaptic transmission. Mutations in a key regulator of sphingolipids, ceramidase, results in defects in release of neurotransmitter and vesicle trafficking (Rohrbough et al., 2004). In addition, sphingolipids and cholesterol make up dense domains within membranes that organize protein function and signaling processes.

Cholesterol contributes to membrane dynamics, particularly the regulation of membrane fluidity and microdomains involved in protein interactions. In the CNS, cholesterol synthesis is primarily de novo and tightly regulated (Spady and Dietschy, 1983; Dietschy et al., 1993; Jurevics and Morell, 1995; Turley et al., 1998). At the synapse, the presence of cholesterol is thought to be important for proper synapse structure and function in the brain. Experiments altering cholesterol levels revealed several roles for cholesterol in neurons including promotion of synaptogenesis, maintenance of synapse organization, and enablement of synaptic vesicle (SV) fusion and endocytosis (Hering et al., 2003, Pfrieger, 2003, Salaun et al., 2004, Rohrbough and Broadie, 2005). During development, glia-derived cholesterol enhances synapse formation (Mauch et al., 2001, Pfrieger, 2003, Goritz et al., 2005). In neuroendocrine cells, cholesterol depletion disrupts syntaxin clusters and decreases evoked catecholamine release (Chamberlain et al., 2001, Lang et al., 2001, Gil et al., 2005, Salaun et al., 2005).

In addition, cholesterol depletion with methyl-β-cyclodextrin (MCD) inhibits clathrin-dependent endocytosis in multiple preparations (Rodal et al., 1999, Subtil et al., 1999). In nerve terminals, cholesterol interacts with several SV proteins (Thiele et al., 2000). In addition, cholesterol has been shown to be a prominent component of SV membranes (Deutsch and Kelly, 1981). However, despite these earlier data, very little is known about the precise functional role of cholesterol homeostasis on neurotransmission and the underlying vesicle trafficking events in CNS nerve terminals.

CHAPTER 2: ACUTE MANIPULATION OF NEURONAL CHOLESTEROL

2.1 Background

Cholesterol is a major lipid component of cellular membranes and regulates the degree of membrane fluidity. The presence of cholesterol is thought to be important for proper synapse structure and function in the brain. Experiments in which cholesterol levels are altered reveal several roles for cholesterol in neurons including promotion of synaptogenesis, maintenance of synapse organization, and enablement of synaptic vesicle (SV) fusion and endocytosis (Hering et al., 2003, Pfrieger, 2003, Salaun et al., 2004, Rohrbough and Broadie, 2005). During development, glia-derived cholesterol enhances the formation of synapses (Mauch et al., 2001, Pfrieger, 2003, Goritz et al., 2005). In neuroendocrine cells, cholesterol depletion disrupts syntaxin clusters and decreases evoked catecholamine release (Chamberlain et al., 2001, Lang et al., 2001, Gil et al., 2005, Salaun et al., 2005). In addition, cholesterol depletion with methyl-β-cyclodextrin (MCD) inhibits clathrin-dependent endocytosis in multiple preparations (Rodal et al., 1999, Subtil et al., 1999). In nerve terminals, cholesterol interacts with several SV proteins (Thiele et al., 2000). In addition, cholesterol is a prominent component of SV membranes (Deutsch and Kelly, 1981) and a possible spatial organizer of synaptic vesicle recycling (Jia et al., 2006).

To explore the role of cholesterol in CNS neurons, I observed the excitatory synaptic function after acute extraction of cholesterol with methyl-β-cyclodextrin, which reversibly binds cholesterol, from dissociated rat hippocampal cultures. The results obtained from these experiments suggest a dramatically different effect of cholesterol removal from neurons on two types of neurotransmission. Cholesterol extraction attenuated the synchronous release of neurotransmitter after the influx of Ca^{2+} through voltage-gated Ca^{2+} channels. This form of neurotransmission is central to the efficient communication between neurons. Synapses also disperse neurotransmitter spontaneously in the absence of action-potential driven Ca^{2+}-influx, and contrary to the effect of cholesterol extraction on the Ca^{2+}-triggered neurotransmitter release, the spontaneous neurotransmission increases dramatically after cholesterol depletion. Thus, cholesterol appears to play a role in balancing these two forms of neurotransmission.

2.2 Results

2.2.1 Depleting neuronal membrane cholesterol using methyl-β-cyclodextrin

The high concentration of cholesterol within synaptic vesicles as well as cholesterol's apparent interactions with synaptic vesicle proteins was the driving factor in the basic design of my experiments. I wanted to explore the function of vesicular cholesterol by isolating the effect of cholesterol within the synaptic vesicle from cholesterol within the plasma membrane. I chose to deplete

cholesterol using the membrane impermeable methyl-β-cyclodextrin from cultures during either the absence of action potentials (remove plasma membrane cholesterol) or depolarization (deplete cholesterol from plasma and synaptic vesicle membranes). Presumably, this approach allows for the discrimination of the effects of plasma membrane depletion from the effects of reducing cholesterol from both sets of membranes, thus discovering unique features of synaptic vesicle cholesterol.

To deplete cholesterol acutely, I treated primary dissociated rat hippocampal cultures with a 15 mM MCD solution for 30 minutes at room temperature in either a normal K^+ (4 mM K^+) containing tetrodotoxin (TTX) to block action potentials or in a depolarizing medium (20 mM K^+). After cholesterol depletion, I measured basic synaptic transmission as well as properties of synaptic vesicle recycling. Using filipin staining to label free cholesterol, I quantified the global reduction of cholesterol levels in this and other cholesterol manipulations. For cultures treated with MCD, the filipin fluorescence intensity was reduced by 38.0 ± 0.0% compared to the fluorescence values of non-treated cultures (No treatment n=4, 20 mM K^+ with MCD n=3, $p<0.001$).

To assess the viability of cells after MCD treatment, I incubated cells with Trypan Blue, which is a dye with a negatively-charged chromophore that only reacts with damaged membranes, and calculated the fraction of viable cells. I did not detect a significant change in cell viability after MCD treatment (non-treated

cultures: 87.1 ± 3.7 % vs. MCD treated cultures: 82.7 ± 0.9 %, calculated from at least 2 coverslips with 5-20 images per coverslip, not significant, n.s. $p>0.3$). In addition, I assessed the integrity of the cell membranes after treatment with MCD by comparing the membrane resistances of cells to control values from untreated cells. The membrane resistances were 2.20 ± 0.31 GΩ for non-treated cultures and 2.00 ± 0.39 GΩ for MCD treated cultures indicating no significant breach of neuronal membrane integrity after MCD treatment (n.s. $p>0.4$).

2.2.1.1 Cholesterol depletion inhibits action-potential dependent neurotransmission

To characterize excitatory transmission after cholesterol depletion, I stimulated MCD-treated cultures with a hypertonic sucrose solution (+500 mOsm, 30 seconds) or field potentials and measured excitatory postsynaptic currents (EPSCs) using whole-cell voltage-clamp methods. Hypertonic sucrose mobilizes a specific set of vesicles, referred to as the readily releasable pool, in a Ca^{2+}-independent manner (Rosenmund and Stevens, 1996). The ability of hypertonic sucrose to trigger release was significantly lower after treatment with MCD (75% reduction) compared to no treatment (Fig. 2.2.1.1 A-B; No treatment n=18, 20 mM K^+ with MCD n=18, $p<0.01$). Treatment with 20mM K^+ alone for 30 minutes did not significantly alter the hypertonic sucrose response, indicating that depolarizing medium was not the cause of the decrease observed after MCD

treatment in 20 mM K^+ solution. Considering the possible effects of vesicle fusion during the 20 mM K^+ with MCD treatment, cultures were treated with MCD alone (in a 4 mM K^+ solution with tetrodotoxin, TTX, to prevent action potentials). The MCD alone treatment should presumably allow depletion of only the exposed membranes (plasma membrane and spontaneously recycling vesicles). Treatment with MCD alone resulted in a 68% reduction in the charge transfer induced by hypertonic sucrose compared to non-treated cultures (No treatment n=18, MCD alone n=16, $p<0.05$).

Using field stimulation to evoke Ca^{2+}-dependent neurotransmitter release, I observed a similar decrease in the EPSCs of MCD-treated cultures (73% reduction) compared to non-treated cultures (Fig. 2.2.1.1 C-D; No treatment n=7, 20 mM K^+ with MCD n=8, $p<0.01$). Consistent with the hypertonic sucrose results, treatment with 20 mM K^+ alone did not affect the amplitude of the evoked EPSCs, while treatment with MCD alone reduced the amplitude by 57% (No treatment n=7, MCD alone n=12, $p<0.05$). These results are in agreement with those reported earlier from other secretory preparations after cholesterol depletion (Chamberlain et al., 2001, Lang et al., 2001, Zamir and Charlton, 2006). After MCD treatment, the reduction in the hypertonic sucrose response and the EPSC amplitudes were reversible by the re-addition of cholesterol using MCD: cholesterol complexes (Fig. 2.2.1.1).

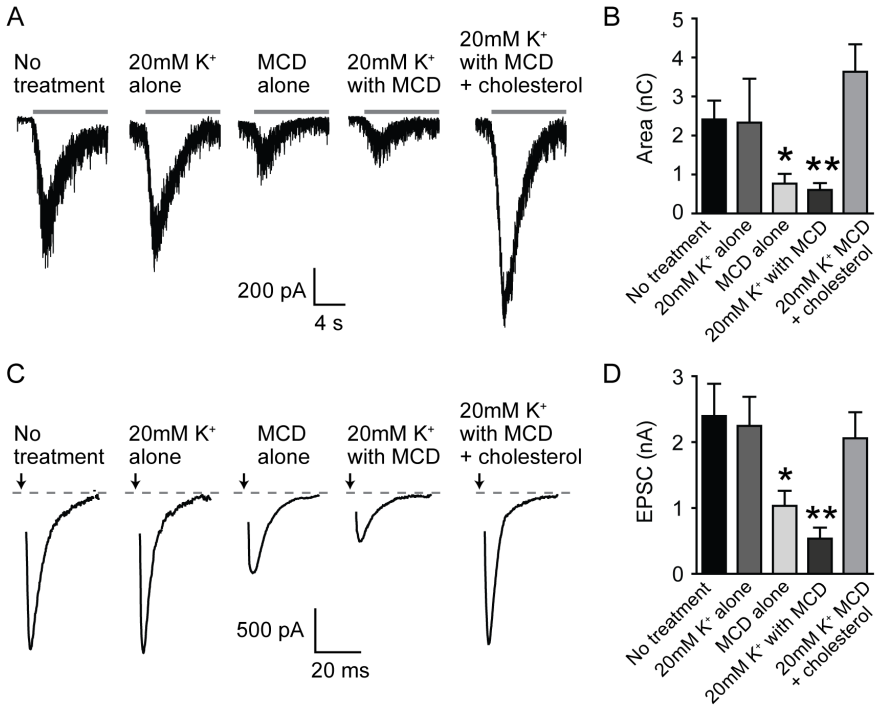

Figure 2.2.1.1 Depletion of cholesterol with MCD reduces evoked responses to hypertonic sucrose and action potentials.

(A-B) Hypertonic sucrose response after MCD treatment (A) Sample traces (B) Summary graph of the average charge transfer of the first 10 s of the 30-s sucrose stimulation showing a 75% decrease in responses in cultures treated in 20 mM K^+ with MCD. Cultures treated with 20 mM K^+ alone were not significantly different from non-treated cultures. Treatment with MCD alone also reduced the response; however, the magnitude of the decrease was less dramatic (68%). The addition of cholesterol to MCD treated cultures rescued the depleted hypertonic sucrose responses to values not significantly different from non-treated cultures. (Horizontal bar represents the presence of hypertonic sucrose, data collected from at least 3 cultures for each condition, No treatment n=18, 20 mM K^+ alone n=3, MCD alone n=16, 20 mM K^+ with MCD n=18, 20 mM K^+ with MCD + cholesterol n=10)

(C-D) Field potential stimulated responses after MCD treatment. (C) Sample traces. (D) Summary graph depicting a 78% reduction in the average maximum EPSC amplitude after treatment in 20 mM K^+ with MCD. Cultures treated with 20 mM K^+ alone were not significantly different from non-treated cultures. Treatment with MCD alone also reduced to a lesser degree (57%). Addition of cholesterol to MCD-treated cultures rescued the reduced EPSC amplitudes to values not significantly different from non-treated cultures (Arrow represents stimulus application, at least 3 cultures, No treatment n=7, 20 mM K^+ alone n=3, MCD alone n=12, 20 mM K^+ with MCD n=8, 20 mM K^+ with MCD + cholesterol n=7).

Error bars represent the standard error of the mean (SEM) (* $p<0.05$, ** $p<0.01$).

2.2.1.2 Cholesterol depletion augments the frequency of spontaneous vesicle fusion events

In the next set of experiments, I characterized the effect of cholesterol depletion on spontaneous fusion events by recording spontaneous miniature EPSCs (mEPSCs) after MCD treatment. The frequency of mEPSCs increased 5-fold in cultures depleted with MCD (Fig. 2.2.1.2.1 A-B; No treatment n=28, 20 mM K^+ with MCD n=31, $p<0.001$), while the amplitudes of the events were not significantly different indicating that the properties of postsynaptic glutamate receptors were not significantly altered by these manipulations (Fig. 2.2.1.2.1 C). Treatment with 20 mM K^+ alone did not affect the frequency or the amplitudes of the mEPSCs. Cultures treated with MCD alone had a 3-fold higher frequency of mEPSCs, however this increase was not significantly different from the non-treated cultures (No treatment n=28, MCD alone n=24, n.s. $p>0.05$). The increased frequency after MCD treatment was reversed by the re-addition of cholesterol from MCD: cholesterol complexes (Fig. 2.2.1.2.1 A-B).

The substantial increase in the spontaneous fusion rate seen in cholesterol-depleted cultures prompted us to determine whether the high mEPSC frequency would persist over time, or alternatively, rapidly diminish suggesting depletion of a vesicle pool that sustains this form of release. To determine the longevity of the increase in the spontaneous fusion rate, I recorded mEPSCs for 20 minutes and compared non-treated and MCD-treated frequencies at the end of the experiment.

I found that the frequency of mEPSCs in MCD-treated cells was still increased 5-fold compared to control cells at 20 minutes (Fig. 2.2.1.2.1 D; at 20 minutes, n=3, $p<0.05$). This finding is consistent with the constant spontaneous recycling of a pool of vesicles to maintain this high fusion rate.

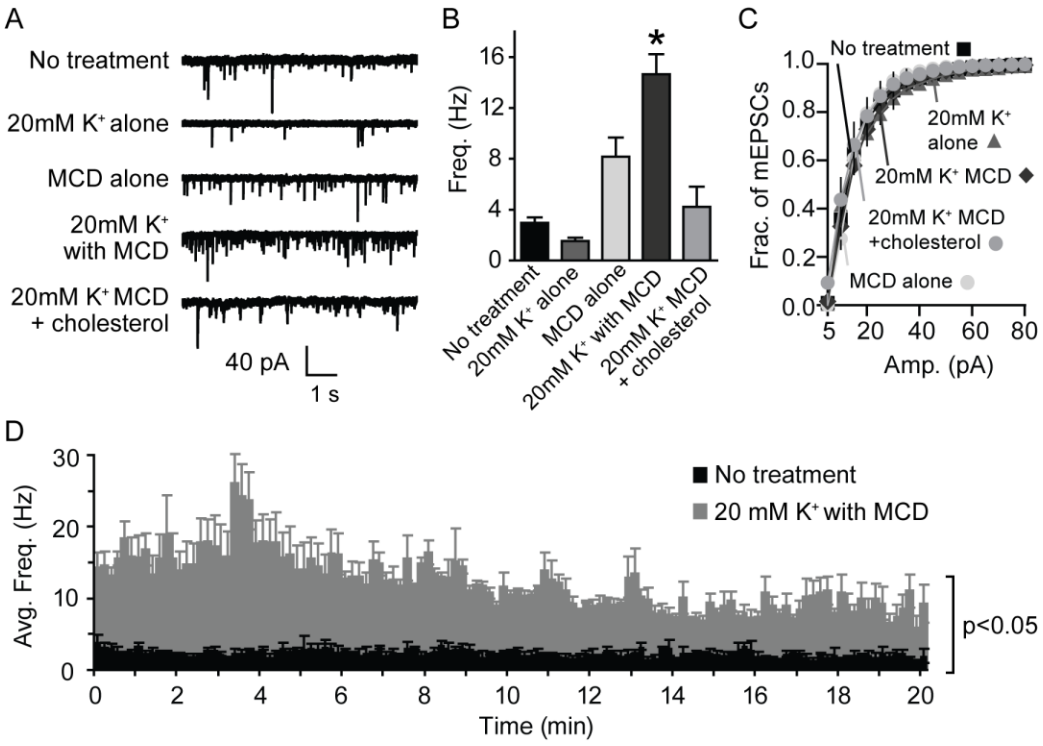

Figure 2.2.1.2.1 Cholesterol depletion augments spontaneous fusion rate

Spontaneous miniature EPSCs (mEPSC) after MCD treatment (A) Sample traces
(B) Summary graph showing a 5-fold increase in the frequency of mEPSCs for MCD-treated cultures compared to non-treated cultures. Treatment with 20 mM K^+ alone did not alter the frequency of mEPSC events. Cultures treated with MCD alone had an average 3-fold higher frequency of mEPSCs; however the rate was not significantly different from the non-treated cultures. (C) Cumulative histograms of the distribution of mEPSC amplitudes showed no differences using Kolmogorov-Smirnov test (K-S test, $p>0.0001$).
(D) Summary graph depicting the persistent 5-fold increase of the average mEPSC frequency (integrated per 10-second intervals) for 20 minutes for non-treated cultures and cultures treated in 20 mM K^+ with MCD.

(at least 3 cultures, No treatment n=28, 20 mM K^+ Only n=6, MCD alone n=24, 20 mM K^+ with MCD n=31, and 20 mM K^+ with MCD + cholesterol n=4).
Error bars represent the SEM (*p< 0.001).

After treating cultures with 20 mM K^+ with MCD and then incubating for 30 minutes with BAPTA-AM (a fast Ca^{2+} buffer), I recorded mEPSC events and found that Ca^{2+} chelation did not prevent the increased frequency of spontaneous events (10-fold) compared to the frequencies observed in BAPTA-AM loaded, non-treated cultures (Fig. 2.2.1.2.2 A-C; No treatment BAPTA-AM n=7, 20 mM K^+ with MCD n=6, $p<0.05$). For non-treated cultures, the rate of spontaneous events was reduced after incubation with BAPTA-AM; however, the reduction was not significant (No treatment no BAPTA-AM n=3, No treatment BAPTA-AM n=7, $p>0.05$). Cultures treated with MCD alone were also increased (6-fold), however this increase was not significant (No treatment BAPTA-AM n=7, MCD alone n=4, n.s. $p>0.05$). Thus, the increased frequency observed after MCD treatment is not dependent on Ca^{2+} or leakiness of neuronal membranes after cholesterol removal.

To examine the Ca^{2+} sensitivity of spontaneous neurotransmission seen in MCD-treated neurons, I perfused cultures with the Ca^{2+} ionophore ionomycin to increase the cytoplasmic Ca^{2+}concentration. Before ionomycin perfusion, the basal mEPSC frequency was 3.5-fold higher in neurons from cultures treated in 20 mM K^+ with MCD compared to those treated with 20 mM K^+ alone (Fig. 2.2.1.2.2 D-E; 20 mM K^+ alone n=4, 20 mM K^+ with MCD n=6, $p<0.05$). After

ionomycin perfusion, the average fold increase in the frequency of spontaneous events was 2- and 5-fold for neurons from cultures treated with 20 mM K^+ alone and with 20 mM K^+ with MCD respectively (Fig. 2.2.1.2.2 F; 20 mM K^+ alone n=4, 20 mM K^+ with MCD n=6, p>0.05). Spontaneous synaptic vesicle fusion is a Ca^{2+} sensitive process albeit to a reduced degree. Therefore, taken together with our observation that spontaneous release is dramatically augmented after cholesterol removal, the increase in the effectiveness of ionomycin to trigger release is consistent with an increase in the number of vesicles available for spontaneous fusion.

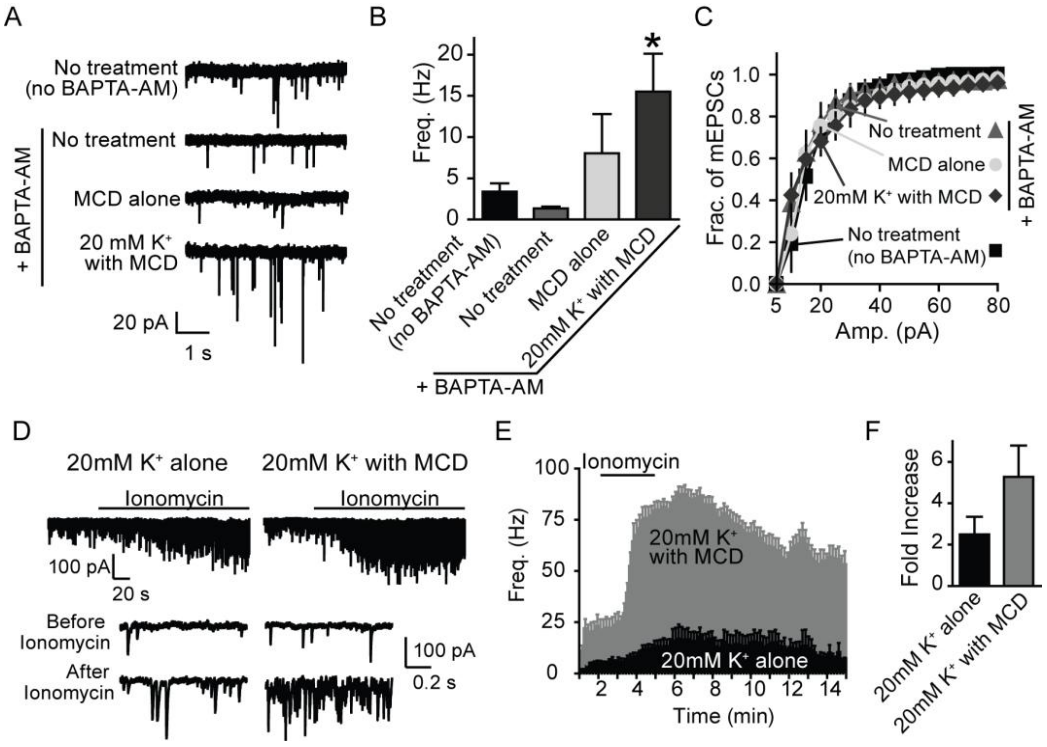

Figure 2.2.1.2.2 Ca^{2+}-dependence of the increased spontaneous event frequency after cholesterol depletion

(A-C) mEPSC recorded after BAPTA-AM loading (1µM for 30 minutes) in MCD-treated cultures (A) Sample traces (B) Summary graph showing a 10-fold increase in the frequency of mEPSCs for cultures treated in 20 mM K^+ with MCD then loaded with BAPTA-AM compared to BAPTA-AM loaded, non-treated cultures. The frequency of mEPSCs in non-treated cultures loaded with BAPTA-AM was 60% of the frequency of non-treated cultures not loaded with BAPTA-AM. The frequency of mEPSCs in cultures treated with MCD alone had a 6-fold increase in frequency; however the difference was not significant from the frequency of BAPTA-AM loaded, non-treated cultures. This demonstrates that the increase in the frequency of mEPSCs after MCD treatment is not due to an increase in Ca^{2+} levels/influx. (C) The distributions of mEPSC amplitudes were not affected by the BAPTA-AM treatment as determined by the K-S test ($p>0.0001$). (1 culture, No treatment no BAPTA-AM n=3, No treatment BAPTA-AM n=7, MCD alone n=4, and 20 mM K^+ with MCD n=6)
(D-F) Ionomycin responses from MCD treated cultures. (D) Sample traces of ionomycin perfusion (1µM for 3 min). Detailed views of the traces before ionomycin and after ionomycin for each treatment are shown below. (E) Histogram of the average frequency over 10-s intervals of both the 20 mM K^+ with MCD and the 20 mM K^+ alone treatments before and after ionomycin perfusion. Cultures treated in 20 mM K^+ with MCD had a 3-fold higher mEPSC frequency before ionomycin treatment than cultures treated with 20 mM K^+ alone. (F) Summary graph of the fold increase in mEPSC frequency after ionomycin perfusion. The average fold increase in the frequency of mEPSCs after ionomycin perfusion was 2.5- and 5-fold for cultures treated with 20 mM K^+ alone and 20 mM K^+ with MCD (respectively), however the difference is not significant. (Horizontal black bar indicates the presence of ionomycin, 1 culture, 20mM K^+ alone n=6, 20mM K^+ with MCD n=3).
Error bars represent the SEM (*$p<0.05$).

2.2.1.3 Altered neurotransmission after cholesterol depletion is not dependent on the presence of glial cells

Next, I explored whether these effects of cholesterol depletion in dissociated hippocampal cultures is specific to neurons or a result of an indirect effect of cholesterol removal from glial cells. To address this issue, I examined excitatory transmission after cholesterol depletion in the absence of glia using Banker-style hippocampal cultures (Goslin et al., 1998). I obtained the Banker-style cultures from the Thomas Südhof laboratory, which kindly donated the

hippocampal neurons plated at embryonic day-18 without serum to prevent glial growth and incubated in a glia-enriched medium. I treated these cultures with 20 mM K^+ alone and 20mM K^+ with MCD and measured both the evoked and spontaneous neurotransmission. The 20 mM K^+ with MCD treatment resulted in a 94 and 85% decrease in the hypertonic sucrose response and field-stimulated EPSCs, respectively (Fig. 2.2.1.3 A-D; hypertonic sucrose: 20 mM K^+ alone n=6, 20 mM K^+ with MCD n=6, $p<0.005$; EPSCs: 20 mM K^+ alone n=6, 20 mM K^+ with MCD n=3, $p<0.05$). After 20mM K^+ with MCD incubation, I also observed a significant increase in the frequency of mEPSCs in the absence of glia (Fig. 2.2.1.3 E-G, 20 mM K^+ alone n=6, 20 mM K^+ with MCD n=9, $p<0.05$), indicating that the effect of cholesterol depletion by MCD on spontaneous and evoked fusion is not dependent on glial cells.

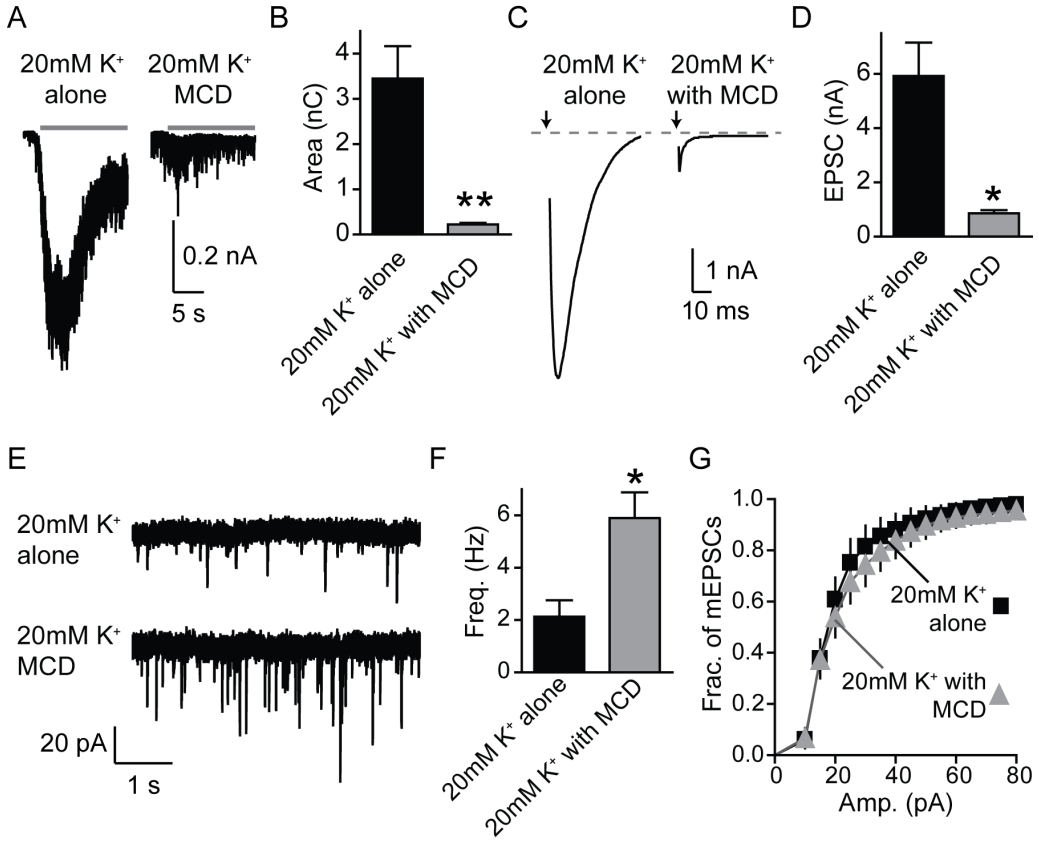

Figure 2.2.1.3 MCD effect is not dependent on the presence of glial cells.

(A-B) Hypertonic sucrose stimulation after MCD treatment in the absence of glia (A) Sample traces (B) Summary graph showing that the average charge transfer during the first 10 seconds of the 30-second sucrose response is decreased 94% after treatment with MCD compared to cultures treated with 20mM K^+ alone. (Horizontal bar represents the presence of hypertonic sucrose, 1 culture, 20mM K^+ alone n=6, 20mM K^+ with MCD n=6)

(C-D) Field stimulation evoked responses after MCD treatment in the absence of glia. (C) Sample traces. (D) Summary graph showing an 85% reduction in the average evoked EPSC amplitude for cultures treated with MCD compared to cultures treated with 20mM K^+ alone. (Arrow represents timing of the stimulation, 1 culture, 20mM K^+ alone n=6, 20mM K^+ with MCD n=3)

(E-G) mEPSCs after MCD treatment in the absence of glia (E) Sample traces (F) Summary graph shows a 3-fold increase in the frequency of mEPSCs for cultures treated with MCD compared to cultures treated with 20mM K^+ alone. (G) The distributions of mEPSC amplitudes were not affected by these treatments as determined by the K-S test ($p>0.001$) (1 culture, 20mM K^+ alone n=6, 20mM K^+ with MCD n=9)

Error bars represent the SEM (*$p<0.05$, **$p<0.005$).

2.2.1.4 Cholesterol depletion leads to decreased evoked uptake and increased spontaneous uptake of horseradish peroxidase

To determine whether acute cholesterol depletion caused structural differences at the presynaptic terminal, I examined the synapses of MCD-treated neurons by analyzing electron micrographs taken by Xinran Liu (Fig. 2.2.1.4 A). In 20 mM K^+ with MCD treated cultures, the number of docked vesicles were normal compared to the control (data not shown); however, I observed an obvious decrease in the total number of vesicles per synapse (44%) in cultures treated with MCD (Fig. 2.2.1.4 B; No treatment n=94, 20 mM K^+ with MCD n=108, $p<0.001$). The significant loss of vesicles after a brief, 30-minute MCD treatment in 20 mM K^+ suggests that some vesicles could not be retrieved after fusion during MCD treatment. In contrast, cultures treated with MCD alone experienced a less dramatic reduction in the total number of vesicles per synapse (8%; No treatment n=94, MCD alone n=68, n.s. $p>0.05$), indicating that this defect in endocytosis required depolarization during MCD incubation.

To monitor SV endocytosis under these conditions, I also observed electron micrographs taken by Xinran Liu from MCD-treated cells after either evoked or spontaneous horseradish peroxidase (HRP) uptake. I performed the evoked uptake of HRP by maximally stimulating cultures for 2 minutes in a high K^+ buffer (47 mM K^+) containing HRP (Fig. 2.2.1.4 C). The number and corresponding percent of HRP-positive vesicles decreased 61 and 64% in cultures treated 20 mM K^+

with MCD (Fig. 2.2.1.4 D-E; No treatment n=11, 20 mM K^+ with MCD n=6, $p<0.01$). After treating cultures with MCD alone, I found a reduction in the number (30%) and corresponding percent (42%) of HRP-positive vesicles compared to non-treated cultures (No treatment n=11, MCD alone n=8, n.s. $p>0.05$). The decrease in the number and overall percent of HRP-positive vesicles is consistent with the decreased responses observed with hypertonic sucrose and field stimulation (Fig. 2.2.1.1).

To explore the spontaneous uptake of HRP, I incubated cultures in a normal K^+ buffer (4 mM K^+) containing HRP in the presence of TTX to prevent action potentials for 15 minutes. After washing and fixing, Xinran took electron micrographs of the synapses, which I then analyzed. While the percentage of vesicles that take up HRP with maximal stimulation is decreased after MCD treatment, I observed a 1.6- and 2.5-fold increase in the number as well as the percent of vesicles that took up HRP spontaneously compared to synapses from non-treated cultures (Fig. 2.2.1.4 F-H; No treatment n=47, 20 mM K^+ with MCD n=72, $p<0.05$). This outcome suggests that within 15-minute incubation with HRP there were more vesicles recycling spontaneously in MCD-treated synapses compared to the controls. This increase could be a result of an elevation in the number of spontaneously fusing vesicles as suggested above (Fig. 2.2.1.2.1 D and Fig. 2.2.1.2.2 D-F) and/or an increase in their rate of recycling.

The 44% decrease in the number of vesicles per synapse after treatment in 20 mM K^+ with MCD (Fig. 2.2.1.4 A-B) suggests that some fused vesicles were unable to endocytose. In agreement with this premise, I detected several stranded endocytic structures in images from neurons treated in 20 mM K^+ with MCD (Fig. 2.2.1.4 I and K) compared to the images from neurons treated with 20 mM K^+ alone (Fig. 2.2.1.4 I and J).

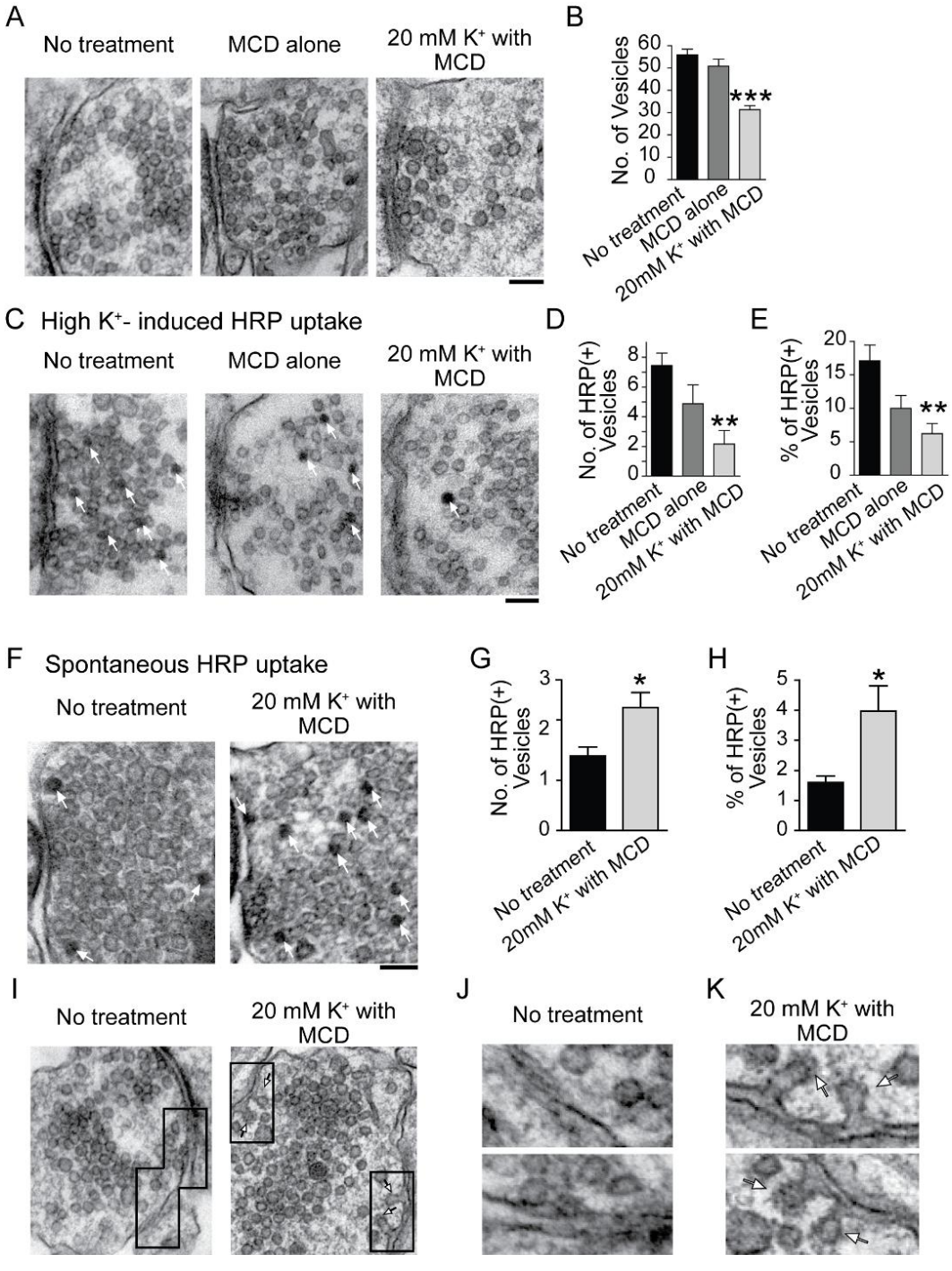
A
No treatment
MCD alone
20 mM K+ with MCD
B
No. of Vesicles
60
50
40
30
20
10
0
***
No treatment
MCD alone
20mM K+ with MCD
C High K+- induced HRP uptake
No treatment
MCD alone
20 mM K+ with MCD
D
No. of HRP(+) Vesicles
8
6
4
2
0
**
No treatment
MCD alone
20mM K+ with MCD
E
% of HRP(+) Vesicles
20
15
10
5
0
**
No treatment
MCD alone
20mM K+ with MCD
F Spontaneous HRP uptake
No treatment
20 mM K+ with MCD
G
No. of HRP(+) Vesicles
3
2
1
0
*
No treatment
20mM K+ with MCD
H
% of HRP(+) Vesicles
5
4
3
2
1
0
*
No treatment
20mM K+ with MCD
I
No treatment
20 mM K+ with MCD
J
No treatment
K
20 mM K+ with MCD

Figure 2.2.1.4 Cholesterol depletion decreases the number of vesicles per synapse and effects depolarization-evoked and spontaneous HRP uptake differentially.

(A-B) Electron micrographs (EMs) of MCD-treated hippocampal cultures (A) Representative synapses (B) Summary plot showing a 44% decrease in the average number of vesicles per synapse for cultures treated in 20 mM K^+ with MCD compared to the non-treated cultures. Cultures treated with MCD alone only showed an 8% decrease in the number of vesicles per synapse, indicating that treatment with MCD with stimulation is necessary for the decrease in vesicles. (No treatment n=94, MCD alone n=68, and 20 mM K^+ with MCD n=108).
(C-E) EMs of MCD-treated cultures loaded with HRP using 47 mM K^+ depolarisation for 2 minutes. (C) Representative synapses (white arrows indicate HRP-positive (HRP+) vesicles). (D) Summary plot showing a 61% decrease in the average number of HRP+ vesicles per synapse for cultures treated in 20 mM K^+ with MCD compared to the non-treated cultures. Cultures treated with MCD alone had a 30% decrease in the number of HRP+ vesicles per synapse compared to the non-treated cultures. (E) Summary plot showing a 64% decrease in the average number of HRP+ vesicles per synapse for cultures treated in 20 mM K^+ with MCD compared to the non-treated cultures. Cultures treated with MCD alone had a 42% decrease in the percent of HRP+ vesicles per synapse compared to the non-treated cultures. (No treatment n=11, MCD alone n=8, and 20 mM K^+ with MCD n=6).
(F-H) EMs of MCD-treated cultures loaded with HRP spontaneously. (F) Representative synapse sections (white arrows indicate HRP-positive vesicles). (G) Summary graph showing a 1.6-fold increase in the average number of HRP+ vesicles per synapse for cultures treated in 20 mM K^+ with MCD. (H) Summary graph showing a 2.5-fold increase in the average percent of HRP+ vesicles per synapse for cultures treated in 20 mM K^+ with MCD. (No treatment n=47 and 20 mM K^+ with MCD n=72).
(I-K) Electron micrographs (EMs) of MCD-treated hippocampal cultures depicting stranded endocytic structures. (I) Representative images. (J) Magnified images of synapses treated with 20mM K^+ alone. (K) Magnified images of synapses treated with 20mM K^+ with MCD.
Error bars represent the SEM (*$p<0.05$, **$p<0.01$, ***$p<<0.001$; scale bar = 100 nm).

2.2.1.5 Cholesterol depletion dependent increase in spontaneous fusion rate does not require synaptobrevin-2

The differential effect of cholesterol depletion on the evoked and spontaneous synaptic vesicle recycling suggested cholesterol depletion was hindering evoked fusion by a mechanism that does not impair spontaneous fusion. To better understand the mechanisms underlying this phenomenon, I repeated the same maneuvers in dissociated hippocampal neurons obtained from mice lacking a major synaptic vesicle SNARE, synaptobrevin-2 (also called VAMP-2). Synaptobrevin-2-deficient (Syb2 –/–) synapses manifest a severe reduction in evoked exocytosis and endocytosis (Schoch et al., 2001, Deak et al., 2004). In initial cholesterol depletion experiments in wild-type rat cultures, I detected a significant decrease in the response to hypertonic sucrose after cholesterol depletion (Fig. 2.2.1.1 A-B). This effect could involve the dispersion of syntaxin clusters, thus impairment of SNARE-mediated fusion, seen after cholesterol depletion in other systems (Lang et al., 2001, Churchward et al., 2005). To determine if the impairment of evoked neurotransmission after cholesterol extraction is dependent on the SNARE machinery, I looked for changes in the hypertonic sucrose responses of neurons without synaptobrevin-2 after cholesterol depletion. As expected, the lack of synaptobrevin-2 resulted in an 80% reduction of the hypertonic sucrose response compared to the wild-type (WT) neurons (WT n=8, Syb2 –/– n=7, $p<0.05$). Consistent with the experiments I performed in wild-

type rat cultures, wild-type synaptobrevin-2 mouse neurons treated with MCD had an 80% decrease in the response to hypertonic sucrose compared to non-treated wild-type neurons (Fig. 2.2.1.5 A-B; WT n=8, WT (MCD) n=4, $p<0.05$). On the contrary, the low-charge hypertonic sucrose responses from non-treated synaptobrevin-2-deficient neurons experienced no further decrease after cholesterol depletion (Fig. 2.2.1.5 A-B; Syb2 –/– n=7, Syb2 –/– (MCD) n=5, n.s. $p>0.05$). Thus, these experiments revealed no further reduction in hypertonic sucrose driven release in synaptobrevin-2-deficient synapses, suggesting that removal of cholesterol impairs evoked release primarily by affecting SNARE-dependent fusion.

I next looked for altered spontaneous fusion after cholesterol depletion in the synaptobrevin-2-deficient neurons. Without depleting cholesterol, the lack of synaptobrevin resulted in a dramatic 97% reduction in the frequency of mEPSC events compared to the wild-type neurons (WT n=7, Syb2 –/– n=7, $p<0.001$). In contrast to the lack of a decrease in hypertonic sucrose responses after cholesterol depletion in synaptobrevin-2-deficient neurons, I could detect a significant increase in the frequency of mEPSCs after MCD treatment in *both* the wild-type (2-fold, WT n=7, WT (MCD) n=5, $p<0.005$) and synaptobrevin-2-deficient neurons (13-fold, Syb2 –/– n=7, Syb2 –/– (MCD) n=4, $p<<0.001$). Even with the increase in frequency after MCD treatment, the frequency in synaptobrevin-2-deficient neurons was still 65% lower than the spontaneous fusion rate in non-

treated wild-type neurons (WT n=7, Syb2 –/– (MCD) n=4, $p<0.05$) (Fig. 2.2.1.5 C-E).

So while the response to hypertonic sucrose stimulation was not affected by MCD treatment in synaptobrevin-2-deficient neurons, I could still detect an increase in the spontaneous fusion rate after MCD treatment without a significant alteration in the amplitudes of individual mEPSCs. This suggests that cholesterol may act downstream of synaptobrevin-2 function to restrain spontaneous fusion.

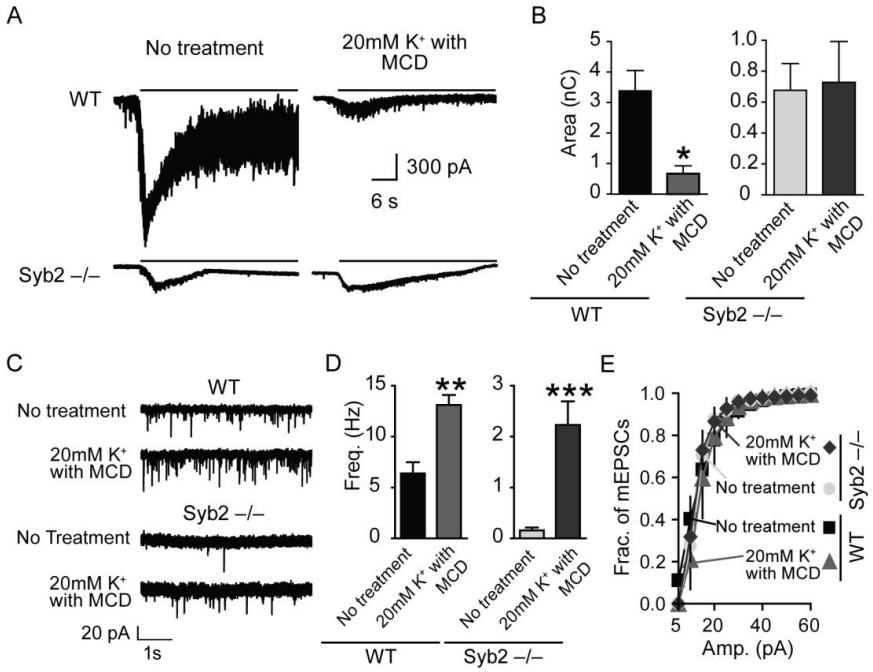

Figure 2.2.1.5 Differential effect of cholesterol depletion in synaptobrevin-2-deficient mice.

(A-B) Hypertonic sucrose stimulation of synaptobrevin-2-deficient (Syb2 –/–) and wild-type littermates (WT) neurons after MCD treatment (A) Sample traces (B) Summary graph of the charge transfer during the first 10 seconds of the 30-second sucrose stimulation depicts an 80% decrease in WT neurons treated in 20mM K^+ with MCD, and an 80% lower response of Syb2 –/– neurons compared to WT. However the sucrose responses of Syb2 –/– cultures treated in 20mM K^+ with MCD were not significantly

different from the responses from non-treated Syb2 –/– cultures. (Horizontal bar represents the presence of hypertonic sucrose, 1 culture, WT n=8, WT MCD n=4, Syb2 –/– n=7, Syb2 –/– MCD n=5)
(C-E) mEPSCs in Syb2 –/– and WT after MCD treatment (C) Sample traces (D) Summary graph shows a 2-fold and 14-fold increase after treatment in 20mM K^+ with MCD in the frequency of mEPSCs in WT and Syb2 –/– neurons, respectively, compared to untreated neurons. Note: The mEPSC frequency in Syb2 –/– neurons is 95% less than WT, and the frequency of Syb2 –/– neurons after MCD treatment is still 71% less than non-treated WT neurons. (E) The distributions of mEPSCs amplitudes did not reveal significant differences under all conditions using K-S test ($p>0.0001$) (1 culture, WT n=7, WT MCD n=5, Syb2 –/– n=7, Syb2 –/– MCD n=4).
Error bars represent the SEM (*$p<0.05$, **$p<0.005$, ***$p<<0.001$)

2.2.2 Inhibitory neurotransmission after acute extraction of cholesterol

To determine if inhibitory synaptic transmission is equally affected by cholesterol depletion, I repeated the recordings of field potential stimulated well as the spontaneous postsynaptic currents from inhibitory synapses of wild-type rat cultured hippocampal neurons. I isolated the inhibitory currents by blocking excitatory neurotransmitter receptors with CNQX and found similar effects of cholesterol depletion at these synapses. I observed a decrease in the field potential stimulated inhibitory post synaptic currents (IPSCs; 2.7-fold; Fig. 2.2.2.1: 20 mM K^+ only 1.9±0.4 nA, n=4; 20 mM K^+ MCD 0.7±0.1 nA, n=3; 20 mM K^+ MCD + Cholesterol 1.8±0.2 nA, n=4) as well as an increase in the frequency of miniature IPSC (mIPSC)(4.8-fold; Fig. 2.2.2.2: 20 mM K^+ only 0.31±0.07 Hz, n=7; 20 mM K^+ MCD 1.52±0.2 Hz, n=5; 20 mM K^+ MCD + Cholesterol 0.69±0.56 Hz, n=5) without a change in the distribution of the mIPSC amplitudes. I could restore both the IPSC amplitudes and mIPSC frequency to levels not significantly different

from non-treated neurons by the addition of cholesterol using MCD: cholesterol complexes.

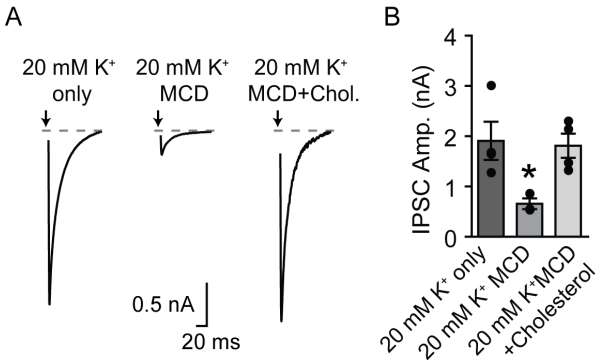

Figure 2.2.2.1 Cholesterol depletion reversibly decreases evoked IPSCs

(A-B) Field stimulation evoked responses after MCD treatment in a 20 mM K^+ solution. (A) Sample traces. (B) Summary graph of the average magnitude of the maximum evoked IPSC amplitude showing a 2.7-fold decrease in cultures treated in 20 mM K^+ with MCD. The addition of cholesterol to MCD-treated cultures rescued the reduced EPSC amplitudes to values not significantly different from non-treated cultures.
Error bars represent the SEM (20 mM K^+ only n=4, 20 mM K^+ with MCD n=3, and 20 mM K^+ with MCD + cholesterol n=4; *p< 0.04).

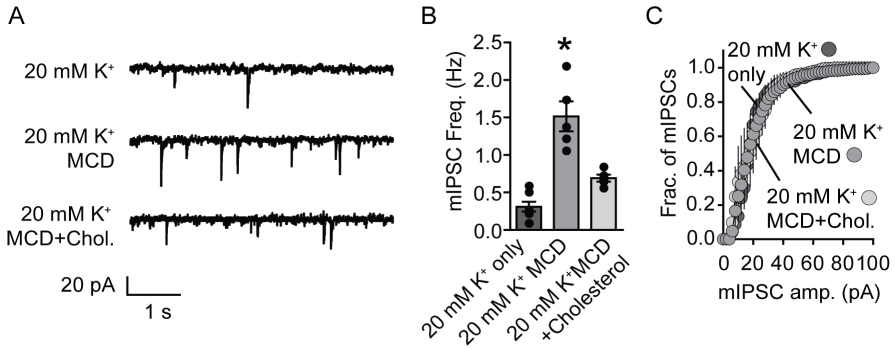

Figure 2.2.2.2 Cholesterol depletion reversibly increases the frequency of mIPSCs.

(A-C) Spontaneous miniature IPSCs (mIPSC) after MCD treatment in a 20 mM K^+ solution
(A) Sample traces (B) Summary graph showing a4.8-fold increase in the frequency of mIPSCs for MCD-treated cultures compared to non-treated cultures. Treatment with 20

mM K^+ alone did not alter the frequency of mIPSC events. (C) Plot of the average mIPSC amplitudes showing no differences.
Error bars represent the SEM (20 mM K^+ only n=4, 20 mM K^+ with MCD n=5, and 20 mM K^+ with MCD + cholesterol n=4; *p<<0.001).

2.2.3 Oxidation of cholesterol using cholesterol oxidase

After acute extraction of cholesterol from neuronal membranes with methyl-β-cyclodextrin, the rate of spontaneous vesicle fusion increases (Fig. 2.2.1.2.1) in a Ca^{2+}-independent manner (Fig. 2.2.1.2.2), while the efficiency of synchronized fusion in response to action potentials decreases (Fig 2.2.1.1). These results suggest that cholesterol plays an integral role in synaptic neurotransmission. However, cholesterol provides at least two different services to the membrane: rigidity and specific interactions with proteins. Thus, cholesterol depletion from the hippocampal neurons results in a decrease in both membrane fluidity as well as cholesterol-specific protein interactions. A loss of membrane rigidity due to cholesterol removal would result in a more flexible lipid bilayer; this flexibility could lead to a reduction in the energy required to fuse two separate and stable lipid bilayers, thus enhancing the probability of spontaneous vesicle fusion. Moreover, disruption of cholesterol-specific interactions within the synaptic membrane could reduce or eliminate necessary membrane organization and even the activity of bound proteins.

To explore whether the effects of cholesterol on either evoked or spontaneous neurotransmission result from an increase in membrane fluidity

and/or a loss of cholesterol-dependent protein interactions, I treated hippocampal neuron cultures with the membrane impermeable enzyme, cholesterol oxidase (ChOx), which converts cholesterol to cholestenone. The structure of cholestenone is different enough from cholesterol that the oxidation of cholesterol leads to the disruption of cholesterol-specific interactions while similar enough to not disrupt membrane fluidity (Lau and Das, 1995, Gimpl et al., 1997). Thus, if the effects of cholesterol extraction are due to decreased membrane fluidity, then oxidation of cholesterol will not mimic the effects of cholesterol depletion because cholestenone does not affect membrane fluidity. If the cholesterol depletion effects are a result of lost cholesterol-specific interactions, then conversion of cholesterol to cholestenone will disrupt the same interactions as cholesterol removal resulting in similar synaptic dysfunction observed after acute extraction of cholesterol.

To identify which effects observed after cholesterol depletion might be due to altered membrane fluidity, I treated cultures with cholesterol oxidase and measured the amplitudes of field potential evoked EPSCs and the mEPSCs and looked for the similarities (protein interactions) or differences (membrane fluidity) in the effects seen after direct extraction of cholesterol (Fig. 2.2.1.1 C-D and 2.2.1.2.1). Like methyl-β-cyclodextrin, cholesterol oxidase is unable to permeate through membranes, so I oxidized cholesterol along only the plasma membrane or in both plasma and synaptic vesicle membranes to dissociate the

effects of cholesterol within each lipid bilayer. Briefly, I added cholesterol oxidase (4U/ml, *Pseudomonas fluorescens*, Sigma) along with either TTX or additional K^+ (20 mM K^+ final concentration) into the original culture medium of dissociated rat hippocampal neuron cultures and incubated the neurons for 30 minutes at 37°C. After washing the coverslips, I whole-cell patch clamped hippocampal neurons and measured synaptic transmission by recording postsynaptic currents. For each experiment, I performed concurrent experiments on neurons treated with only TTX or elevated K^+ to control for these variables.

After oxidizing cholesterol within only the plasma membrane or both the plasma and synaptic vesicle membranes, I observed a 40 and 57% decrease in the field-potential stimulated EPSCs compared to recordings from neurons treated in the same medium without cholesterol oxidase (Fig 2.2.3.1: TTX alone 2.7±0.3 nA, n=12; 20 mM K^+ alone 2.4±0.3 nA, n=11; ChOx TTX 1.6±0.3 nA, n=13; ChOx 20 mM K^+ 1.0±0.1 nA, n=12). The similarity between each cholesterol oxidase treatment suggests that the decreased EPSC amplitudes are a function of the oxidation of plasma membrane cholesterol; however, the treatment of both membranes further attenuated the EPSC amplitudes, which indicate that the loss of cholesterol by conversion to cholestenone exacerbates the defect in action potential-dependent neurotransmission. Moreover, the changes in EPSC amplitudes after cholesterol oxidation demonstrate that the decreased amplitudes after cholesterol depletion most likely involve the loss of cholesterol-specific

protein interactions. This is logical considering the volume of evidence linking cholesterol-dependent organization of synaptic proteins with both exo- and endocytosis.

As for spontaneous neurotransmission after cholesterol oxidase treatments, I observed obvious differences between the oxidation effect of only plasma membrane cholesterol and that of cholesterol from both the plasma and synaptic vesicle membranes. Cholesterol oxidase treatment in the absence of action potentials resulted in no change in spontaneous neurotransmitter release compared to TTX only treated neurons (Fig 2.2.3.2: TTX alone 2.2±0.8 Hz, n=10; ChOx TTX 2.2±0.3 Hz, n=13; p=0.997). Conversely, I observed a 2.2-fold increase in the frequency of mEPSCs without affecting the event amplitude distributions compared to neurons treated with elevated K^+ alone (Fig. 2.2.3.2: 20 mM K^+ alone 2.2±0.4 Hz, n=18; ChOx 20 mM K^+ 4.7±1.1 Hz, n=8; $p<0.02$). Considering the lack of altered spontaneous release after plasma membrane oxidation, the non-significant upward trend in the frequency of mEPSCs after acute cholesterol depletion (Fig 2.2.1.2.1, MCD alone) appears to be a function of decreased membrane fluidity, not loss of protein function. Moreover, the oxidation of cholesterol in both the plasma membrane and synaptic vesicles does affect the rate of spontaneous vesicle fusion, indicating that this defect involves the loss of a protein interaction leading to the increased efficiency of spontaneous neurotransmitter release.

These experiments suggest that cholesterol participates in specific interactions within the neuronal plasma membrane and the disruption of these interactions by either oxidation or removal of cholesterol results in attenuated neurotransmitter release. Moreover, cholesterol-specific interactions within vesicle membranes appear to at least partially inhibit spontaneous neurotransmitter release.

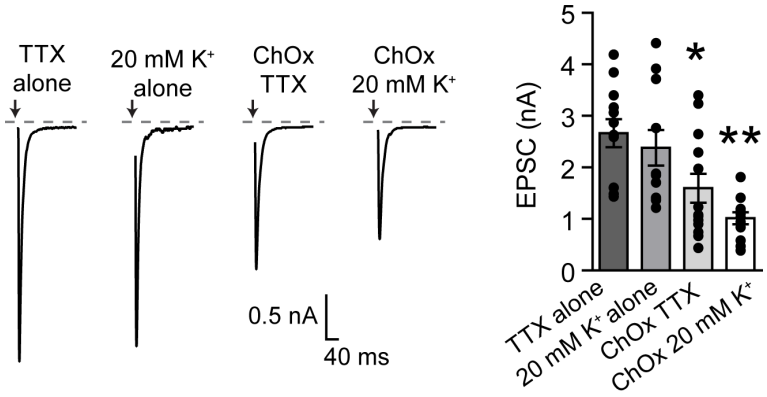

Figure 2.2.3.1 Cholesterol oxidation in the plasma membrane or in synaptic vesicles decreases EPSCs amplitudes

(A) Sample traces of field potential stimulated EPSCs with or without cholesterol oxidase treatment in the absence of action potentials (TTX) or in elevated K^+ (20 mM K^+).
(B) Field stimulation evoked EPSCs displaying a 40 and 57% decrease after cholesterol oxidation in TTX or 20 mM K^+. (2 cultures; TTX n=12; ChOx + TTX n=13; 20 mM K^+ n=11; ChOx + 20 mM K^+ n=12).
Error bars represent the SEM. (*$p<0.04$, **$p<0.001$)

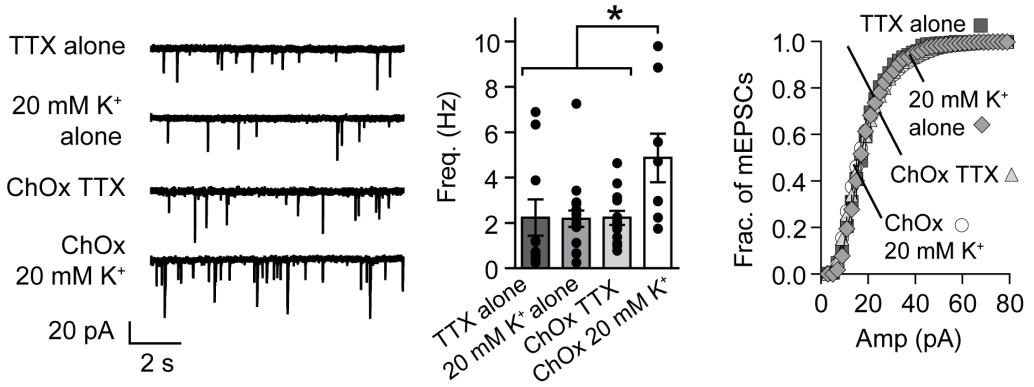

Figure 2.2.3.2 Altered cholesterol-specific interactions within recycling pool vesicles by cholesterol oxidation leads to enhanced spontaneous neurotransmitter release.

(A) Sample traces of the miniature excitatory postsynaptic currents (mEPSCs)
(B) Summary graph showing a 2.2-fold increase in the mEPSC frequency in neurons treated with ChOx in elevated K^+ (C) The mEPSCs amplitudes were not significantly different between the treatment groups.
Error bars represent the SEM. (2 cultures; TTX n=10; ChOx + TTX n=13; 20 mM K^+ n=18; ChOx + 20 mM K^+ n=8; * $p<0.02$)

2.3 Summary

As an integral member of membranes, cholesterol interacts with both lipids and proteins to control the organization and functions along lipid bilayers ((Gimpl et al., 1997, Lee, 2004, Pucadyil and Chattopadhyay, 2005)). Implicated in exocytosis and endocytosis in other secretory systems, I pursued the exploration of cholesterol's role in synaptic neurotransmission (Rodal et al., 1999, Subtil et al., 1999, Chamberlain et al., 2001, Lang et al., 2001, Gil et al., 2005, Salaun et al., 2005). Evidence for cholesterol as a player in exocytosis came from several studies demonstrating localization of SNARE and other synaptic proteins to cholesterol-rich domains as well as decreased exocytosis after acute cholesterol removal (Chamberlain et al., 2001, Lang et al., 2001, Gil et al., 2005, Salaun et

al., 2005), one even showed the preferential docking of vesicles at sites of cholesterol-dependent syntaxin1 clusters (Lang et al., 2001). As for defects in endocytosis, acute extraction of cholesterol blocked the recruitment of clathrin, which is essential for classical membrane retrieval (Rodal et al., 1999, Subtil et al., 1999, Xia et al., 2004).

My initial experiments implicate cholesterol in both exocytosis and endocytosis within synapses of the CNS. Sudden loss of cholesterol from neuronal membranes did in fact disrupt the release of neurotransmitter measured by postsynaptic currents during field potential or hypertonic sucrose stimulations (Fig. 2.2.1.1). The reduced hypertonic sucrose depended on the presence of synaptobrevin-2, suggesting a SNARE-dependence which supports the prior studies in other systems showing a correlation between exocytosis and SNARE protein clustering (Fig. 2.2.1.5). I also found that the decreases in EPSCs after cholesterol depletion are most likely a product of disruptions in the cholesterol-specific interactions suggested by the reduced EPSC amplitudes after converting cholesterol to cholestenone with cholesterol oxidase (Fig. 2.2.3.1). Moreover, electron micrographs of synapses obtained after high K^+ stimulated uptake of HRP exposed a decrease in the percentage of vesicles recycling after cholesterol depletion indicating an interruption in the cycle of exocytosis and subsequent endocytosis of synaptic vesicles (Fig. 2.2.1.4 C-E).

Interestingly, I detected obvious defects in endocytosis as measured by a near 50% decrease in the percent of vesicles per synapse after cholesterol extraction during depolarization (Fig. 2.2.1.4 A-B). This deficit only appeared after exposure to MCD during depolarization indicating that cholesterol depletion from action potential-dependent recycling vesicles plays a significant role in the efficiency of endocytosis. Consistent with this observation, synapses exhibited a more dramatic decrease in the percentage of HRP positive vesicles after cholesterol extraction from both membranes compared to synapses after depletion of only the plasma membrane, demonstrating that not only are there fewer vesicles at these synapses but also that the lost vesicles were most likely part of the recycling pool.

Under these experimental conditions, I observed a substantial increase in spontaneous SV fusion, coupled to enhanced endocytosis, and a concomitant decrease in evoked neurotransmission and vesicle recycling. Differential regulation of evoked and spontaneous recycling is consistent with earlier findings that spontaneously fusing SVs may be distinct from those that fuse in response to presynaptic action potentials (Sara et al., 2005). Although the mechanisms underlying spontaneous fusion are not well understood, these observations suggest that synaptic cholesterol is a crucial component of the machinery that prevents spontaneous fusion of SVs at rest.

2.4 Methods

2.4.1 Cell culture

The hippocampus was dissected and dissociated from postnatal day 0–3 (P0–3) Sprague-Dawley rats as previously described in Kavalali et al. (1999). Rats were rapidly killed by decapitation after sedation by chilling on an ice-cold metal plate. Dissociated cells were plated on zero thickness 12mm glass coverslips and stored at 37°C with 5% CO_2 in a humidified incubator. Synaptobrevin-2-deficient dissociated hippocampal cultures (courtesy of Dr. Thomas C. Südhof) were prepared following previously published protocols (Schoch et al. 2001). Banker-style glia-free hippocampal cultures were prepared from hippocampi from embryonic day 18 (E18) Sprague-Dawley rats following published protocols (Goslin et al. 1998).

2.4.2 Electrophysiology

A modified Tyrode's solution was used for all experiments (except where noted otherwise) that contained (mM): 140 NaCl, 4 KCl, 2 $MgCl_2.6H_2O$, 10 glucose, 10 HEPES and 2 $CaCl_2$ (pH 7.4, osmolarity 300 mosmol l^{-1}). Pyramidal cells were whole-cell voltage clamped at –70 mV with borosilicate glass electrodes (3–5 MΩ). Electrode solutions contained (mM): 105 cesium methanesulphonate, 10 CsCl, 5 NaCl, 10 Hepes, 20 TEA.Cl hydrate, 4 Mg-ATP, 0.3 GTP, 0.6 EGTA and 10 Lidocaine N-ethyl bromide, sodium-channel blocker (QX-314). For spontaneous mEPSCs, recordings were performed in the modified Tyrode's solution containing 1 μM tetrodotoxin (TTX) and 50 μM picrotoxin (PTX). For Ca^{2+}-buffered spontaneous mEPSCs recordings, cells were incubated for 30 min with 1 μM BAPTA-AM in Ca^{2+}-free modified Tyrode's solution before recording mEPSCs in a Ca2+-free modified Tyrode's solution containing 1 μM TTX and 50 μM PTX. For ionomycin experiments, mEPSCs were recorded from treated cultures for at least 2 min before perfusing an ionomycin solution for 3 min

followed the removal of ionomycin by washing with the spontaneous mEPSC solution to prevent excessive insertion of the ionophore. The ionomycin solution consisted of the modified Tyrode's solution containing 1 μM ionomycin, 1 μM TTX and 50 μM PTX. Sucrose recordings were performed by infusing Tyrode's solution containing 500mm sucrose and 1 μM TTX with 50 μM PTX for 30 seconds. Evoked response experiments were performed using field stimulation with platinum electrodes at 20 mA for 1 ms per action potential in the Tyrode's solution containing 50 μm PTX.

2.4.3 Methyl-β-cyclodextrin (MCD) treatment

Elevated K^+ Tyrode solution used for MCD treatments contained (mM): 106 NaCl, 20 KCl, 2 $MgCl_2.6H_2O$, 10 glucose, 10 Hepes, 2 $CaCl_2$ (pH 7.4, osmolarity 280 mosmol l^{-1}), and 15 mM MCD (Sigma; approximately 20 $mgml^{-1}$; average methyl substitution, 10.5–14.7) with 10 μM NBQX (2,3-dioxo-6-nitro-1,2,3,4-tetrahydrobenzo[f]quinoxaline-7-sulphonamide) and 50 μM AP5 (dl-2-amino-5-phosphonovaleric acid). NBQX and AP5 were added to these solutions to prevent recurrent activity and toxicity due to excessive glutamate signaling during the treatments. For 20 mm K^+ alone treatments, cultures were incubated in an elevated K^+ Tyrode's solution containing (mM): 126 NaCl, 20 KCl, 2 $MgCl_2.6H_2O$, 10 glucose, 10 Hepes, 2 $CaCl_2$ (pH 7.4, osmolarity 300 mosmol l^{-1}) with 10 μM NBQX and 50 μM AP5. For MCD alone treatments, cultures were incubated in a Tyrode's solution containing (mM): 131 NaCl, 4 KCl, 2 $MgCl_2.6H_2O$, 10 glucose, 10 Hepes, 2 $CaCl_2$ (pH 7.4, osmolarity 280 mosmol l^{-1}) with 15 mM MCD, 1 μm TTX, 10 μM NBQX and 50 μM AP5. Hippocampal cultures (10–15 days in vitro, DIV) were incubated for 30 min in the treatment solution at room temperature (22–25°C). After treatment, the cells were washed thoroughly, and then experiments were performed.

2.4.4 Cholesterol addition

In order to produce MCD: cholesterol complexes (molar ratio, 9.78 : 1), a 5% MCD solution was heated to 80°C and 30 mg of cholesterol dissolved in 9 ml of chloroform: methanol (1:2) was added drop-wise until all of the solution was dissolved. The solution was crystallized and re-dissolved in 5 ml of distilled water and stored at –20°C (adapted from (Klein et al., 1995)). For cholesterol addition, cells were incubated at room temperature for 1 hour in 0.61mM of complexed cholesterol (about 6mM MCD saturated with cholesterol) with 10 μM NBQX, and 50 μM AP5 in either a 20 mm K^+ Tyrode's solution (depolarization) or 4 mm K^+ Tyrode's solution with 1 μM TTX (no depolarization). The solution was thoroughly washed away and experiments were performed.

2.4.5 Filipin staining

Cultures were fixed with 4% paraformaldehyde (ice-cold) for 30 min and incubated overnight with filipin III, 0.125 mg ml^{-1} (diluted from 0.4 mg ml^{-1} DMSO :H_2O (1: 4), Sigma). Coverslips were thoroughly washed and mounted. Images were taken with a confocal microscope (Nikon D-Eclipse C1) and analyzed using MetaFluor software (Universal Imaging Corp., Downingtown, PA, USA). At least three coverslips (n =3) were imaged, using five images per coverslip.

2.4.6 Trypan blue staining

After MCD treatments, cultures were washed for 10 min with modified Tyrode's solution. Then a 0.4% Trypan Blue solution (Sigma) was added to the cells at a final concentration of 0.2% (200 μl modified Tyrode's solution: 200 μl Trypan Blue 0.4%) for 10 min. Cells were washed again for 10 min and DIC images (at least 5 per coverslip) were acquired with a CCD camera (Roper Scientific, Trenton, NJ, USA) under bright field illumination. To calculate the per cent of viable neurons, the number of blue (non-viable) and non-blue (viable) cells in a 0.01mm2 region were counted, and the number of viable neurons were divided by

the total number of neurons per area (×100). Then the values for the areas of one coverslip were averaged.

2.4.7 Electron microscopy

For high K^+ HRP uptake, treated cells were incubated with horseradish peroxidase (10 mg ml^{-1} HRP, Sigma) for 2 min in a modified Tyrode's solution with 47mm K^+, 10 μM NBQX and 50 μM AP5, then washed twice with buffer. The cells were fixed with 2% glutaraldehyde in 0.1 M sodium phosphate buffer, pH 7.4 at 37°C then washed with

Tris-Cl (100 mM, pH7.4). The cells were then incubated with 3,3'-diaminobenzidine (0.1%DAB, Sigma) in Tris-Cl buffer and H_2O_2 (0.02%) for 15 min. After washing with distilled water, cells were incubated in1%OsO_4 for 30 min at room temperature then stained en bloc with 2% aqueous uranyl acetate for 15 min, dehydrated in ethanol, and embedded in Poly/Bed 812, polysciences Inc, Warrington, PA, USA for 24 hours. Sections (60 nm) were post-stained with uranyl acetate and lead citrate and viewed with JEOL1200 EX transmission microscope. For the spontaneous HRP uptake, the procedure was the same as above except that the cells were treated with 25 mg ml^{-1} HRP for 15 min in a modified Tyrode's solution with 1 μM TTX, 10 μM NBQX and 50 μM AP5. For structural analysis, rat hippocampal cultures were treated as described except cells were not incubated with HRP or DAB solutions.

2.4.8 Cholesterol oxidase treatment

Hippocampal cultures (10-21 days in vitro, DIV) were treated with cholesterol oxidase (4U/ml, *Pseudomonas fluorescens*, Sigma) for 30 minutes at 37°C in cell culture medium with either 1 μM TTX or 20 mM K^+. After treatment, the cells were washed thoroughly and then experiments were performed.

CHAPTER 3: ALTERING HMG-COA REDUCTASE ACTIVITY

3.1 Background

To investigate the role of cholesterol homeostasis in synaptic function, I measured the evoked and spontaneous neurotransmission in dissociated hippocampal cultures after inhibiting cholesterol synthesis. By inhibiting HMG-CoA reductase, the rate limiting enzyme of cholesterol biosynthesis, I reduced the total neuronal cholesterol to determine if this would result in the same decreased evoked and increased spontaneous neurotransmitter release seen after acute manipulation of membrane cholesterol (Chapter 2).

3.2 Results

3.2.1 Manipulation of HMG-CoA reductase activity with an exogenous inhibitor

In the next set of experiments, I asked whether impairing cholesterol synthesis in neurons would mimic the results obtained after acute depletion of membrane cholesterol with MCD. For this purpose, I used mevastatin, a 'statin' compound that inhibits HMG-CoA reductase (the rate-limiting enzyme in cholesterol synthesis) in a cholesterol-free medium. To quantify the relative reduction in cholesterol, I treated cells with mevastatin for 6 hours and then labelled with filipin. The level of filipin fluorescence was reduced by 36. 0± 0.1% compared to cells that were not treated with mevastatin (No mevastatin n=4, Mevastatin n=3, $p<0.001$).

Treatment with mevastatin for 6 hours significantly decreased the hypertonic sucrose response and the field-stimulation evoked EPSC amplitude 80 and 70% (respectively) compared to non-treated cultures (Fig. 3.2.1.1 A-D; hypertonic sucrose: No mevastatin n=7, Mevastatin n=12, $p<0.01$; EPSCs: No mevastatin n=5, Mevastatin n=5, $p<0.05$). Interestingly, after mevastatin treatment, I observed the same upward trend in the frequency of the spontaneous events (Fig. 3.2.1.2 A-B; 3-fold; No mevastatin n=24, Mevastatin n=13, $p<0.001$) with no effect on the amplitude of the events, indicating no significant change in postsynaptic receptors by this manipulation (Fig. 3.2.1.2 A, C). Both the decreased evoked responses and increased frequency after mevastatin treatment were reversed by the addition of cholesterol from MCD: cholesterol complexes. After cholesterol addition, the filipin fluorescence was increased 1.4-fold compared to mevastatin-treated cultures, which is 11.1 ± 0.1% less than the fluorescence levels in non-treated cells (No mevastatin n=4, Mevastatin n=3, Mevastatin + cholesterol n=3, $p<0.05$).

The mevastatin treatments were performed in the presence of 0.25 mM mevalonate, which is the product of the reaction that mevastatin inhibits. Mevalonate is the precursor molecule for the synthesis of cholesterol and isoprenoids. This concentration of mevalonate during mevastatin treatment can maintain the level of isoprenoids, while not generating sufficient levels of cholesterol (Alberts et al., 1980, Brown and Goldstein, 1980, Goldstein and

Brown, 1990, Simons et al., 1998). To rule out the effect of mevalonate on evoked and spontaneous neurotransmission, cultures were treated with mevastatin in the presence or absence of mevalonate and the lack of mevalonate did not result in a loss of the effect seen with mevastatin and mevalonate (data not shown).

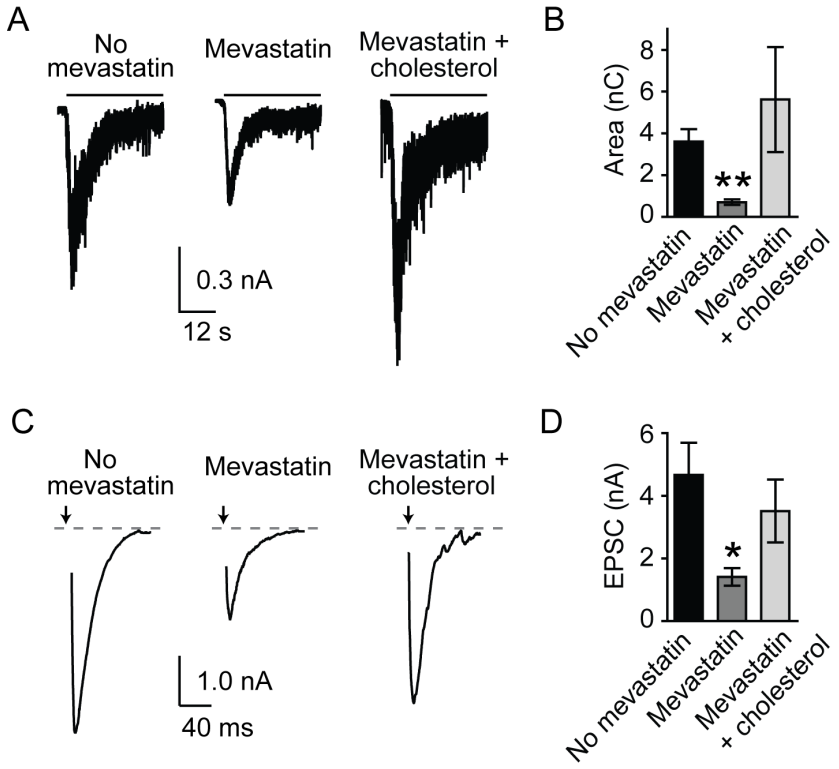

Figure 3.2.1.1 Inhibition of cholesterol synthesis with mevastatin mimics the effect of acute depletion on evoked neurotransmitter release

(A-B) Hypertonic sucrose stimulation after 6-hour mevastatin treatment (A) Sample traces (B) Summary graph showing that the average charge transfer during the first 10 seconds of the 30-second sucrose response is decreased 5-fold after treatment with mevastatin for 6 hours compared to non-treated cultures. The addition of cholesterol after mevastatin treatment rescued the depleted hypertonic sucrose responses to values not significantly different from non-treated cultures. (Horizontal bar represents the presence of hypertonic sucrose, at least 2 cultures, No mevastatin=7, Mevastatin n=12, Mevastatin + cholesterol n=3)

(C-D) Field stimulation evoked responses after 6-hour mevastatin treatment (C) Sample traces (D) Summary graph depicting a 3.4-fold reduction in the average evoked EPSC amplitude for cultures treated with mevastatin compared to non-treated neurons. The addition of cholesterol after mevastatin treatment rescued the reduced EPSC amplitudes to values not significantly different from non-treated cultures (Arrow represents timing of the stimulation, at least 2 cultures, No mevastatin=5, Mevastatin n=5, Mevastatin + cholesterol n=4).
Error bars represent the SEM (*p<0.05, **p<<0.001).

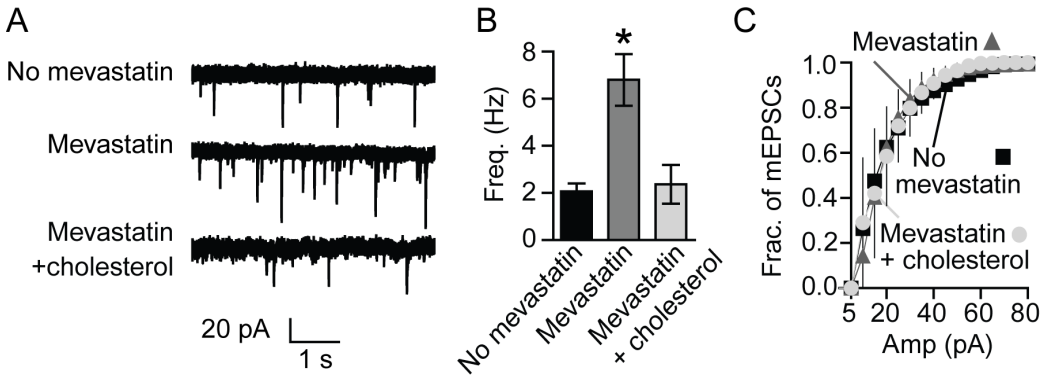

Figure 3.2.1.2 Effect of cholesterol synthesis inhibition on spontaneous neurotransmission mimics acute cholesterol depletion

(A) Sample traces of mEPSCs recordings. (B) Summary graph shows a 3.2-fold increase in the frequency of mEPSCs for cultures treated for 6 hours with mevastatin compared to untreated neurons. The increased frequency was reduced to non-treated frequency levels after incubation with MCD: cholesterol complexes. (C) The distributions of mEPSC amplitudes were not affected by these treatments as determined by the K-S test ($p>0.0001$)
Error bars represent the SEM (*p<<0.001; at least 2 cultures, No mevastatin=24, Mevastatin n=13, Mevastatin + cholesterol n=4).

3.2.2 Endogenous inhibition of HMG-CoA Reductase activity

Next, I wanted to inhibit cholesterol synthesis through an endogenous pathway, which will help demonstrate the effects observed with mevastatin were not due to non-specific interactions. AMP levels rise within a cell when the energy level is low. Increased levels of AMP activate the AMP-activated kinase

(AMPK) which in turn phosphorylates HMG-CoA reductase, thus inhibiting activity of this enzyme (Omkumar et al., 1994, Istvan et al., 2000).Therefore, I incubated wild-type rat hippocampal neurons with 0.5 mM AICAR for 2 hours at 37°C (5-aminoimidazole-4-carboxamide riboside), a potent activator of AMPK, resulting in the endogenous inhibition of HMG-CoA reductase, which then diminishes the cholesterol levels within the cell. After inhibiting cholesterol synthesis using AICAR activation of AMPK, I measured spontaneous fusion events as well as the responses to both hypertonic sucrose and field potential stimulation. Compared to non-treated neurons, I found decreased responses to both hypertonic sucrose application (1.8-fold; Fig. 3.2.2.1 A-B: No AICAR 3.8±0.6 nC, AICAR 2.1±0.1 nC; n=3; $p<0.05$) and field potential stimulation (2.4-fold; Fig. 3.2.2.1 C-D: No AICAR 2.6±0.4 nA, AICAR 1.1±0.3 nA; n=3; $p<0.04$) after AICAR treatment. Moreover, the frequency of mEPSCs also increased 3.4-fold in AICAR-treated neurons compared to non-treated neurons (Fig. 3.2.2.2 A-B: No AICAR 2.0±0.2 Hz, AICAR 6.7±1.4 Hz; n=3; $p<0.03$) while not affecting the distribution of the mEPSC amplitudes. Thus, the attenuated evoked neurotransmission and enhanced spontaneous neurotransmitter release after inhibiting cholesterol synthesis with AICAR treatment argue that the effect of mevastatin treatment on synaptic transmission is not a result of non-specific interactions.

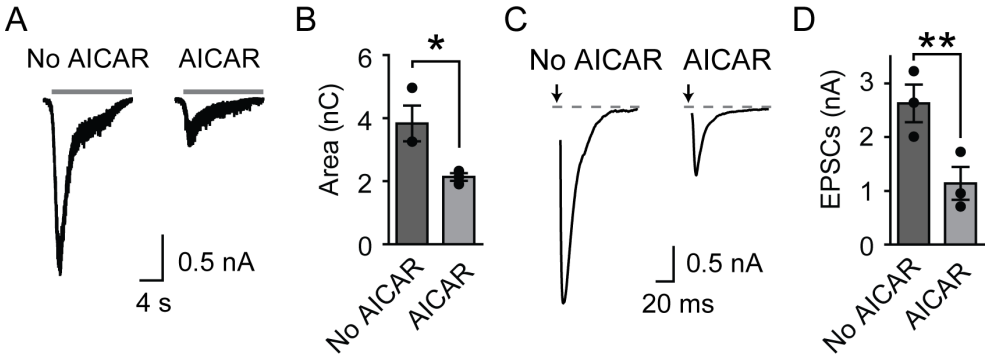

Figure 3.2.2.1 Inhibition of rate-limiting enzymes by a protein kinase inhibitor (AICAR) decreases evoked neurotransmitter release

(A-B)Hypertonic sucrose responses with and without AICAR treatment (A) Representative traces (D) Summary graph depicting 1.8-fold decrease in the average charge of the first 10 s of the 30 s application. (black bars represent the presence of hypertonic sucrose)
(C-D) Field potential stimulated EPSCs with and without AICAR treatment. (C) Representative traces of EPSCs from AICAR treated cultures. (D) Summary chart showing a 2.4-fold decrease in the average maximum EPSC in AICAR-treated cultures compared to non-treated cultures. (Arrows indicate the initiation of the field potential stimulation)
Error bars represent the SEM. (*p<0.05, ** p<0.03; n=3)

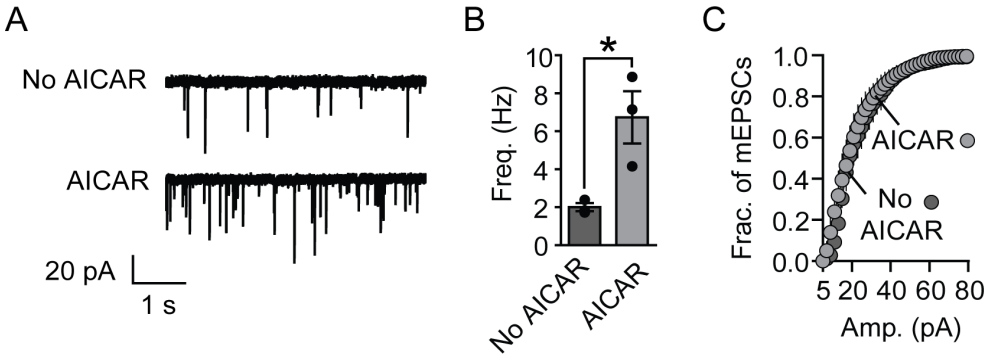

Figure 3.2.2.2 Inhibition of rate-limiting enzymes by a protein kinase inhibitor (AICAR) increases spontaneous neurotransmitter release

mEPSC recordings with and without AICAR incubation (A) Representative traces of mEPSCs (B) Summary plot of the average mEPSC frequency depicting a 3.4-fold increase in AICAR-treated neurons. (C) Distribution of the mEPSC amplitudes showing no significant differences between groups.
Error bars represent the SEM. (*p<0.03; n=3)

3.3 Summary

Acute manipulations of neuronal cholesterol by direct removal or oxidation of membrane cholesterol modified synaptic transmission resulting in inefficient action potential-dependent vesicle fusion and endocytosis while augmenting spontaneous neurotransmission. Altering the concentration of cholesterol through exogenous and endogenous inhibition of HMG-CoA reductase activity demonstrate that a reduction in the total neuronal cholesterol level also provokes defective neurotransmitter release. This supports the proposal that cholesterol provides a balance between these two forms of synaptic transmission.

3.4 Methods

3.4.1 Cell culture

The hippocampus was dissected and dissociated from postnatal day 0–3 (P0–3) Sprague-Dawley rats as previously described in Kavalali et al. (1999). Rats were rapidly killed by decapitation after sedation by chilling on an ice-cold metal plate. Dissociated cells were plated on zero thickness 12mm glass coverslips and stored at 37°C with 5% CO2 in a humidified incubator.

3.4.2 Electrophysiology

A modified Tyrode's solution was used for all experiments (except where noted otherwise) that contained (mM): 140 NaCl, 4 KCl, 2 $MgCl_2.6H_2O$, 10 glucose, 10 Hepes and 2 $CaCl_2$ (pH 7.4, osmolarity 300 mosmol l^{-1}). Pyramidal cells were whole-cell voltage clamped at –70 mV with borosilicate glass electrodes (3–5 MΩ). Electrode solutions contained (mM): 105 cesium methanesulphonate, 10 CsCl, 5 NaCl, 10 Hepes, 20 TEA.Cl hydrate, 4 Mg-ATP, 0.3 GTP, 0.6 EGTA and 10 Lidocaine N-ethyl bromide, sodium-channel blocker (QX-314). For

spontaneous mEPSCs, recordings were performed in the modified Tyrode's solution containing 1 μM tetrodotoxin (TTX) and 50 μM picrotoxin (PTX). Sucrose recordings were performed by infusing Tyrode's solution containing 500mm sucrose and 1 μM TTX with 50 μM PTX for 30 seconds. Evoked measurements were obtained by recording EPSC response after applying field potentials with platinum electrodes at 20 mA for 1 ms per action potential in the Tyrode's solution containing 50 μm PTX.

3.4.3 Mevastatin treatment

Hippocampal cultures (12–15 DIV) were treated with mevastatin (4 μM,Sigma) and mevalonate (0.25mM, Sigma) in a serum-free medium supplemented with double B-27 supplement (Invitrogen) at 37°C for 6 hours in a humidified incubator with 5% CO_2.

3.4.4 AICAR treatment

Hippocampal cultures (12–15 DIV) were treated with AICAR (5-Aminoimidazole-4-carboxaide 1-beta-D-ribofuranoside, 0.5 mM) at 37°C for 2 hours in a humidified incubator with 5% CO_2.

3.4.5 Cholesterol addition

In order to produce MCD: cholesterol complexes (molar ratio, 9.78 : 1), a 5% MCD solution was heated to 80°C and 30 mg of cholesterol dissolved in 9 ml of chloroform: methanol (1 : 2) was added drop-wise until all of the solution was dissolved. The solution was crystallized and re-dissolved in 5 ml of distilled water and stored at –20°C (adapted from (Klein et al., 1995)). For cholesterol addition, cells were incubated at room temperature for 1 hour in 0.61mM of complexed cholesterol (about 6mM MCD saturated with cholesterol) with 10 μM NBQX, and 50 μM AP5 in either a 20 mm K^+ Tyrode's solution (depolarization) or 4 mm K^+

Tyrode's solution with 1 μM TTX (no depolarization). The solution was thoroughly washed away and experiments were performed.

3.4.6 Filipin staining

Cultures were fixed with 4% paraformaldehyde (ice-cold) for 30 min and incubated overnight with filipin III, 0.125 mg ml^{-1} (diluted from 0.4 mg ml^{-1} DMSO :H_2O (1: 4), Sigma). Coverslips were thoroughly washed and mounted. Images were taken with a confocal microscope (Nikon D-Eclipse C1) and analyzed using MetaFluor software (Universal Imaging Corp., Downingtown, PA, USA). At least three coverslips (n =3) were imaged, using five images per coverslip.

3.4.7 Trypan blue staining

After MCD treatments, cultures were washed for 10 min with modified Tyrode's solution. Then a 0.4% Trypan Blue solution (Sigma) was added to the cells at a final concentration of 0.2% (200 μl modified Tyrode's solution: 200 μl Trypan Blue 0.4%) for 10 min. Cells were washed again for 10 min and DIC images (at least 5 per coverslip) were acquired with a CCD camera (Roper Scientific, Trenton, NJ, USA) under bright field illumination. To calculate the per cent of viable neurons, the number of blue (non-viable) and non-blue (viable) cells in a 0.01mm^2 region were counted, and the number of viable neurons were divided by the total number of neurons per area (×100). Then the values for the areas of one coverslip were averaged.

CHAPTER 4: NIEMANN-PICK TYPE C1 DEFICIENCY

4.1 Background

Acute decreases in cholesterol over minutes or hours demonstrated an important role for cholesterol in synaptic transmission; however, these experiments reduced total neuronal cholesterol. To further understand the dynamics of cholesterol in the synapse specifically, I examined the neurons obtained from a line of mice with a mutation in the Niemann-Pick type C1 (NPC1) gene, which experience a defect in cholesterol trafficking resulting in decreased cholesterol at distal axons (Karten et al., 2002). In humans, the NPC1 disease presents with a wide variety of symptoms at ages from < one month to > 20 years. Hepatic, neurological and even psychiatric abnormalities occur in patients afflicted with the NPC1 disease. The most common age of diagnosis is between childhood and adolescent and this group can suffer from liver disease, ataxia, seizures, and even a decline in school performance (Vanier and Millat, 2003). Most times this disease results from a mutation in the NPC1 gene resulting in the loss of function of the NPC1 protein (Loftus et al., 1997). Ultimately the loss of NPC1 function results in the disruption of normal trafficking of cholesterol from the late endosome/ lysosome pathway resulting in the accumulation of cholesterol within these organelles in all cells of the body (Kobayashi et al., 1999, Vanier and Millat, 2003).

The NPC1 protein is an integral membrane protein of 1278 amino acids with 13 transmembrane domains and contains a putative sterol sensing domain (Carstea et al., 1997, Davies and Ioannou, 2000).There are several mouse models of this disease, one of which is a model with a complete loss of the NPC1 protein due to a mutation which truncates the protein resulting in the loss of the sterol sensing domain as well as 11 of the 13 transmembrane domains (BALB/cNctr-NPC1^{m1N}/J) (Loftus et al., 1997). As a result of this loss of function, NPC1-deficient mice present with weight loss and motor deficits and die within two to four months of age (Mukherjee and Maxfield, 2004).

In the brain, all regions express the NPC1protein; however, higher expression occurs in the cerebellum and brainstem (Prasad et al., 2000). At around 3 months, neuronal death is obvious in the cerebellum, prefrontal cortex and thalamus in NPC1-deficient mice (about 96, 28, and 20%, respectively). The loss of Purkinje cells in the cerebellum strongly correlates with the onset of ataxia (Li et al., 2005). Cholesterol levels in the whole brain are only slightly decreased in the NPC1 mutants (Li et al., 2005), but the cellular distribution of the remaining cholesterol is altered with an accumulation of cholesterol in the soma and a loss of cholesterol at distal axons (Karten et al., 2002, 2003) which may contribute to defective vesicle trafficking in presynaptic nerve terminals (Karten et al., 2006).

In the following experiments, I examine the excitatory and inhibitory neurotransmission in NPC1-deficient hippocampal and cortical neurons and those from wild-type littermates to gain insight into the repercussions of decreased synaptic cholesterol.

4.2 Results

4.2.1 Synaptic Dysfunction

To measure synaptic transmission in neurons with a cholesterol trafficking defect due to the lack of NPC1 protein function, I first measured the responses to hypertonic sucrose application and field potential stimulated excitatory postsynaptic currents (EPSCs). The charge of the first ten of the thirty-second hypertonic sucrose application was 65% less that the responses measured from wild-type littermate neurons(Fig. 4.2.1.1 A-B, WT: 3.9±0.7 nC, n=10; NPC1:1.3±0.3 nC, n=9; $p<0.01$).NPC1-deficient hippocampal neurons experienced a 77% reduction in the average EPSC amplitude compared to similar recordings from wild-type cultures (Fig. 4.2.1.1 C-D, WT: 3.2±0.5 nA, n=4; NPC1: 0.7±0.1 nA, n=4; $p<0.05$).The lack of NPC1 also resulted in a significant increase in the frequency of miniature EPSCs (mEPSCs) with no effect on the amplitude of these events (Fig. 4.2.1.2A-C, 2.4-fold; WT: 1.9±0.3 Hz, n=16; NPC1: 4.6±0.8 Hz, n=17; $p<0.004$). Because the NPC1-deficient phenotype might be altered by culturing the neurons, another member of the lab, Mert

Ertunc, measured the rate of spontaneous events in hippocampal slices obtained from the same mice and found a similar increase (3.4-fold) in the frequency of mEPSCs (WT: 0.6±0.1 Hz n=6, NPC1: 2.1±0.4 Hz , n=5; $p<0.005$). The addition of cholesterol to the NPC1-deficient hippocampal cultures rescued the evoked responses and the frequency of spontaneous mEPSCs to a level not significantly different from the wild-type values (Fig. 4.2.1.1&2).

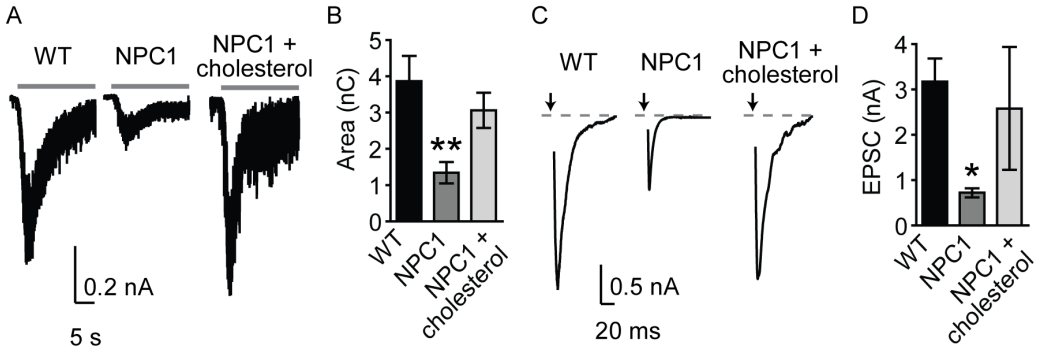

Figure 4.2.1.1 Altered cholesterol trafficking in Niemann Pick C1-deficient mice causes abnormalities in neurotransmission mimicking the effect of acute cholesterol depletion

(A-B) Hypertonic sucrose stimulation (A) Sample traces (B) Summary graph showing a 3-fold decrease in the average charge transfer during the first 10 seconds of the 30-second sucrose response in NPC1 neurons compared to WT neurons. The incubation of NPC1 neurons with MCD: cholesterol complexes resulted in an increased response to hypertonic sucrose that was not significantly different from WT neurons. (Horizontal bar represents the presence of hypertonic sucrose, 4 cultures, WT n=10, NPC1 n=9, NPC1 + cholesterol n=5).
(C-D) Field stimulation evoked responses (C) Sample traces (D) Summary chart depicting a 4.6-fold decrease in the average evoked EPSC amplitude for NPC1 neurons compared to WT neurons. The addition of cholesterol to NPC1 neurons rescued the reduced EPSCs to values not significantly different from WT cultures (Arrow represents timing of the stimulation, 4 cultures, WT n=4, NPC1 n=4, NPC1 + cholesterol n=4). Error bars represent the SEM (*$p<0.03$, **$p<0.01$).

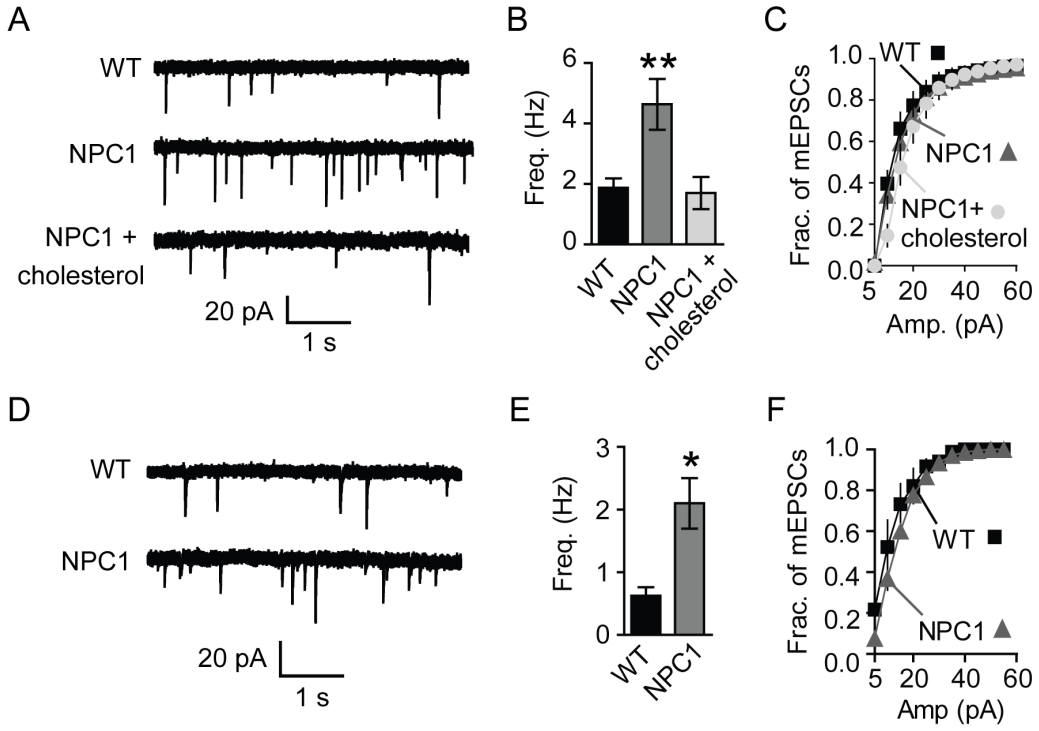

Figure 4.2.1.2 Altered cholesterol trafficking in NPC1-deficient mice causes abnormalities in neurotransmission mimicking the effect of acute cholesterol depletion.

(A-C) mEPSCs recordings from cultured NPC1 and WT neurons (A) Sample traces (B) Summary graph shows a 2.5-fold increase in the frequency of mEPSCs for NPC1 neurons compared to WT neurons. The increased frequency in NPC1 neurons was reduced to the WT frequency levels after incubation with MCD: cholesterol complexes. (C) The distributions of mEPSC amplitudes were not different under all conditions as determined by the K-S test ($p>0.0001$) (4 cultures, WT n=16, NPC1 n=17 NPC1 + cholesterol n=9). (D-F) mEPSC recordings from NPC1 and WT hippocampal slices (D) Sample mEPSC traces (E) Summary graph of the frequency of mEPSCs showing a 3.4-fold increase in the frequency of mEPSCs in the NPC1 neurons. (F) The distributions of mEPSC amplitudes were not different as determined by the K-S test ($p>0.0001$) (WT n=6, NPC1 n=5).
Error bars represent the SEM (*$p<0.005$, ** $p<0.004$).

A number of studies examine the neuronal phenotypes of this mutation in cortical neurons (in particular (Karten et al., 2002, Karten et al., 2006)), so I wanted to analyze the effect of the mutation in both the hippocampus and the cortex. In cortical neurons, the affect of the NPC1 mutation resulted in a 60% increase in the frequency of mEPSC, while not affecting the event amplitudes (Fig. 4.2.1.3, A-C;WT: 2.1±0.3 Hz, n=13; NPC1: 5.5±0.8 Hz, n=11; p<<0.001) as well as a 54% reduction in EPSCs amplitudes (Fig. 4.2.1.3 D-E, WT: 3.7±0.5 nA, n=13; NPC1: 1.7±0.3 nA, n=13; p<0.02), which reflects the changes seen in hippocampal neurons (Figs. 4.2.1.1, 2).

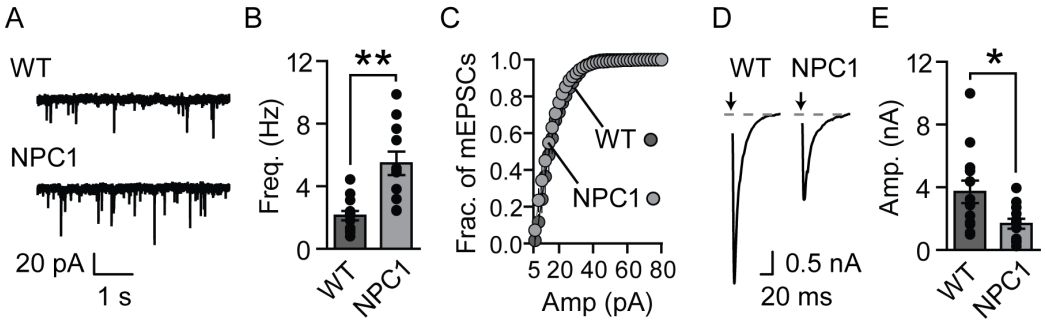

Figure 4.2.1.3 Enhanced spontaneous fusion and decreased amplitudes of EPSCs in cortical excitatory neurotransmission

(A-C) mEPSCs recordings from cultured cortical NPC1 and WT neurons (A) Sample traces (B) Summary chart showing a 2.6-fold increase in the frequency of mEPSCs for NPC1 neurons compared to WT neurons. (C) The distributions of mEPSC amplitudes were not different as determined by the K-S test (p>0.0001) (2 cultures, 2 cultures, WT n=13, NPC1 n=11)

(D-E) Field stimulation evoked responses from cortical neuron cultures of NPC1-deficient and wild-type littermate mice (D) Sample traces (E) Summary plot depicting a 2.2-fold decrease in the average evoked EPSC amplitude for NPC1 neurons compared to WT neurons. (Arrow represents timing of the stimulation, 2 cultures, WT n=13, NPC1 n=13).

Error bars represent the SEM (*p<0.02, **p<<0.001).

The consistency of the findings from dissociated hippocampal and cortical neuronal cultures and intact hippocampal slices from the NPC1-deficient mice argues for a crucial role of neuronal cholesterol homeostasis in setting the balance between evoked and spontaneous fusion. Furthermore, this fundamental abnormality in synaptic transmission can be detected irrespective of whether cholesterol levels are altered acutely (Chapters 2 & 3; depletion or synthesis inhibition) or chronically (NPC1 mutants).

4.2.2 Inhibitory Neurotransmission

After acute cholesterol depletion with methyl-β-cyclodextrin, I observed attenuated responses to field potential stimulation as well as enhanced spontaneous vesicle fusion in both excitatory and inhibitory neurotransmission (Chapter 2). When compared to the effect of acute cholesterol extraction, the excitatory synapses in neurons from NPC1-deficient mice experience the same reciprocal changes in spontaneous and evoked synaptic transmission (Fig. 4.2.1.1, 2). To determine whether the NPC1-deficient neurons also mimic the effect of cholesterol depletion on inhibitory neurotransmission, I measured the inhibitory postsynaptic currents (IPSCs) and miniature IPSC (mIPSC) in both hippocampal and cortical neurons. I observed decreases in the field potential stimulated IPSCs in both NPC1-deficient hippocampal (Fig. 4.2.2D-E ; 4.2-fold: WT 2.5±0.6 nA, n=13; NPC1 0.6±0.1nA, n=9; $p<0.01$) and cortical neurons (Fig. 4.2.2 I-J; 2.6-

fold: WT 2.1±0.2 nA, n=12; NPC1 0.8±0.2 nA, n=8; $p<0.004$); however, the frequency of mIPSCs profoundly decreased 2-fold in both hippocampal (Fig. 4.2.2 A-C; WT 3.7±0.8 Hz, n=5; NPC1 1.8±0.2 Hz, n=10; $p<0.002$) and cortical NPC1-deficient neurons (Fig. 4.2.2 F-H; WT 3.6±0.5 Hz, n=15; NPC1 1.7±0.3 Hz, n=11; $p<0.01$), which is contrary to the effect of cholesterol extraction on mIPSC frequency (Fig. 2.2.2.1) and inconsistent with the increases in mEPSC frequency in both NPC1-deficient (Fig. 4.2.1.2) and cholesterol depleted neurons (Fig. 2.2.1.2.1, 3.2.1.2, 3.2.2.2).

Reduced spontaneous fusion is indicative of either decreased levels of postsynaptic receptors, reduced efficacy of spontaneous vesicle recycling within a synapse or decreased number of synapses onto the postsynaptic neuron. In my experiments, I observed no change in the average amplitude of mIPSC events (Figs. 4.2.2 C, H), which suggests that the NPC1-neurons have the same distribution of inhibitory postsynaptic receptors as wild-type neurons. Thus, the decreased frequency of mIPSCs is most likely a result of fewer inhibitory synapses and/or decreased spontaneous release per synapse.

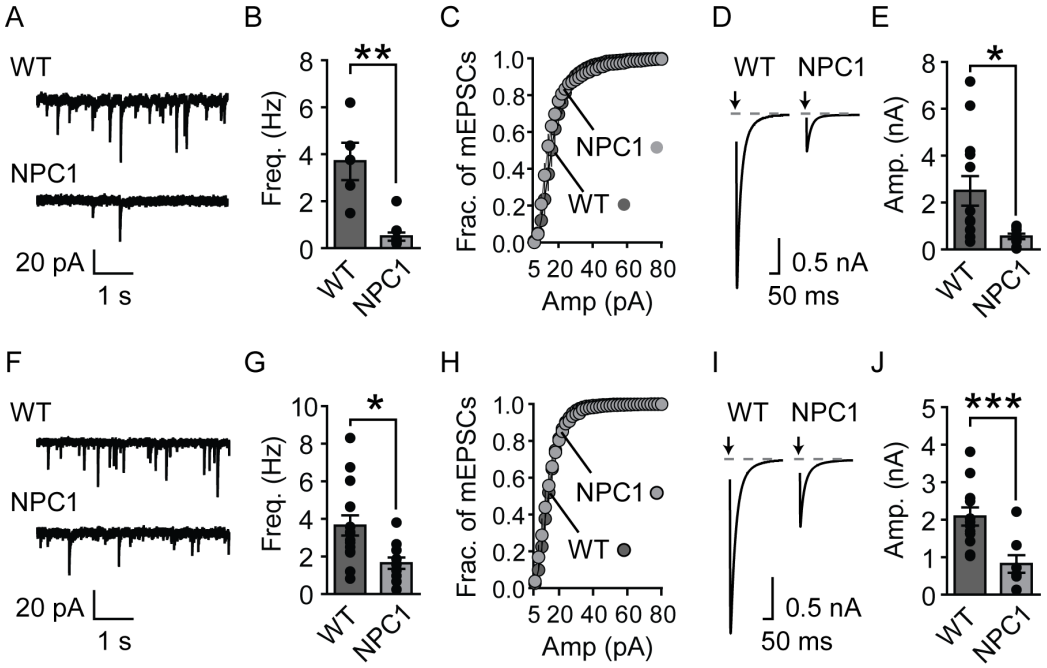

Figure 4.2.2 Attenuated inhibitory neurotransmission in NPC1-deficient neurons

(A-E) Hippocampal neurons; (F-J) Cortical neurons
(A-C, F-H) mIPSCs recordings from cultured hippocampal (A-C) and cortical (F-H) NPC1 and WT neurons (A,F) Sample traces (B,G) Summary chart showing a 2-fold decrease in the frequency of mIPSCs in mutant hippocampal (B) and cortical (G) neurons compared to the wild-type littermate neurons. (C, H) The distributions of mIPSC amplitudes were not different in either neuron type ($p>0.0001$) (2 cultures, Hippocampal: WT n=5, NPC1 n=10; Cortical: WT n=15, NPC1 n=11)
(D-E, I-J) Field potential stimulated IPSC responses from hippocampal (D-E) and cortical *I-J) neuron cultures of NPC1-deficient and wild-type littermate mice (D, I) Sample traces (E, J) Summary plot of the average IPSC amplitude depicting an amplitude decrease of 4.2- and 2.6-fold in NPC1-deficient hippocampal and cortical neurons (respectively) compared to amplitudes of wild-type littermate neurons. (Arrow represents timing of the stimulation, 2 cultures, Hippocampal: WT n=13, NPC1 n=9; Cortical: WT n=12, NPC1 n=8)
Error bars represent the SEM (*$p<0.01$, **$p<0.004$, ***$p<0.002$).

4.2.3 Vesicle Recycling

Central synapses have limited synaptic vesicles and must employ a recovery method for vesicles that exocytose to maintain neurotransmitter release when repeatedly stimulated at higher frequencies. To explore the effect of the NPC1 mutation on vesicle fusion and recycling, I measured the dynamics of neurotransmitter release by employing two different methods. The first involved measuring postsynaptic currents using the whole-cell voltage clamp technique during repetitive stimulation, which gives insight into the availability and reavailability of vesicles during constant stimulation. The other approach utilized the lipophillic fluorescent dye FM1-43 to track recycling vesicles. Upon stimulation, vesicles that fuse and endocytose in the presence of FM1-43 take up the dye and become fluorescent. Whereby, fluorescence uptake and the release upon vesicle re-fusion provide the information about the number of actively fusing vesicles as well as the dynamics of their reuse. Together, these techniques provide valuable insight into synaptic efficiency.

4.2.3.1 Decreased excitatory and normal inhibitory synaptic depression in NPC1-deficient hippocampal neurons

Prior experiments demonstrated that the NPC1-deficit result in a decrease in the magnitude of EPSCs in primary dissociated hippocampal cultures (Figure 4.2.1.1 C-D). To understand whether the NPC1 mutation also affects synaptic

vesicle recycling, I first observed the changes in EPSC amplitudes during a 10 Hz train of field potentials for 80 seconds in NPC1- deficient hippocampal neurons. The lack of NPC1 results in a less pronounced decrease in the release rate of neurotransmitter compared to neurons from wild-type littermates; however, the probability of release is unaffected (Fig. 4.2.3.1.1). Interestingly, the fast and slow decay constants of wild-type 10 Hz depression are 1.4 ± 0.3 and 34.1±5.2 s, respectively, while the NPC1-deficient synaptic depression was best fit by a one-fit decay equation with a time constant (τ) of 47.0±8.1 s (Fig. 4.2.3.1.1C- D). This suggests that the first few vesicles might fuse normally, however the following fusion events occur at a slower pace.

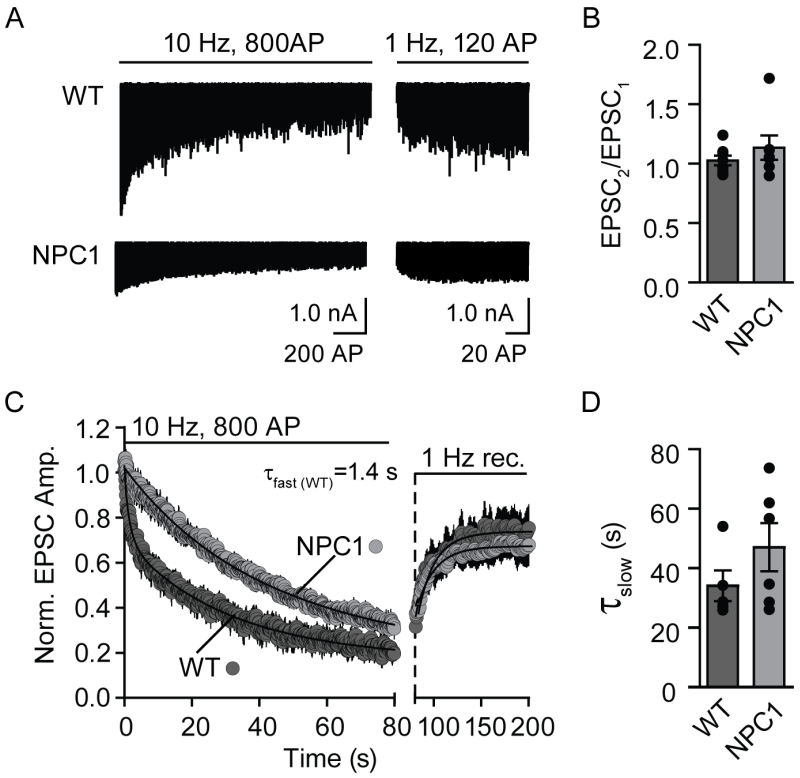

Figure 4.2.3.1.1 Probability of release is unaffected while synaptic depression is attenuated in cultured NPC1-deficient hippocampal neurons.

(A) Representative traces of the EPSCs recorded during a 10 Hz 80s stimulus (left) and recovery measured at 1 Hz for 2 min in NPC1-deficient hippocampal neurons (NPC1) and neurons from wild-type littermates (WT). Note the EPSC amplitudes are significantly less (Fig. 4.2.1.1)
(B) Average ratio of the second EPSC to the first EPSC in a 10 Hz stimulus train showing no change in the probability of vesicle release (P_r).
(C) Plot of the average normalized EPSC magnitude per stimulus during a 10 Hz train followed by the recovery of the responses measured at 1 second intervals depicting a slower depletion in neurotransmitter in NPC1- deficient neurons compared to wild-type depression kinetics.
(D) Summary plot of the average slow rate constant from the 10 Hz WT trace (two-phase decay fit) and the tau from the NPC1 (one-phase decay). The fast component of neurotransmitter release in WT neurons (τ_{WT} fast= 1.4 ± 0.3 s, panel C) is lost in NPC1 neurons, while retaining the slow component.
Error bars represent the SEM (n=7).

Conversely, the synaptic depression at inhibitory synapses of both hippocampal and cortical neurons appeared unaffected despite the reduced amplitude of IPSCs. I found no significant differences in the probability of release or the rate of IPSC amplitude decay during a 10 Hz train of 800 stimuli in NPC1-deficient and wild-type hippocampal neurons. The rate of recovery in NPC1-deficient hippocampal neurons seemed slower but was not significant (Fig. 4.2.3.1.2). I observed a more pronounced deficit in the recovery rate after a 10 second field potential stimulation at 20 Hz in hippocampal neurons lacking NPC1 compared to wild-type without a significant difference in the rate of depression of the IPSC amplitudes (Fig. 4.2.3.1.3 A-D). Cortical neurons behaved similarly, however the defect in the rate of recovery was less dramatic (Fig. 4.2.3.1.3 C-D).

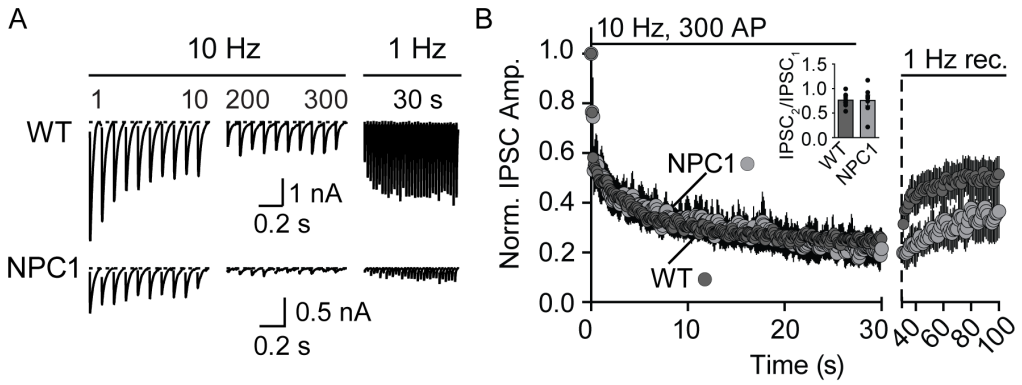

Figure 4.2.3.1.2 Evoked inhibitory neurotransmission decreases without affecting the rate of release during 10 Hz stimulus train in NPC1-deficient hippocampal neurons.

(A) Representative traces of the first and last 10 IPSCs of a 10 Hz 30s stimulus train and the 30s of recovery measured at 1 Hz frequency in NPC1-deficient hippocampal neurons (NPC1) and neurons from wild-type littermates (WT).
(B) Plot of the average normalized IPSC per stimulus during a 10 Hz train followed by the recovery of the responses measured at 1 second intervals demonstrating not

significant difference in the rate of neurotransmitter release during 10 Hz stimulation. Inset: Average ratio of the second IPSC to the first IPSC in a 10Hz stimulus train showing no change in the probability of vesicle release (Pr).
Error bars represent the SEM (n=6).

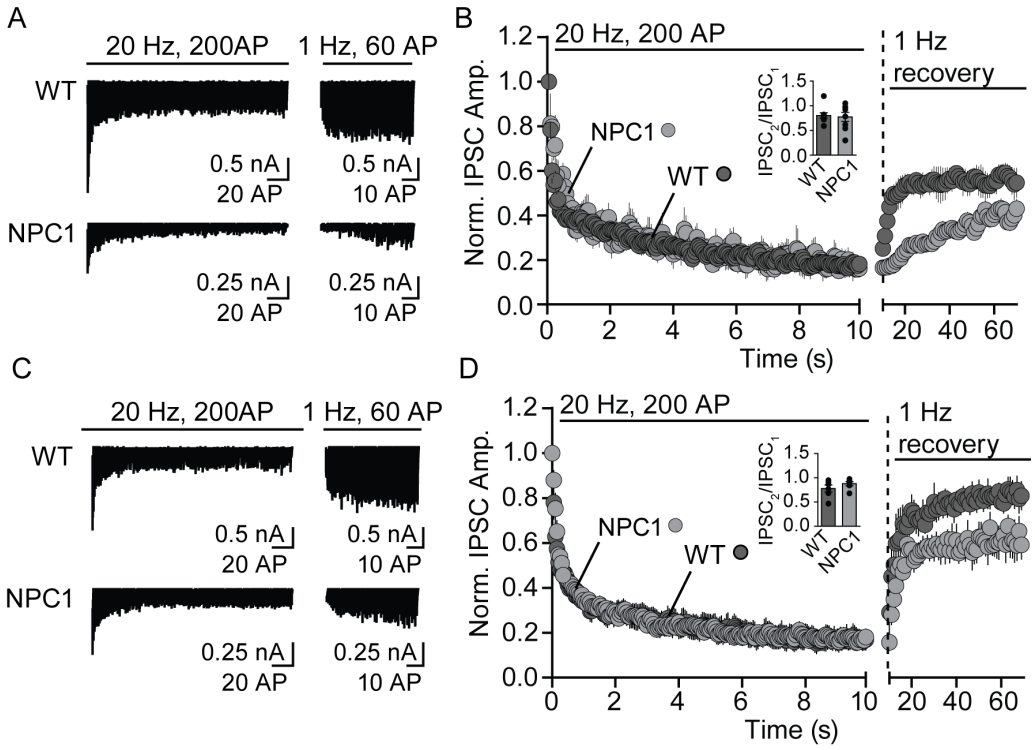

Figure 4.2.3.1.3 20 Hz inhibitory synaptic depression and release probability are unaffected in NPC1-deficient neurons

(A-B) Hippocampal neurons (C-D) Cortical neurons
(A, C) Sample traces recorded during a 20 Hz 200 AP train followed by a sixty second measurement of inhibitory postsynaptic current (IPSC) amplitude recovery in cultured hippocampal (A) and cortical (C) neurons from mutant and wild-type littermate mice.
(B, D) Plot summarizing the averaged IPSC amplitude change during a 20 Hz stimulus train followed by 1 Hz stimulation to measure IPSC amplitude recovery. Both hippocampal (B) and cortical (D) neurons experience no defect in 20Hz synaptic depression or the probability of release , however the recovery from vesicle depletion is slower for both types of neurons.
Error bars represent the SEM. (Hippocampal: WT n=5, NPC1 n=6; Cortical n=5)

4.2.3.2 Recycling of action potential-dependent and –independent synaptic vesicles in NPC1-deficient neurons

In NPC1-deficient neurons, excitatory and inhibitory synapses experience a decrease in the efficacy of evoked synaptic transmission and an increase in spontaneous neurotransmitter release as measured by a population of synaptic input into a postsynaptic neuron. Increased number of synapses and number of vesicles or even enhanced recycling of spontaneously fusing vesicles could account for the augmented spontaneous neurotransmission. Likewise, the attenuated response to stimulation might result from a decreased number of available vesicles, number of synapses or ability for available vesicles to fuse. To gain insight into the contributions of individual synapses, I used the fluorescent marker FM1-43 to label and track the recycling of synaptic vesicles in NPC1-deficient hippocampal neurons.

I began my experiments by exploring the spontaneously fusing vesicles of NPC1-deficent and wild-type neurons by incubating them in a low K^+ buffer containing FM1-43 and TTX (to block action potentials and isolate spontaneously fusing vesicles) for 15 minutes. During this incubation, vesicles fusing spontaneously take up the lipophillic dye upon endocytosis and become fluorescent. After washing away the extracellular FM1-43, I monitored the loss of fluorescence due to dye-containing vesicle exocytosis over 20 minutes in the presence of TTX and then challenged the synapses with a combination of field

potential stimulation and high K^+ to release the remaining available FM1-43 (Fig. 4.2.3.2 A). I found no differences in the dynamics of dye release at NPC1-deficient synapses (Fig. 4.2.3.2 B) indicating that spontaneous fusion of dye-containing spontaneous vesicles fused at the same rate as fluorescent wild-type vesicles. In addition, the initial intensity of fluorescence per bouton (a measure of the number of spontaneously fusing vesicles) was no different from the values observed in wild-type boutons. This suggests that 10 minutes after incubating neurons in the absence of action potentials the NPC1-deficient and wild-type synapses contain about the same number of labeled spontaneously fusing vesicles. After monitoring for 20 minutes, I stimulated the neurons with a series of field potential trains and a high K^+ challenge (Fig. 4.2.3.2 D). The final fluorescence values were similar between the genotypes, thus the NPC1-deficient synapses appeared no different in any aspect of this experiment.

Taken from this, a couple things could be happening. If the number of spontaneously fusing vesicles increase in NPC1-deficient neurons, then I should presumably see an increase in the initial bouton fluorescence; however, this is not the case. I can think of two reasons for this: (1) there are the same numbers of spontaneously fusing vesicles and more synapses allowing for an increased frequency of mEPSCs; (2) There are more spontaneously fusing vesicles, but they release their dye during the wash. I attempted to address this by infecting NPC1-deficient and wild-type cultures with a synaptophysin-pHlorin lentiviral construct;

however, prenatal lethality along with inefficient infection prevented the completion of this study. Synaptophysin-pHlorin is a fusion of the synaptic vesicle protein synaptophysin with a luminal pH sensitive chromophore. Inside the acidic vesicle, the pHlorin domain is quenched; however, upon exocytosis the protein fluoresces. With this system I could monitor spontaneous fusion, and by blocking vesicle reacidification after exocytosis with folimycin (blocker of vATPase) I could determine the total number of vesicles fusing spontaneously per synapse.

After completing the spontaneous vesicle recycling, I incubated the same boutons with FM1-43 in a high K^+ buffer containing FM1-43 to label the entire recycling pool. After washing for 10 minutes to remove excess dye, I monitored the loss of fluorescence from boutons during an 80 second 10 Hz field stimulation followed by more field potentials and one round of high K^+.(Fig. 4.2.3.2 D). In NPC1-deficient synapses, I observed a significant decrease in the initial fluorescence as well as a marked decrease in the rate of fluorescence loss (Fig. 4.2.3.2 E-F) (one-phase decay rate constant: WT 29.9±1.6 s, n=5; NPC1 49.4±9.1, n=4; $p<0.05$; data not shown). The total amount of dye released was significantly less that that of the wild-type neurons (Fig. 4.2.3.2 F). These results suggest that after washing away the excess FM1-43, NPC1-deficient synapses have fewer recycling pool vesicles per synapse and these vesicles fuse at a slower rate than the recycling pool vesicles in wild-type synapses.

In combination with the electrophysiological data, these results suggest that a decreased number of recycling pool vesicles may cause the reduced evoked postsynaptic currents. However, there are at least two problems I see with these assumptions. First, the decreased postsynaptic currents could result from a decreased number of synapses, and I cannot rule this out. Second, as with the spontaneous FM1-43 experiment, an increased loss of FM1-43 during the wash due to enhanced spontaneous fusion may cause the attenuated initial fluorescence intensity. I attempted to address the possible increase in spontaneous fusion from recycling pool vesicles by stimulating the uptake of FM1-43 in NPC1-deficient and wild-type neurons, then monitoring the quantity and rate of fluorescence loss spontaneously. Unfortunately, I cannot conclusively state the results of these experiments, because I obtained some of the data with a different camera and I cannot compare the fluorescence values confidently.

What I can say is that the decreased initial fluorescence indicates that the vesicles of the recycling pool within NPC1-deficient synapses are either more likely to fuse spontaneously or are present in smaller numbers at the synapse. Moreover, the decreased EPSC depression observed during the 10Hz 800 AP train (Fig. 4.2.3.1.1) is consistent with the slower rate of fluorescence loss from NPC1-deficient neurons. In fact for wild-type synapses, the slow time constant of 10Hz 800 AP fluorescence loss and EPSC depression are 29.9±1.6 s and 34.1±5.2 s, respectively; while the time constants were 49.4±9.1s and 47.0±8.1 s for the

NPC1-deficient neurons. The close agreement of the decay time constants for both the electrophysiology and the FM1-43 imaging strongly supports the idea that recycling pool vesicles of NPC1-deficient synapses can fuse but do so slowly.

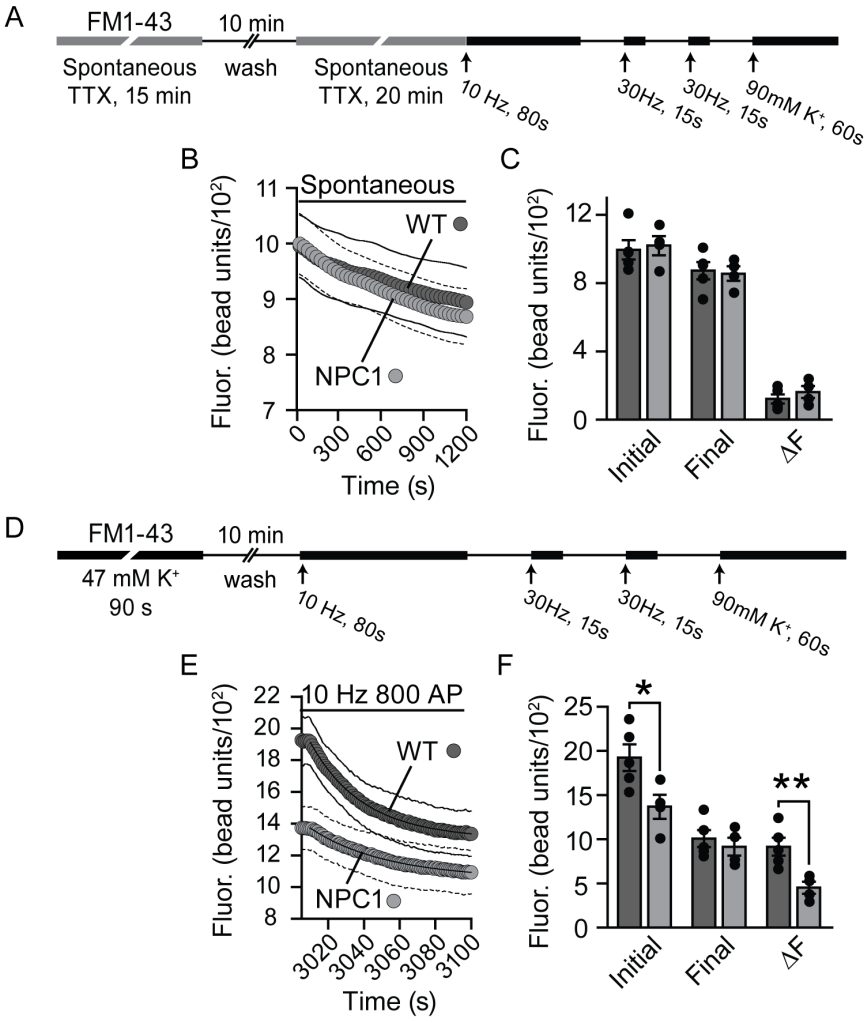

Figure 4.2.3.2 Recycling of action potential-dependent and -independent synaptic vesicles in NPC1-deficient hippocampal synapses.

(A-D)Spontaneous FM1-43 uptake and release (A) Diagram of the protocol for spontaneous uptake of FM1-43 (B) Summary plot of the average loss of fluorescence measured during dye release after FM1-43 uptake during the spontaneous portion of the protocol. The graph depicts no difference between NPC1-deficient (NPC1) and wild-type

(WT) boutons in the rate of spontaneous release of FM1-43 from vesicles labeled spontaneously. (C) Chart of the average fluorescence values per coverslips showing no change in the initial or final fluorescence (also see panel B) as well as no change in the total amount of FM1-43 released by the end of the experiment (ΔF).
(E-H) Maximal uptake of FM1-43 into recycling synaptic vesicles (E) Diagram of the high K^+ stimulated uptake of FM1-43 and the following field-potential and high K^+ stimulation employed for FM1-43 release. (F) Summary graph of the fluorescence values during the first stimulation after washing showing an obvious decrease in the initial fluorescence and a decrease in the rate of release during the 10 Hz 800 AP stimulation. (C) Average fluorescence values from each coverslip demonstrating a significant decreases (about 40%) in the initial and the total amount of fluorescence lost after completing the protocol in NPC1-deficient boutons compared to wild-type.
Error bars represent the SEM. (2 cultures, WT n=5, Npc1 n=4; *$p<0.04$, ** $p<0.009$)

4.2.4 Altered spontaneous network activity in the absence of inhibitory neurotransmission in NPC1-deficient cortical neurons

The decreased basal inhibitory input and increased excitatory neurotransmitter exposure in NPC1-deficient neurons in culture indicate the potential for an increase in spontaneous network activity. By measuring the postsynaptic currents in the absence of TTX, I measured the network activity of NPC1-deficient neurons in dissociated cultures with and without inhibitory neurotransmission. To determine the basal network activity, I recorded the postsynaptic currents without blocking inhibitory neurotransmitter receptors with picrotoxin (PTX). Surprisingly, the frequency of the spontaneous postsynaptic currents (sPSCs) was no different than the rate of events observed in wild-type neurons (Fig. 4.2.4.1 A-B). In addition to the frequency, the NPC1-deficiency resulted in no changes in the amplitudes, charges, or durations of these events

(Fig. 4.2.4.1 C-E). This suggests that the increased spontaneous vesicle fusion at excitatory synapses does not increase the activity of postsynaptic neurons

To explore whether inhibitory input maintains the normal culture network activity, I recorded spontaneous EPSCs (sEPSCs) in the presence of picrotoxin to block inhibitory neurotransmitter receptors. The NPC1-deficiency resulted in an increase in the frequency of sEPSCs with a decrease in the duration of the bursts (Fig. 4.2.4.2). Interestingly, the amplitudes of these bursts were not significantly different between NPC1-deficient neurons compared to the wild-type neurons. This is curious considering the decreased magnitude of evoked EPSCs in NPC1-deficient cultures (Fig. 4.2.1.1C-D).

To examine the properties of spontaneous action potential (sAP) firing in NPC1-deficient and wild-type cortical neurons, I observed the sAP events by current-clamping cortical neurons in culture without QX-314 in the electrode solution (presynaptic action potentials were not blocked) (Fig.4.2.4.3, 4). I first measured the sAP firing without blocking inhibitory neurotransmitter receptors, and like the spontaneous network activity I found no significant changes in NPC1-deficient neurons (Fig.4.2.4.3) With inhibitory neurotransmission blocked by PTX, I found an increase in the frequency of sAP firing accompanied by a decrease in the duration of the events (Fig. 4.2.4.4 B-C). There was a trend towards a diminished number of AP per sAP burst; however, the initial and

average sAP amplitude, half-width and threshold were not significantly different from the values obtained from wild-type neurons (Fig. 4.2.4.3 D-G).

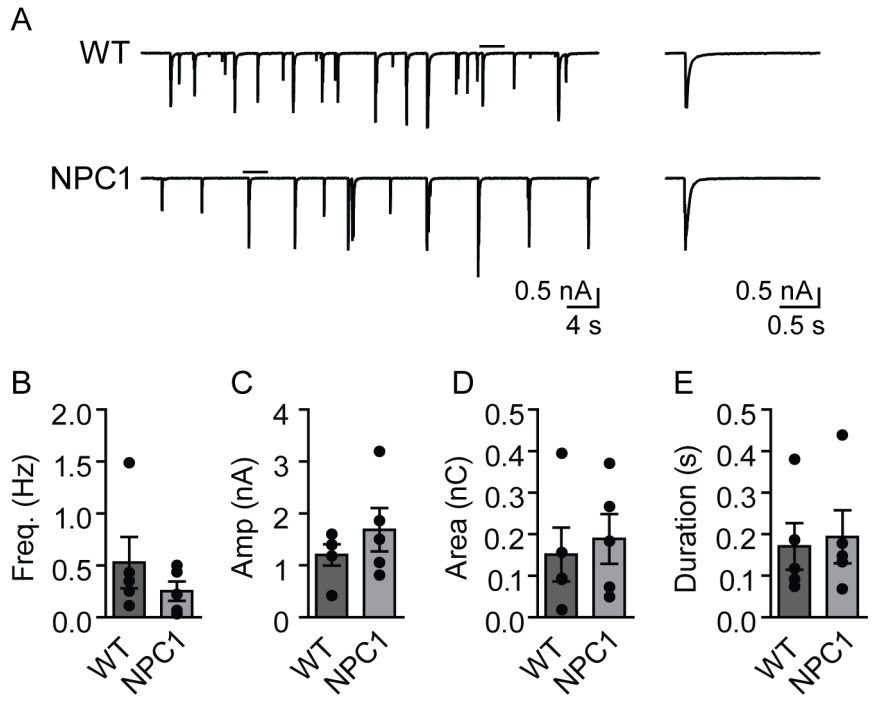

Figure 4.2.4.1 Spontaneous activity is not altered in the presence of both excitatory and inhibitory input in cortical neurons lacking NPC1.

(A) Representative traces of spontaneous bursts of PSCs (sPSCs) from cortical neurons of NPC1-deficient (NPC1) and wild-type (WT) mice (left). Magnified image of a sPSC burst (right).
(B-E) Charts summarizing the average sPSC measurements: NPC1-deficient cortical neurons display no changes in the frequency (B), amplitudes (C) charge (D) or duration (E) in the sAP events.
Error bars represent the SEM. (n=5)

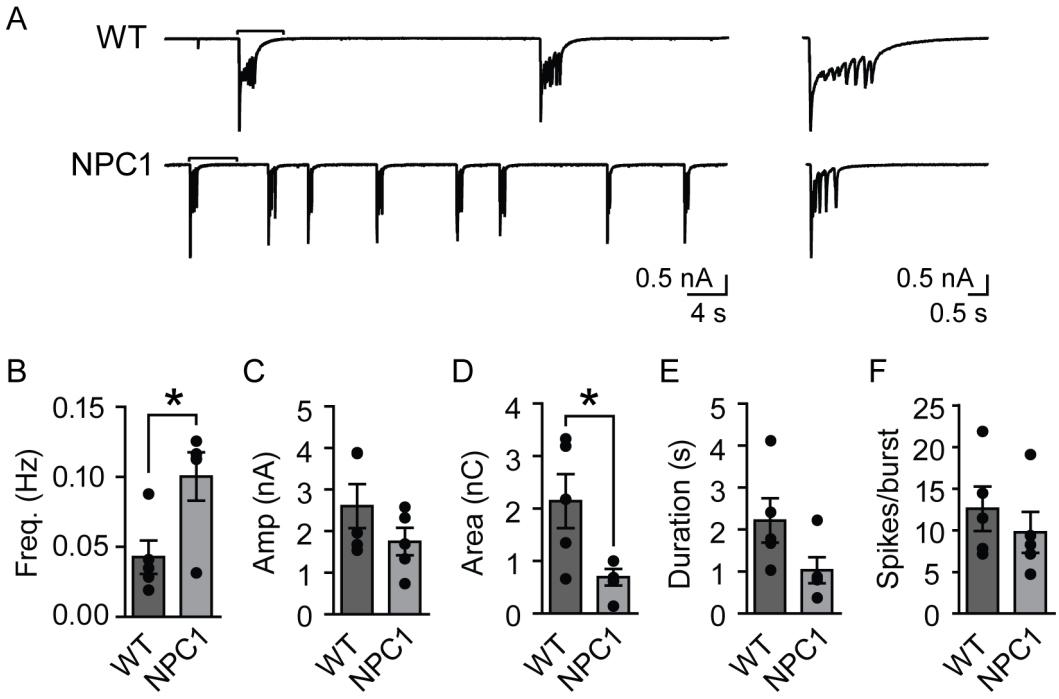

Figure 4.2.4.2 Increased excitatory spontaneous activity in NPC1-deficient cortical cultures.

(A) Representative traces of spontaneous bursts of EPSCs (sEPSCs) from NPC1-deficient (NPC1) and wild-type (WT) cortical neurons (left). Magnified view of the sEPSC burst (right) marked by the bracket on the left trace.
(B-F) Charts summarizing the average measurements of bursts of sEPSCS: The sEPSC bursts of NPC1-deficient cortical neurons occur more frequently (B) with no change in the average maximum amplitude of each event (C). Mutant neurons released less charge per burst (D), however the duration (E) and numbers of spikes following the initial event peak (F) were not significantly different from wild-type neurons.
Error bars represent the SEM. (* $p<0.03$; $n=5$)

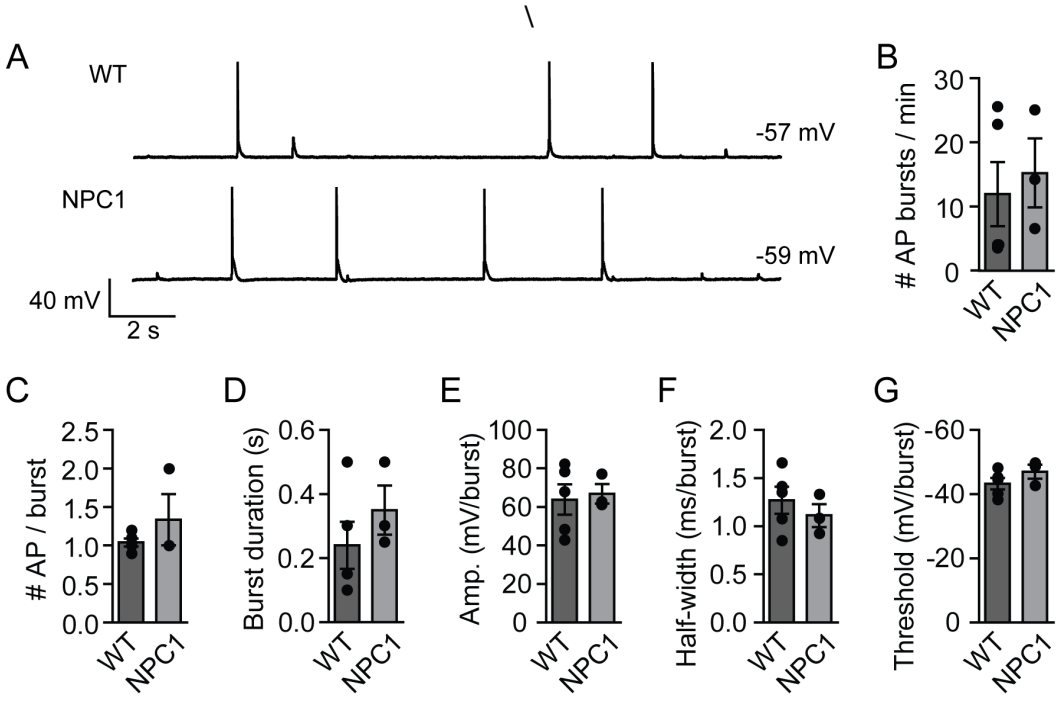

Figure 4.2.4.3 Spontaneous action potential firing is unaffected in NPC1 deficient cortical neurons

(A) Representative traces of spontaneous bursts of action potentials (sAPs) from NPC1-deficient (NPC1) and wild-type (WT) cortical neurons without blocking inhibitory neurotransmitter receptors.
(B-G) Summary charts of the properties of spontaneous bursts of APs. The NPC1-deficient neurons experienced no alterations in the frequency of sAP (B), number of AP per burst (C), durations of the bursts (D), amplitudes of the bursts (E), half-width (F) or threshold of AP firing (G).
Error bars represent the SEM. (WT n=5, NPC1, n=3)

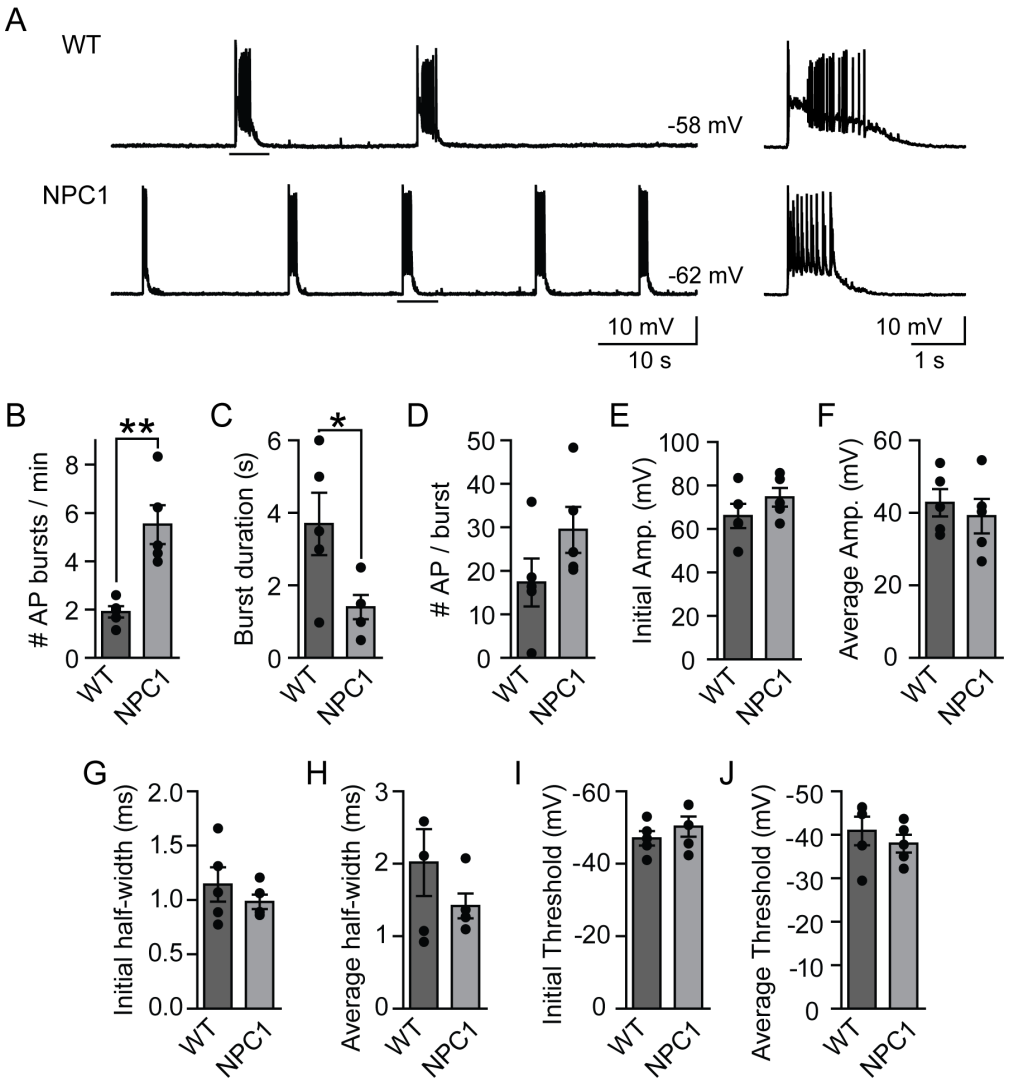

Figure 4.2.4.4 Shorter, more frequent bursts of spontaneous action potential firing in NPC1 deficient cortical neurons

(A) Representative traces of spontaneous bursts of action potentials (sAPs) from NPC1-deficient (NPC1) and wild-type (WT) cortical neurons. The traces on the right are enlarged portions of those on the left.
(B-G) Summary charts of the properties of spontaneous bursts of APs. The frequency of sAP increased while the durations of the bursts shortened (C). The sAPs from the NPC1-deficient neurons experience no differences in the initial or average amplitudes (E-F), half-widths (G-H), and thresholds (I-J) of each burst.
Error bars represent the SEM. (* $p<0.04$, ** $p<0.003$, n=5)

4.3 Summary

In NPC1-deficient hippocampal neurons, a loss of the initial fast depression of excitatory neurotransmitter release during a 10 Hz 800 AP stimulus train accompanied the decreased evoked neurotransmission. In wild-type neurons, the 10 Hz stimulation evoked EPSCs which decreased in amplitude quickly followed by a slower reduction in amplitude during the rest of the stimulus train. The loss of the fast, synchronous release coupled with the initial attenuated EPSC amplitude is likely a result of inefficient priming of vesicles before fusion which would lead to decreased number of release ready vesicles. Interestingly, fluorescent tracking of synaptic vesicles in NPC1-deficient synapses revealed that all actively recycling are reusable, although at a slower pace compared to wild-type counterparts. This rate of reuse is comparable to the decay rate of EPSC amplitudes during 10 Hz stimulation. The NPC1 protein is present in synaptic endosomes (Karten et al., 2005), which play a role in repackaging synaptic vesicles (Sudhof, 2004). Therefore, the lack of this component of neurotransmitter release could be a product of inadequate packaging of synaptic vesicles; however, I cannot rule out altered organization of the plasma membrane, specifically the active zone, which could reduce the number of release sites. At inhibitory synapses, responses to field potentials also decreased; however, while there was a delay in the rate of recovery, I found no deficit in the IPSC decay during 10 Hz 30

s stimulation. This suggests that inhibitory synaptic vesicles can prepare for fusion efficiently.

The NPC1 mutation appears to affect spontaneous excitatory and inhibitory neurotransmitter release differently. Spontaneous release of excitatory neurotransmitter increased, mimicking the effect of acute depletion of cholesterol. Conversely, the frequency of inhibitory neurotransmitter release slowed even though acute cholesterol extraction increased this fusion. The lack of change in the mIPSC amplitude argues against changes in inhibitory neurotransmitter receptors, thus the opposing effect of the NPC1 mutation in culture is most likely a function of compensatory decreases in spontaneous vesicle recycling at each synapse and/or a decrease in the number of inhibitory synapses.

When observing spontaneous network activity and spontaneous action potential firing within the NPC1 cultures, I found no change in the occurrence or efficiency of spontaneous bursts of postsynaptic current or the firing of action potentials in the postsynaptic neuron in the presence of both inhibitory and excitatory input. Considering the increased excitatory neurotransmitter release into the synaptic cleft at rest and the coincident decrease in the inhibitory output, one would expect to see more spontaneous action potentials and network activity. In fact, blocking inhibitory neurotransmitter receptors resulted in augmentation of both spontaneous activity and action potential firing, demonstrating that the

normal excitability of NPC1-deficient neurons requires the attenuated inhibitory input.

The NPC1-deficient neurons display defects in both excitatory and inhibitory neurotransmitter release. Action potential-triggered vesicle fusion decreased in both synapses, and vesicles that do fuse have a slower rate of reuse. Excitatory synapses of NPC1-deficient released neurotransmitter more frequently, while hindering spontaneous inhibitory neurotransmission. Interestingly, the increased excitatory neurotransmitter within the synaptic cleft did not result in augmented spontaneous network activity in the presence of inhibitory input. Therefore, NPC1-deficient neurons experience opposing changes in excitatory and inhibitory neurotransmission, but somehow these defects balance out within the neuronal circuitry of the culture. While at face value, this appears to diminish the impact of the findings, further investigations into how these synaptic defects affect the brain as it ages may provide insight into the disease pathology.

4.4 Methods

4.4.1 Cell culture

The hippocampus was dissected and dissociated from postnatal day 0–3 (P0–3) NPC1-deficient mice (Jackson Laboratory, BALB/cNctr-NPC1m1N/J) as previously described in Kavalali et al. (1999).Mice were rapidly killed by decapitation after sedation by chilling on an ice-cold metal plate. Dissociated cells were plated on zero thickness 12mm glass coverslips and stored at 37°C with 5% CO_2 in a humidified incubator.

4.4.2 Hippocampal slice preparation

After Nembutal (20 mg kg−1; Abbott Laboratories, IL, USA) anesthesia, mice were rapidly killed by decapitation, hippocampi were removed, and transverse slices (400 μm) were cut in oxygenated, ice-cold dissection (lowCa^{2+}–high Mg^{2+} artificial cerebrospinal fluid; ACSF) solution using a Vibratome (St Louis, MO, USA) and incubated at 34°C for 30 min. Slices were kept at room temperature for at least 60 min in ACSF containing (mM): 124 NaCl, 5 KCl, 12 NaH_2PO_4, 26 $NaHCO_3$, 10 D-glucose, 2 $CaCl_2$ and 1 $MgCl_2$, gassed with 95% O_2 and 5% CO_2. After removal of the CA3 region, slices were transferred to the recording chamber, perfused with oxygenated ACSF. All the handling and killing procedures for animals were approved by the Institutional Animal Care and Use Committee of U.T. Southwestern Medical Center.

4.4.5 Electrophysiology

Hippocampal Cultures: A modified Tyrode's solution was used for all experiments (except where noted otherwise) that contains (in mM) 140 NaCl, 4 KCl, 2 $MgCl_2(6H_2O)$, 10 glucose, 10 HEPES, 2 $CaCl_2$ (pH 7.4, osmolarity 300 mOsM). Pyramidal cells were whole-cell voltage clamped at –70 mV with borosilicate glass electrodes (3-5 MΩ). Electrode solutions contained (in mM): 105 Cs-methanesulphonate, 10 CsCl, 5 NaCl, 10 HEPES, 20 TEA.Cl hydrate, 4 Mg-ATP, 0.3 GTP, 0.6 EGTA, 10 QX-314. All solutions contained 50 μM aminophosphonopentanoic acid (AP-5) to block NMDA receptors. For hypertonic sucrose recordings, a Tyrode's solution containing 500 mM sucrose and 1 μM TTX with 50 μM PTX was perfused over cultures for 30 seconds. EPSC measurements were performed using field stimulation with platinum electrodes at 20 mA for 1 ms per action potential in the Tyrode's solution containing 50 μM PTX. For spontaneous mEPSCs, recordings were performed in the modified Tyrode's solution containing 1 μM tetrodotoxin (TTX). Inhibitory or excitatory

currents were isolated using 50 µM PTX or 10 µM 6-cyano-7-nitroquinoxaline-2,3-dione (CNQX) (respectively). Spontaneous network activities were recoded from neurons immerged in a Tyrode's solution without TTX to allow spontaneous action potentials. The presence of QX3-14 within the internal pipette solution prevented action potential firing in the postsynaptic neuron. Spontaneous action potentials were measured by current clamping neurons in a plain Tyrode's solution and a pipette solution containing (in mM): 110 K-gluconate, 20 KCl, 10 NaCl, 10 HEPES , 0.6 EGTA, 4 Mg-ATP, 0.3 GTP, 10 QX-314 and buffered to pH 7.2-7.3 with CsOH (280-290 mOsm) .

Hippocampal Slices: Electrophysiological recordings were carried out in the whole-cell voltage-clamp configuration on the CA1 pyramidal neurons. Patch pipettes had resistance of 3-6 MΩ when filled with pipette solution containing (in mM): 110 K-gluconate, 20 KCl, 10 NaCl, 10 HEPES , 0.6 EGTA, 4 Mg-ATP, 0.3 GTP, 10 QX-314 and buffered to pH 7.2-7.3 with CsOH (280-290 mOsm). Recordings were obtained with an Axopatch-200B patch-clamp amplifier (Molecular Devices, Union City, CA, USA). Signals were low-pass filtered at 2 kHz and digitized at 10 kHz.

4.4.3 Cholesterol addition

In order to produce MCD: cholesterol complexes (molar ratio, 9.78 : 1), a 5% MCD solution was heated to 80°C and 30 mg of cholesterol dissolved in 9 ml of chloroform: methanol (1: 2) was added drop-wise until all of the solution was dissolved. The solution was crystallized and re-dissolved in 5 ml of distilled water and stored at –20°C (adapted from (Klein et al., 1995)). For cholesterol addition, cells were incubated at room temperature for 1 hr in 0.61mM of complexed cholesterol (about 6 mM MCD saturated with cholesterol) with 10 µM NBQX, and 50 µM AP5 in either a 20 mm K^+ Tyrode's solution or 4 mm K^+ Tyrode's

solution with 1 µM TTX. The solution was thoroughly washed away and experiments were performed.

4.4.6 Fluorescent detection of synaptic vesicle recycling

Synaptic boutons were loaded with 8 µM FM1-43 (Molecular Probes, Eugene, OR) under conditions described in Results. The modified Tyrode's solution used in all experiments contained (in mM): 150 NaCl, 4 KCl, 2 $MgCl_2$, 10 glucose, 10 HEPES, and 2 $CaCl_2$, (pH 7.4, ≈ 310 mOsm). High K^+ solutions contained equimolar substitution of KCl (90 mM) for NaCl. All staining and washing protocols were performed with 10 µM 6-cyano-7-nitroquinoxaline-2,3-dione (CNQX) and 50 µM aminophosphonopentanoic acid (AP-5) to prevent recurrent activity. For spontaneous FM1-43 uptake, cultures were incubated in a modified Tyrode's solution containing 1 µM TTX, which inhibits action potentials induced by network activity inherent in the culture. For spontaneous FM1-43 release, synapses were monitored for 20 minutes in a modified Tyrodes solution containing TTX and images were captured every 30 s. After 20 minutes, images were taken every second during a 10 Hz 800 AP train of field potentials followed by two rounds of 30 Hz 450 AP and then one 60 s high K^+ challenge. Each stimulus train was separated by a 60 s rest. After washing for 10 minutes, the same boutons were incubated with FM1-43 in a 47 mM K^+ solution (1:1 solution, modified Tyrode's solution: 90 mM K^+ Tyrode's solution) for 90 s to label total recycling pool of vesicles in a given synapse (Harata et al., 2001). Stimulation after washing away the dye was performed like the spontaneous uptake and destaining except for the 20 minutes spontaneous monitoring. In all experiments I selected isolated boutons (1 μm^2) for analysis and avoided apparent synaptic clusters (Kavalali et al., 1999b). All statistical analyses were performed using the student's t test using the number of coverslips as n unless stated otherwise. Experimental results are represented as mean ± SEM. Images obtained by a

cooled, intensified digital CCD camera (Roper Scientific, Trenton, NJ) during illumination at 480 nm via an optical switch (Sutter Instruments, Novato, CA). Images were acquired and analyzed using Metafluor Software (Universal Imaging, Downingtown, PA).

4.4.6 Statistical analysis

All statistics for pairwise comparisons were calculated using a two-tailed paired t test. Statistics for experiments comparing more than two variables were performed using one-way ANOVA. To determine the significance of mEPSC amplitude distributions, the Kolmogorov-Smirnov test (K-S test, $p>0.0001$) was used.

CHAPTER 5: SPHINGOSINE & NEUROTRANSMISSION

5.1 Background

Communication between neurons requires the release of neurotransmitter from synaptic vesicles. This process is highly regulated by many proteins to provide synchronous vesicle fusion in response to Ca^{2+} influx after an action potential. For a synaptic vesicle, proteins known as SNAREs (soluble-N-ethylmaleimide sensitive factor attachment protein receptors) reside on the vesicle (synaptobrevin) and the plasma membrane (syntaxin and SNAP-25) (Sollner, 2003, Sudhof, 2004, Jahn and Scheller, 2006). These proteins contain a SNARE motif consisting of 60 amino acids, and a four helical bundle forms when the SNARE motifs come together with synaptobrevin and syntaxin contributing one motif each and two from SNAP-25 (Sutton et al., 1998). Interestingly, the spontaneous intertwining of these four amino acid chains does not happen often (Hu et al., 2002). Thus, other factors must play a role in regulating these proteins to allow for efficient SNARE complex formation.

Some factors implicated in this regulation are other vesicle proteins (Edelmann et al., 1995, Yelamanchili et al., 2005) as well as lipids in the membrane(Humeau et al., 2001, Bankaitis and Morris, 2003, Lesa et al., 2003, Rigoni et al., 2005, Rohrbough and Broadie, 2005). To further understand the lipid modifications on synaptobrevin action (Quetglas et al., 2000, Caccin et al., 2003), the group lead by Bazbek Davletov at the MRC Laboratory of Molecular

Biology in Cambridge in the UK isolated synaptic vesicles from rat hippocampal neurons and incubated them in the presence of syntaxin and SNAP-25. They then added different lipids from a library and quantified the number of SNARE complexes present. They categorized lipids which lead to a larger number of SNARE complexes as positive synaptobrevin regulators (+) and those resulting in no changes as ineffective synaptobrevin modulators (-) (Fig. 5.1).

Sphingosine was one of the positive modulators of SNARE complex formation and is an essential membrane sphingolipid shown to exist in the cytoplasm after enzymatic release. The regulation of SNARE complex formation by sphingosine was concentration dependent and was not a result of the loss of vesicle integrity or interactions with synaptic vesicle proteins other than synaptobrevin (data not shown). The next phase of this project involved the study of neurotransmitter release. In the following experiments, we have shown that sphingosine addition to neuronal cultures results in augmented neurotransmitter release in a synaptobrevin-dependent manner and this is most likely a direct result of increased SNARE formation.

Sphingomyelin	-
D-erythro-Sphingosine	+
L-erythro-sphingosine	+
D-erythro-N,N-Dimethylsphingosine	+
D-erythro-N,N,N-trimethylsphingosine	+
D-erythro-Dihydrosphingosine	+
DL-threo-Dihydrosphingosine	+
D-erythro-Sphingosylphosphoryl choline	+
D-erythro-Sphingosine-1-phosphate	-
Dihydro-sphingosine-1-phosphate	-
D-erythro-N-Acetylsphingosine	-
D-erythro-N-Acetylsphinganine	-
D-erythro-N-Octanoylsphingosine	-
D-erythro-N-Octanoylsphinganine	-
D-erythro-N-Palmitoylsphingosine	-
DL-PDMP	
DL-PPMP	-
MAPP, D-erythro	-
MAPP, L-erythro	-

Figure 5.1 Lipid regulators of synaptobrevin

(Left column) List of sphingosine derivatives tested for synaptobrevin modulation of SNARE-complex formation (Right column) Shows whether the lipid increased (+) or had no effect on SNARE formation through modulation of synaptobrevin.
Modified from Darius et al. manuscript

5.2 Results

5.2.1 Addition of sphingosine augments the number of immediately releasable vesicles

To further test the impact of sphingosine on neurotransmission, we applied sphingosine onto dissociated neuron cultures obtained from mice lacking synaptobrevin-2 and measured the neurotransmitter release evoked by field-stimulation or by application of hypertonic sucrose solution (+500 mOsm, 30 seconds). Mice deficient in synaptobrevin-2 die immediately after birth; however, embryonic neurons from these animals survive in culture. Synaptobrevin-2-deficient neurons have a severe reduction in evoked exocytosis and endocytosis (Schoch et al., 2001; Deak et al., 2004) especially in response to stimulation at

low frequencies (≈1 Hz). Nevertheless, in some cells one can detect occasional responses to stimulation. In heterozygous cultures treatment with 50 µM sphingosine caused a 2.7-fold increase in the amplitudes of excitatory postsynaptic currents (EPSCs) induced by field-stimulation (Syb2 +/–, n = 5 (with or without Sphingosine), $p < 0.03$) (Fig. 5.2.1 A). The responses recorded from synaptobrevin-2-deficient (Syb2 –/–) synapses, however, did not show an increase after sphingosine treatment (Syb2 –/–, n = 5, n.s. p=0.72).

In contrast to action potential evoked stimulation, synaptobrevin-2 deficient neurons reproducibly respond to hypertonic sucrose stimulation albeit at a reduced level (about 6% compared to non-treated wild-type neurons; Syb2 +/– , n=11; Syb2 –/–, n=14; $p< 0.001$). Heterozygous neurons treated with sphingosine had a 2-fold increase in their responses to hypertonic sucrose application compared to neurons from non-treated heterozygous cultures (Syb2 +/–, n=11; Syb2 +/– (Sphingosine), n=17; $p<0.002$). In contrast culture from synaptobrevin deficient mice did not show a significant increase in their hypertonic sucrose responses (Syb2 –/–, n=14; Syb2 –/– (Sphingosine), n=17; n.s. p=0.22) compared to non-treated Syb2 –/– neurons (Fig. 5.2.1 B). These experiments revealed no further increase in responses evoked by field simulation or hypertonic sucrose application in synaptobrevin-2-deficient synapses, which is consistent with the premise that sphingosine enhances neurotransmitter release by regulating the synaptobrevin-2-dependent fusion machinery.

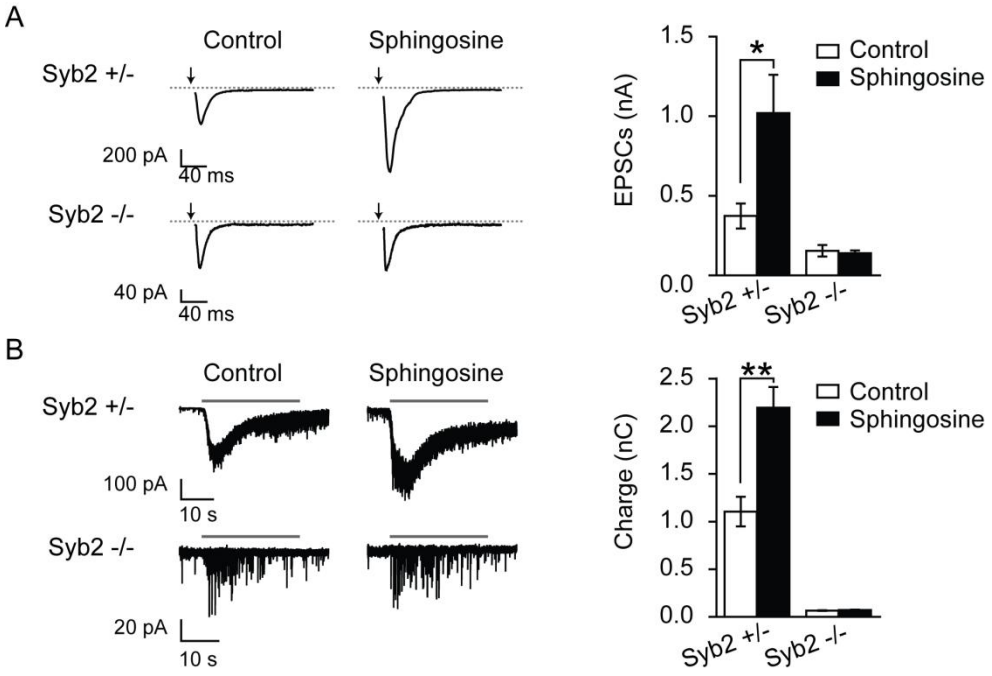

Figure 5.2.1 Synaptobrevin-2 transmitter release mediated by sphingosine

(A) Left panel, representative traces of excitatory postsynaptic currents (EPSCs) evoked by field stimulation in synaptobrevin-2-deficient (Syb2 –/–) and wild-type (Syb2 +/–) neurons treated with 50 µM sphingosine (Sphingosine) or an equal volume of vehicle (Control). As Syb2 –/– cells respond to stimulation only sporadically (Schoch et al., 2001), to assess the sphingosine effect we only analyzed responding cells (n=5). Right panel, a bar chart showing a 2.7-fold increase in the average maximum EPSC amplitudes of sphingosine-treated wild-type neurons compared to non-treated control neurons (EtOH, n=5; Sphingosine, n=5). In contrast, no difference in amplitudes detected in sphingosine-treated synaptobrevin-2-deficient neurons compared to non-treated synaptobrevin-2-deficient neurons (EtOH, n=5; Sphingosine, n=5).
(B) Left panel, representative traces of hypertonic sucrose-induced transmitter release in synaptobrevin-2-deficient (Syb2 –/–) and wild-type (Syb2 +/–) neurons treated with 50 µM sphingosine (Sphingosine) or an equal volume of vehicle (Control). Right panel, summary graph of the charge transfer during the first 10 s of the 30 s sucrose stimulation depicting a 2-fold increase in wild-type (EtOH, n=11; Sphingosine, n=17) and no increase in synaptobrevin-2-deficient neurons (EtOH, n=14; Sphingosine, n=17) after sphingosine addition. Note the ≈95% decrease in the charge transfer in synaptobrevin-2-deficient neurons compared wild-type amplitudes in the absence of sphingosine treatment (Syb2 +/–, n=11; Syb2 –/–, n=14; $p<<0.001$).
Error bars represent the SEM. Syb2, synaptobrevin; * $p< 0.03$, ** $p< 0.002$.

5.2.2 Addition of sphingosine augments the frequency of spontaneous vesicle fusion events

At the neuromuscular junction, sphingosine addition increases the rate of spontaneous neurotransmitter release. To characterize the effect of sphingosine on spontaneous vesicle fusion, we incubated cortical neuron cultures from synaptobrevin2-deficient (Syb2 –/–) and wild-type/heterozygous (Syb2 +/–) littermates with 50 μM D-sphingosine or an equal volume of ethanol (EtOH) for 10 minutes at room temperature. Compared to EtOH-treated neurons, the frequency of miniature EPSCs (mEPSCs) increased 2.4-fold in Syb2 +/– neurons (Fig. 5.2.2 A-B; EtOH, 1.2 ± 0.2 Hz; Sphingosine, 2.9 ± 0.3 Hz) and 3.4-fold in Syb2 –/– neurons (Fig. 5.2.2 A-B; EtOH, 0.29 ± 0.03 Hz; Sphingosine, 0.96 ± 0.17 Hz) after sphingosine addition without a significant change in the amplitudes of individual events (Fig. 5.2.2 C. Syb2 +/–: EtOH, 17.6 ± 2.3 pA; Sphingosine, 17.1 ± 1.6 pA. Syb2 –/–: EtOH, 17.8 ± 1.6 pA; Sphingosine, 20.3 ± 1.7 pA).

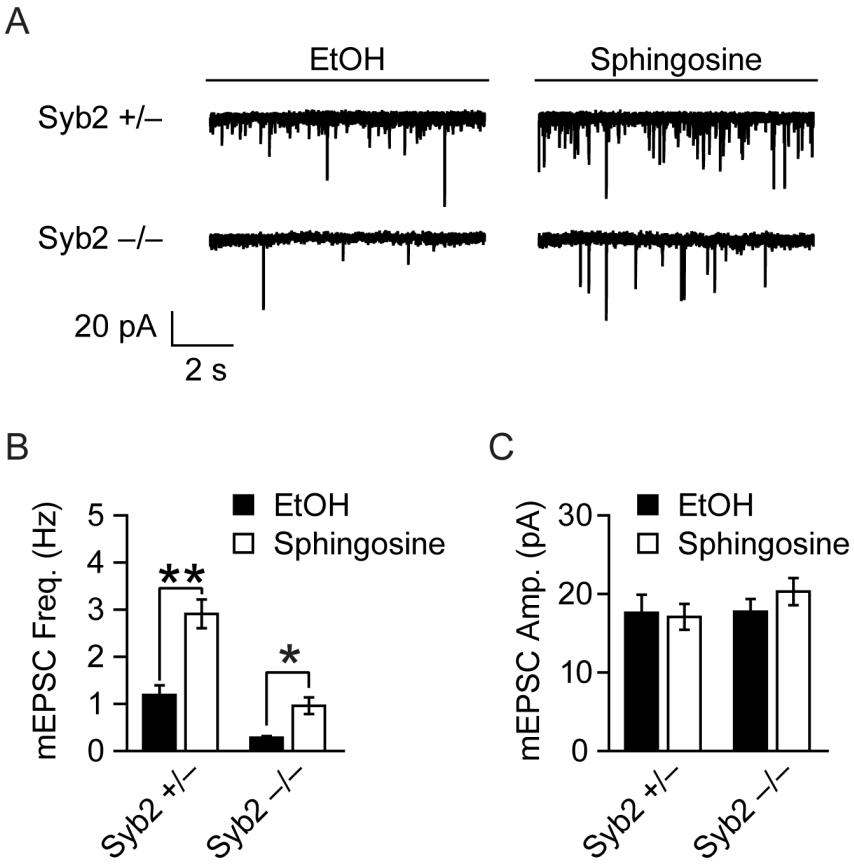

Figure 5.2.2 Addition of sphingosine increases spontaneous neurotransmitter release in a synaptobrevin2-independent manner

(A) Representative traces of mEPSCs recorded from Syb2 +/– and Syb2 –/– neurons incubated with sphingosine or an equal volume of vehicle (ethanol, EtOH)
(B) Summary graph of the average frequency of mEPSC events. In Syb2 +/– neurons, the average mEPSC frequency was 2.4-fold larger when treated with sphingosine compared to incubation with only EtOH. Similarly, sphingosine addition to Syb2 –/– neurons resulted in a 3.4-fold increase in the frequency of mEPSCs. Note: The mEPSC frequency in Syb2 –/– neurons is 76% smaller than the rate observed in Syb2 +/– neurons.
(C) Plot summarizing the average amplitudes of mEPSCs depicting no significant differences between either treatment in both Syb2 +/– and Syb2 –/– neurons.
Error bars represent the SEM. (2 cultures; Syb2 +/–: EtOH n=14, Sphingosine n=16; Syb2 –/–: EtOH n=13, Sphingosine n=16) (*$p < 0.003$, **$p << 0.001$)

5.2.3 Augmentation of neurotransmitter release by another positive regulator of synaptobrevin while an ineffective modulator has no effect

To understand whether enhanced neurotransmission after sphingosine addition to hippocampal neurons is directly related to the increased synaptobrevin activity, we incubated neurons with two additional sphingosine derivatives. The first was sphinganine, another positive regulator of synaptobrevin, and the second was C_2-dihydroceramide, which is ineffective in enhancing synaptobrevin activity (Fig. 5.1). We incubated neurons with 50 µM sphinganine (Biomol**)** or an equal volume of vehicle (DMSO) for 10 minutes at room temperature. Sphinganine addition resulted in an increase in both average maximum amplitudes of field potential-stimulated EPSCs (Fig. 5.2.3.1 A; 2.2-fold; DMSO, 2.3 ± 0.3 nA; Sphinganine, 5.2 ± 1.0 nA) and the hypertonic sucrose responses (Fig. 5.2.3.1 B; 1.7-fold; DMSO, 3.5 ± 0.2 nC; Sphinganine, 6.0 ± 0.9 nC) compared to neurons treated with only DMSO. The sphinganine incubation also led to an increase in the frequency of miniature EPSCs (mEPSCs) compared to DMSO-treated neurons (Fig. 5.2.3.2 A-B; 2.2-fold; DMSO, 3.1 ± 0.4 Hz; Sphinganine, 6.9 ± 0.7 Hz) without affecting the amplitudes of the events (Fig. 5.2.3.2 A and C; p=0.87; DMSO, 22.7 ± 2.8 pA; Sphinganine, 21.9 ± 3.4 pA). These results are consistent with the proposal that positive regulators of synaptobrevin activity also enhance neurotransmitter release.

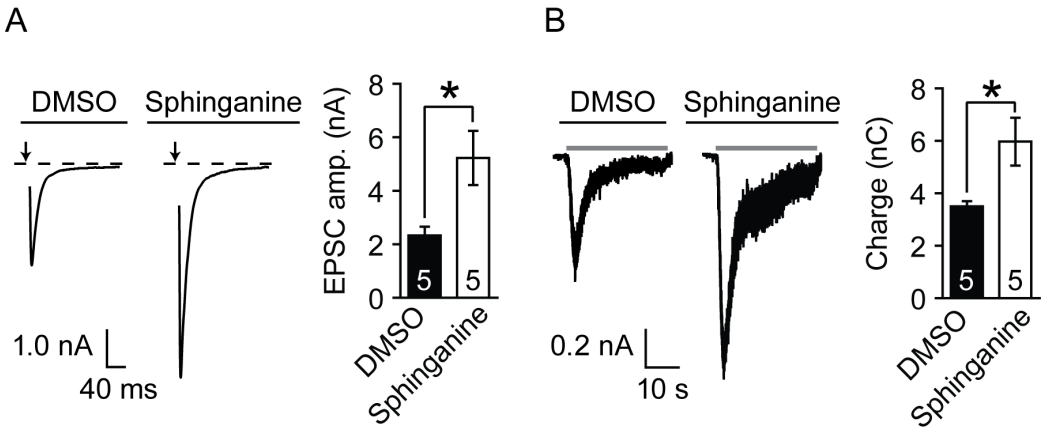

Figure 5.2.3.1 Sphinganine addition potentiates neurotransmitter release evoked by either field potentials or hypertonic sucrose in hippocampal neurons.

(A) Field potential stimulation: Left panel, representative traces of excitatory postsynaptic currents (EPSCs) evoked by field potential stimulation in wild-type rat hippocampal neurons (DIV 15-20) after a 10 minute treatment with 50 µM sphinganine (Sphinganine) or an equal volume of vehicle (DMSO). Right panel, a plot of the average maximum EPSC amplitudes depicting a significant increase (2.2-fold) in the amplitudes from neurons treated with sphinganine compared to DMSO-treated neurons.
(B) Hypertonic sucrose stimulation: Left panel, representative traces of hypertonic sucrose responses from neurons incubated with either DMSO or sphinganine. Right panel, graph summarizing the average charge transfer during the first 10 s of the 30 s hypertonic sucrose stimulation showing a 1.7-fold increase from sphinganine-treated neurons compared to neurons incubated with only DMSO.
Error bars represent the SEM. Arrows indicate the application of current. Gray bars represent the presence of 500 mM sucrose. (DMSO, n=5; Sphinganine, n=5) (* $p < 0.03$)

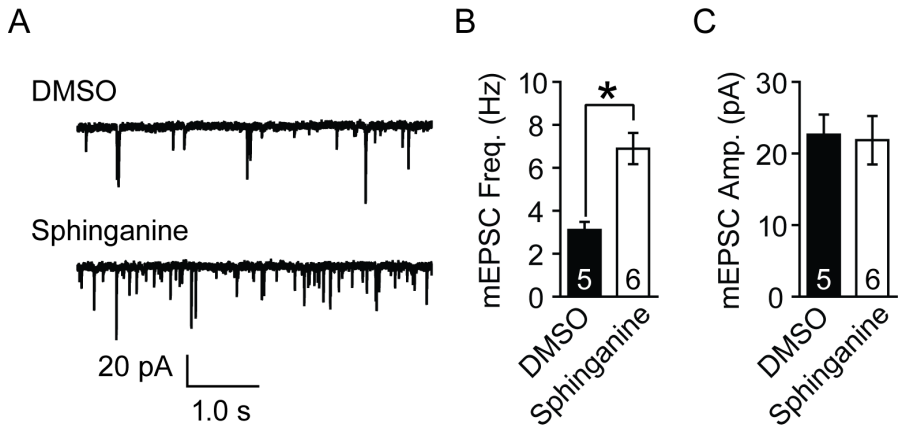

Figure 5.2.3.2 Sphinganine addition enhances frequency of spontaneous release of neurotransmitters in hippocampal neurons.

(A) Representative traces of miniature EPSCs (mEPSCs) current recordings wild-type rat hippocampal neurons (DIV 15-20) incubated for 10 minutes in 50 µM sphinganine (Sphinganine) or an equal volume of vehicle (DMSO). (B) Graph summarizing the average frequency of mEPSC events depicting a 2.2-fold increase after sphinganine addition compared to neurons incubated with only DMSO. (C) Plot of the average amplitude of mEPSC event showing no significant differences between the groups. Error bars represent the SEM. (DMSO, n= 5; Sphinganine, n =6) (* $p < 0.002$)

Moreover, a 10-minute incubation of neurons with 50 µM C_2-dihydroceramide or equal volumes of vehicle (ethanol, EtOH) resulted in no significant differences in either EPSC amplitudes (Fig. 5.2.3.3 A; p=0.99, EtOH, 2.3 ± 0.3 nA; C_2-dihydroceramide, 2.3 ± 0.7 nA) or hypertonic sucrose responses (Fig. 5.2.3.3 B; p=0.59; EtOH, 2.0 ± 0.4 nC; C_2-dihydroceramide, 2.3 ± 0.5 nC). C_2-dihydroceramide-treated neurons experience no significant alterations in either the mEPSC frequency (Fig. 5.2.3.4 A-B; p=0.47; EtOH, 3.3 ± 0.3 Hz; C_2-dihydroceramide, 2.9 ± 0.5 Hz) or amplitudes (Fig. 5.2.3.4 A and C; p=0.47, EtOH, 16.6 ± 0.8 pA; C_2-dihydroceramide, 15.6 ± 1.0 pA) compared to EtOH-treated neurons. Thus, the lack of an effect of C_2-dihydroceramide on both

synaptobrevin and neurotransmission suggests that the enhanced neurotransmitter release after neuronal incubation with positive regulators of synaptobrevin is not an indirect effect of addition of any sphingosine derivative.

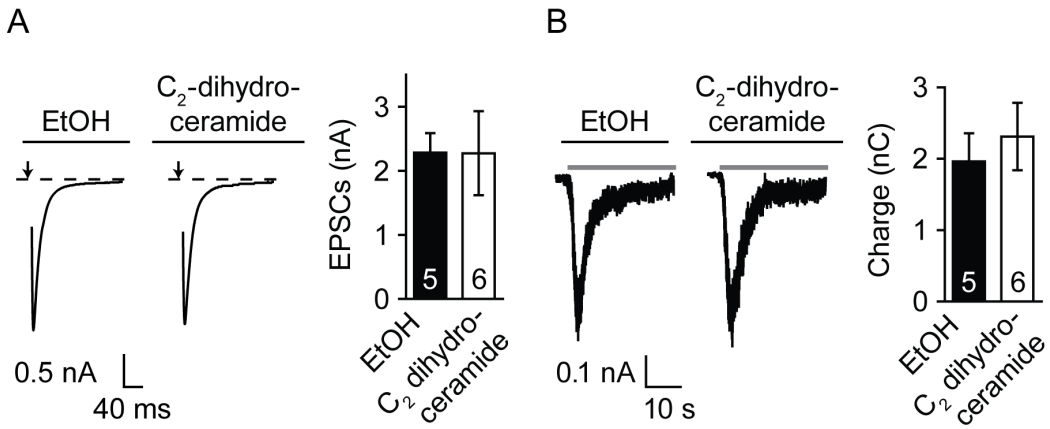

Figure 5.2.3.3 Addition of C_2-dihydroceramide to hippocampal neurons does not affect the neurotransmitter release evoked by either field potentials or hypertonic sucrose.

(A) Field potential stimulation: Left panel, representative traces of excitatory postsynaptic currents (EPSCs) evoked by field potential stimulation in wild-type rat hippocampal neurons (DIV 15-20) after a 10 minute treatment with 50 µM C_2-dihydroceramide (C_2-dihydroceramide) or an equal volume of vehicle (Ethanol, EtOH). Right panel, a summary graph depicting no significant change in the average maximum EPSC amplitudes from neurons treated with C_2-dihydroceramide compared to EtOH-treated neurons.
(B) Hypertonic sucrose stimulation: Left panel, representative current traces from EtOH- and C_2-dihydroceramide-treated neurons after hypertonic sucrose application. Right panel, graph summarizing the average charge transfer during the first 10 s of the 30 s hypertonic sucrose stimulation depicting no significant difference between the charge of the responses from C_2-dihydroceramide- and EtOH-treated neurons.
Error bars represent the SEM. Arrows indicate the application of current. Gray bars represent the presence of 500 mM sucrose. (EtOH, n=5; C_2-dihydroceramide, n=6)

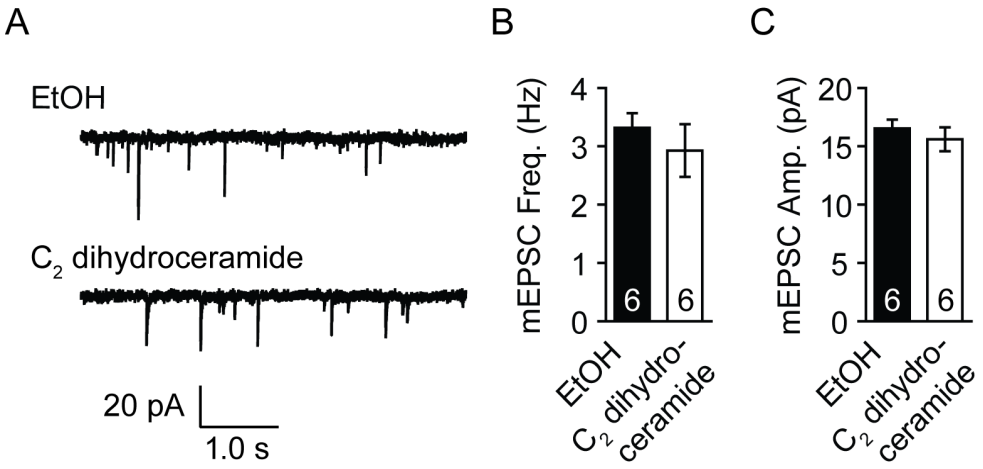

Figure 5.2.3.4 C_2-dihydroceramide addition does not affect spontaneous neurotransmitter release in hippocampal neurons.

(A) Representative traces of miniature EPSCs (mEPSCs) current recordings wild-type rat hippocampal neurons (DIV 15-20) incubated for 10 minutes in 50 µM C_2-dihydroceramide (C_2-dihydroceramide) or an equal volume of vehicle (ethanol, EtOH). (B) Graph summarizing the average frequency of mEPSC events depicting no change in the rate of mEPSC events after C_2-dihydroceramide addition compared to EtOH- treated neurons. (C) Plot of the average amplitude of mEPSC event showing no significant differences between the groups.
(B) Hypertonic sucrose stimulation: Left panel, representative current traces from EtOH- and C_2-dihydroceramide-treated neurons after hypertonic sucrose application. Right panel, graph summarizing the average charge transfer during the first 10 s of the 30 s hypertonic sucrose stimulation depicting no significant difference between the charge of the responses from C_2-dihydroceramide- and EtOH-treated neurons.
Error bars represent the SEM. Arrows indicate the application of current. Gray bars represent the presence of 500 mM sucrose. (EtOH, n=5; C_2-dihydroceramide, n=6)

In summary, incubation of cultured neurons with sphingosine or sphinganine, both shown to enhance synaptobrevin activity (Fig. 5.1), results in the potentiation of excitatory neurotransmitter release (Figs. 5.2 and 5.2.3.1). Conversely, both synaptobrevin activity (Fig. 5.1) and neurotransmitter release remain unchanged in the presence of C_2-dihydroceramide, an ineffective synaptobrevin modulator (Fig. 5.2.3.3).

5.2.4 Inhibition of sphingosine conversion from ceramide does not affect neurotransmitter release

Sphingosine enhances synaptobrevin activity (Fig. 5.1) in a concentration-dependent manner, and neurons treated with sphingosine experience a synaptobrevin-dependent increase in neurotransmitter release (Fig. 5.2.2). Using two sphingosine derivatives, we demonstrated that the augmented synaptic transmission is most likely a result of the positive-regulation of synaptobrevin (Figs. 5.2.3.1 - 5.2.3.4).

To further test the effects of sphingosine manipulation, we incubated neurons with the ceramidase inhibitor, d-*erythro*-MAPP (d-MAPP, Calbiochem), which prevents the conversion of ceramide to sphingosine, thus decreasing the levels of sphingosine. We treated neurons with 20 µM d-MAPP or an equal volume of vehicle (ethanol, EtOH) for 30 minutes at room temperature and measured the properties of synaptic transmission. After d-MAPP treatment, the hypertonic sucrose response did not differ from vehicle-treated neurons (Fig. 5.2.4 A-B; $p = 0.64$; EtOH, 3.7 ± 0.8 nC; d-MAPP, 4.1 ± 0.5 nC). The mEPSC frequency (Fig. 5.2.4 C-D; $p = 0.11$; EtOH, 4.3 ± 1.8 Hz; d-MAPP, 10.9 ± 2.7 Hz) and amplitudes (Fig. 5.2.4 C and E; $p = 0.16$; EtOH, 19.7 ± 2.2 pA; d-MAPP, 24.1 ± 1.9 pA) were also unchanged.

This data indicates that decreased sphingosine levels do not result in altered neurotransmission. In addition, d-MAPP is also an ineffective regulator of

synaptobrevin, providing more support for the direct connection between synaptobrevin modulation and the efficiency synaptic transmission.

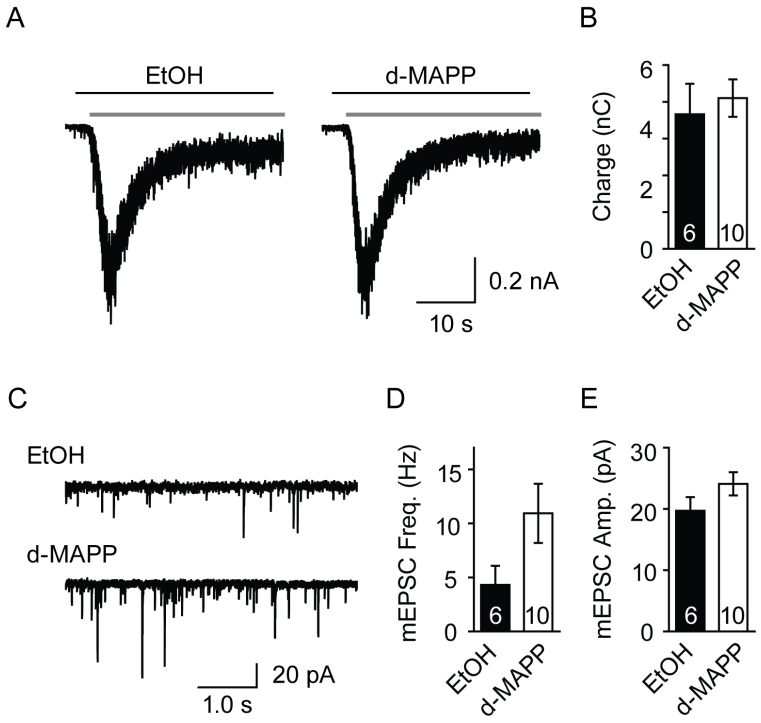

Figure 5.2.4 Inhibition of sphingosine conversion from ceramide by d-*erythro*-MAPP in hippocampal neurons does not affect neurotransmitter release.

(A-B) Hypertonic sucrose stimulation of EtOH- and d-MAPP- treated neurons: (A) Representative traces neurons treated with EtOH or d-MAPP. (B) Summary graph of the average charge transfer during the first 10 s of the 30 s hypertonic sucrose stimulation displaying no significant difference between the charge of responses from d-MAPP- and EtOH-treated neurons.
(C-E) mEPSC frequency and amplitudes from neurons treated with EtOH or d-MAPP. (C) Representative traces of miniature EPSCs (mEPSCs) recordings from wild-type rat hippocampal neurons (DIV 15-20) incubated for 10 minutes with 20 µM d-*erythro*-MAPP (d-MAPP) or an equal volume of vehicle (ethanol, EtOH). (D) Summary plot of the average frequency of mEPSC events depicting significant difference between neurons treated with d-MAPP and EtOH- treated neurons. (E) Graph summarizing the average amplitude of mEPSC events showing no significant differences between the groups. Error bars represent the SEM. Gray bars represent the presence of 500 mM sucrose. (EtOH, n=6; d-MAPP, n=11)

5.3 Summary

Synaptobrevin is a key player in the release of neurotransmitter. The binding of vesicular synaptobrevin to syntaxin and SNAP-25 on the plasma membrane provides vesicles with the ability to approach and stay in close proximity to the plasma membrane. This proximity allows for the synchronous vesicle fusion after action potential-driven Ca^{2+} influx (references for SNARE KOs). Sphingosine, as well as other sphingosine derivatives, positively regulates synaptobrevin binding to the plasma membrane SNARE proteins (Fig. 5.1). Incubation of neurons with these modulators also enhances neurotransmission (Fig 5.2.2 and 5.2.3.1 and 2). However, neuronal synaptic function is unchanged after treatment with either ineffective modulators of the vesicular SNARE protein (Figs. 5.2.3.3, 5.2.3.4, 5.2.4) or an inhibitor of sphingosine production (Fig 5.2.4). Thus, enhanced synaptobrevin activity appears to be a directly related to the augmented synaptic function.

5.4 Methods

5.4.1 Cell culture

Synaptobrevin-2-deficient dissociated cortical cultures (courtesy of Dr. Thomas C. Südhof) were prepared following previously published protocols (Schoch et al., 2001). The cortex was dissected and dissociated from embryonic day 18, and dissociated cells were plated on zero-thickness 12-mm glass coverslips and stored at 37°C with 5% CO_2 in a humidified incubator. For wild-type rat hippocampal cultures, the hippocampus was dissected and dissociated from postnatal day 0-3

(P0-3) Sprague-Dawley rats as previously described in (Kavalali et al., 1999). Dissociated cells were plated on zero thickness 12-mm glass coverslips and stored at 37°C with 5% CO_2 in a humidified incubator.

5.4.2 Electrophysiology

A modified Tyrode's solution was used for all experiments (except where noted otherwise) that contained (in mM): 145 NaCl, 4 KCl, 2 $MgCl_2 \bullet (6H_2O)$, 10 glucose, 10 HEPES, 2 $CaCl_2$ (pH 7.4, osmolarity 300 mOsM). Pyramidal neurons were whole-cell voltage clamped at –70 mV with borosilicate glass electrodes (3-5 MΩ). Electrode solutions contained (in mM): 105 Cs-methanesulphonate, 10 CsCl, 5 NaCl, 10 HEPES, 20 TEA.Cl hydrate, 4 Mg-ATP, 0.3 GTP, 0.6 EGTA, 10 QX-314 (pH 7.3, osmolarity 290 mOsM). To measure excitatory postsynaptic current (EPSC) amplitudes, neurons were washed with a modified Tyrode's solution containing 50 μM PTX and 50 μM AP5 (DL-2-Amino-5-phosphonovaleric acid, NMDA receptor blocker), and field potentials were induced with a 0.1-ms pulse of 10 mA of current through a bipolar platinum electrode. Hypertonic sucrose responses were recorded by infusing modified Tyrode's solution containing 500 mM sucrose and 1 μM TTX with 50 μM PTX for 30 seconds. Spontaneous neurotransmitter release was measured by recording miniature EPSC (mEPSC) frequency and amplitudes in a modified Tyrode's solution containing 1 μM TTX, 50 μM PTX and 50 μM AP5.

5.4.3 Sphingosine addition

Cortical cultures (10-21 days in vitro, DIV) were treated with sphingosine (50 μM, Sigma) for 10 minutes at room temperature (22-25°C). Briefly, 2 μl of 50 μM sphingosine (in ethanol) or an equal volume of ethanol was added to 2 ml of modified Tyrode's solution. After treatment, the cells were washed thoroughly and then experiments were performed.

5.4.4 Sphinganine Addition

Rat hippocampal cultures (15-21 DIV) were treated with sphinganine (50 μM, Biomol) for 10 minutes at room temperature (22-25°C). Briefly, 2 μl of 50 mM sphinganine (in warm DMSO) or an equal volume of DMSO was added to 2 ml of modified Tyrode's solution containing 1 μM TTX, 50 μM PTX, and 50 μM AP5. After treatment, the cells were washed thoroughly (10 minutes) and then experiments were performed.

5.4.5 C_2-Dihydroceramide Addition

Rat hippocampal cultures (15-21 DIV) were treated with C_2-dihydroceramide (50 μM, Biomol) for 10 minutes at room temperature (22-25°C). Briefly, 40 μl of 2.5 mM C_2-dihydroceramide (in ethanol, EtOH) or an equal volume of EtOH was added to 2 ml of modified Tyrode's solution containing 1 μM TTX, 50 μM PTX, and 50 μM AP5. After treatment, the cells were washed thoroughly (10 minutes) and then experiments were performed.

5.4.6 d-*erythro*-MAPP (D-MAPP) treatment

Rat hippocampal cultures were treated with 20 μM d-erythro-MAPP (d-MAPP, Calbiochem) for 30 minutes at room temperature., A 2 μl aliquot of 20 mM d-MAPP (in ethanol) or an equal volume of vehicle was added to 2ml of modified Tyrode's solution containing 1 μM TTX and 50 μM PTX. Neurons were washed and then experiments were performed.

5.4.7 Statistical Analysis

The Student's t-test (two-tailed) was used for pair-wise comparisons.

CHAPTER 6: LONG-TERM RECYCLING SYNAPTIC VESICLE POOL STABILITY

6.1 Background

Vesicles residing in a synapse play different roles in synaptic transmission. As described in detail in the introduction, these roles define several synaptic vesicle pools. The vesicles which fuse in response to action potentials, as well as hypertonic sucrose application, belong to the recycling pool and make up approximately ten to twenty percent of the entire synaptic population. The remaining vesicles constitute the resting pool, which remains dormant even during extreme stimulation, i.e. high K^+ depolarization. What we scientists have yet to show is whether these vesicle pools are stable or dynamic. Do the same vesicles of the recycling pool continually occupy this group or do they switch around with the resting pool? To address this question, I employed several approaches to investigate not only the stability of the recycling, but also the origin and reuse of vesicles which fuse spontaneously.

6.2 Results

6.2.1 Recycling vesicle pool does not mix with the resting pool for up to six hours

To explore the dynamics of recycling vesicles over time, I depolarized the membranes of dissociated rat hippocampal neuron cultures in the presence of the fluorescent dye FM1-43. This lipophilic dye enters into exocytosing vesicles and

takes the dye up upon endocytosis. FM1-43 incorporates into the vesicle membrane and fluoresces, where upon subsequent fusion of these vesicles results a visible fluorescence decrease as the dye escapes into the synaptic cleft. This method is commonly used to measure the properties of the recycling vesicle pool, such as total vesicle pool size as well as the rate of vesicle reavailability. However, to determine how long recycling vesicles reside within this pool, ChiHye Chung began these experiments by labeling recycling pool vesicles during depolarization with FM1-43 and waiting from one to four hours before observing the release of the dye. I picked up these experiments with incubations of four to twenty-four hours (Figs. 6.2.1 and 6.2.2.1). This method addresses whether recycling pool vesicles become dormant over time or remain active. If these vesicles remain within the function recycling pool during prolonged periods, then the dye within them will be readily available for release. Alternatively, if they switch out with vesicles from the resting pool or even fuse spontaneously, then the amount of dye available will decrease and may also affect the kinetics of the fluorescence loss (due to the simultaneous fusion of new non-fluorescent vesicles after extended incubation). As a control, in the same synapses, I measured the normal size and functional properties of the recycling pool for each synapse after completing the experiment. More precisely, after releasing all available dye, I repeated the FM1-43 uptake and release to define the basal recycling pool size and rates of dye release for each bouton and used this

information to determine whether the recycling pool is stable or dynamic over time.

I first examined the effect of a one hour delay before releasing FM1-43 from recycling pool vesicles. Interestingly, the rate and the amount of fluorescence lost were comparable to the basal properties of each synapse (Fig. 6.2.1 C-D). I observed similar results when I increased the delay to two, four and even six hours (Fig.6.2.1 B, E-J), which suggests that the recycling pool is highly stable and that the resting pool of vesicles may be intrinsically fusion-incompetent rather than just slow in their mobility for up to six hours.

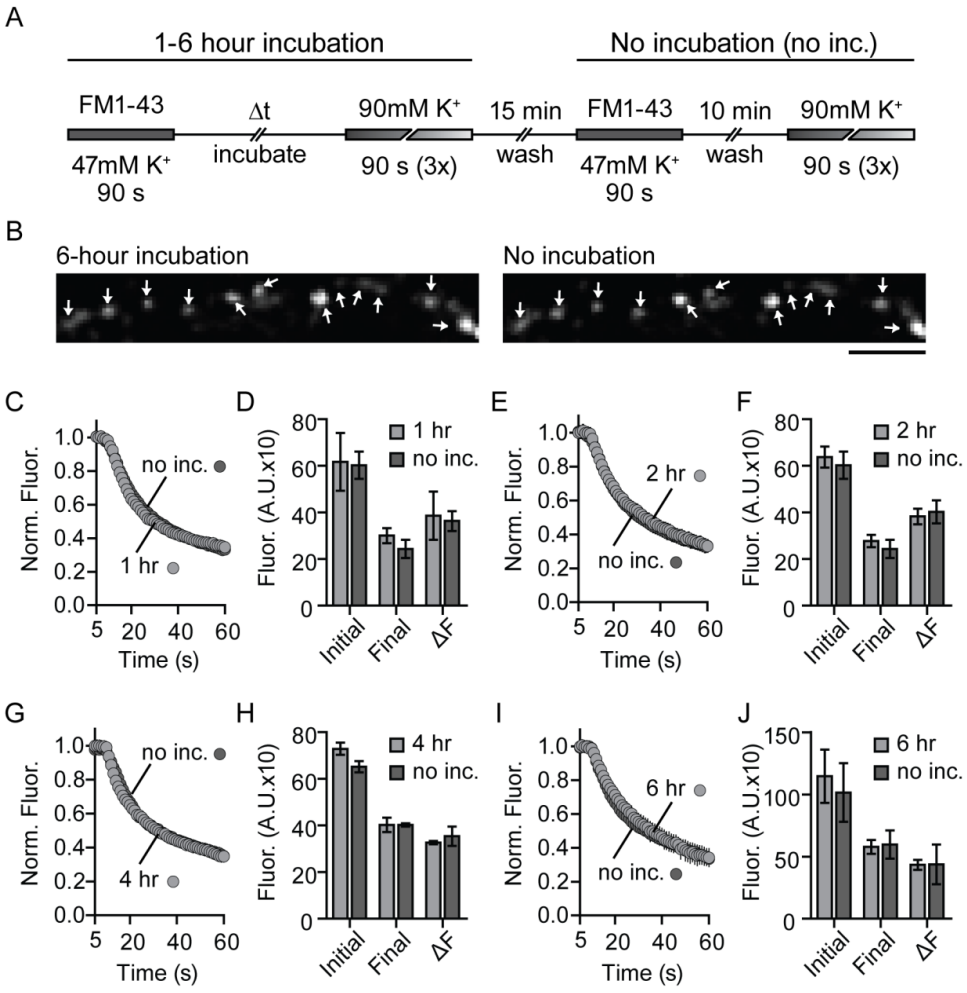

Figure 6.2.1 Vesicles of the recycling pool remain active up to six hours.

(A) Diagram of the protocol used for the uptake and release of FM1-43 (B) Sample images of fluorescent of boutons 6 hours after FM1-43 uptake (left) and of the same synapses labeled again after washing for only 10 minutes (right).
(C, E, G, I) Summary plot of the average normalized fluorescence loss during stimulation after incubation for the indicated time displaying no significant changes in the rate of dye release in synapses incubated for 1 hour (C), 2 hours (E), 4 hours (G) or 6 hours (I) compared to the rate of release in the same synapses without incubation.
(D, F, H, J) Average quantity of the fluorescence values before (initial) and after (final) dye release along with the amount of dye released (DF, initial minus final) showing no significant differences between any parameter for synapses washed for 1 hour (D), 2 hours (F), 4 hours (H) or 6 hours (J) compared to the values measured in the same synapse after washing for only 10 minutes.
Error bars represent the SEM. (1-hr, n=3 coverslips (180 boutons total); 2-hr, n=4 (275); 4-hr, n=3 (300); 6-hr, n=3 (180)). (A.U. arbitrary fluorescence units, scale bar= 2 μm)

6.2.2 Recycling vesicle pool does not mix with a resting pool for up to 24 hours

To determine whether the stability of the recycling pool continues past 6 hours, I repeated the FM1-43 experiments with the delay extended to 24 hours. To do this, I had to stimulate cultures with a high K^+ buffer containing FM1-43 under sterile conditions so that I could replace the culture medium and place them back in to the incubator without contamination. Because I was changing the protocol, I repeated the 6 hour delay experiment at 37°C as well to control the new variable. The nature of these experiments depends on our ability to differentiate between FM dye trapped and FM dye lost spontaneously during incubation.

After incubation for 6 hours at 37°C in the absence of action potentials, I stimulated the FM1-43 synapses and measured the fluorescence values as well as the loss over time. The rate of fluorescence loss was not altered after the incubation period as determined by the rate of loss in the same synapses after the experiment (Fig. 6.2.2.1 C). The initial fluorescence present within the synapse after incubation as well as the total amount of dye release was also not significantly different, however both showed a noticeable downward trend (Fig 6.2.2.1 D). These results are consistent with the data gathered from the six hour incubation at room temperature (Figure 6.2.1 I-J) indicating no major effect of increased temperature on the vesicle dynamics. Interestingly, only 12% of the total recycling pool contained FM1-43 after the 24-hour incubation as inferred

from the quantity of the total recycling pool at these synapses after the experiment (Fig. 6.2.2.1F). The remaining dye released with normal kinetics (Fig 6.2.2.1 E). I observed a marked decrease in the amount of fluorescence initially present after incubation just by looking at the neurons. I found a region of the coverslip where I could distinguish fluorescent boutons to assure a proper focus. By selecting boutons to image from the second round of FM1-43, I was able to measure the amount of dye initially present. Only 40% of the FM1-43 in the original recycling pool remained after incubation compared to the initial fluorescence in the following FM1-43 uptake and release experiment performed afterward in the same synapses. The total quantity of initial fluorescence and amount of dye released both show a similar decrease in intensity suggesting that these reductions are due to slow spontaneous fusion of FM1-43 from the recycling pool dye during the 24-hour incubation.

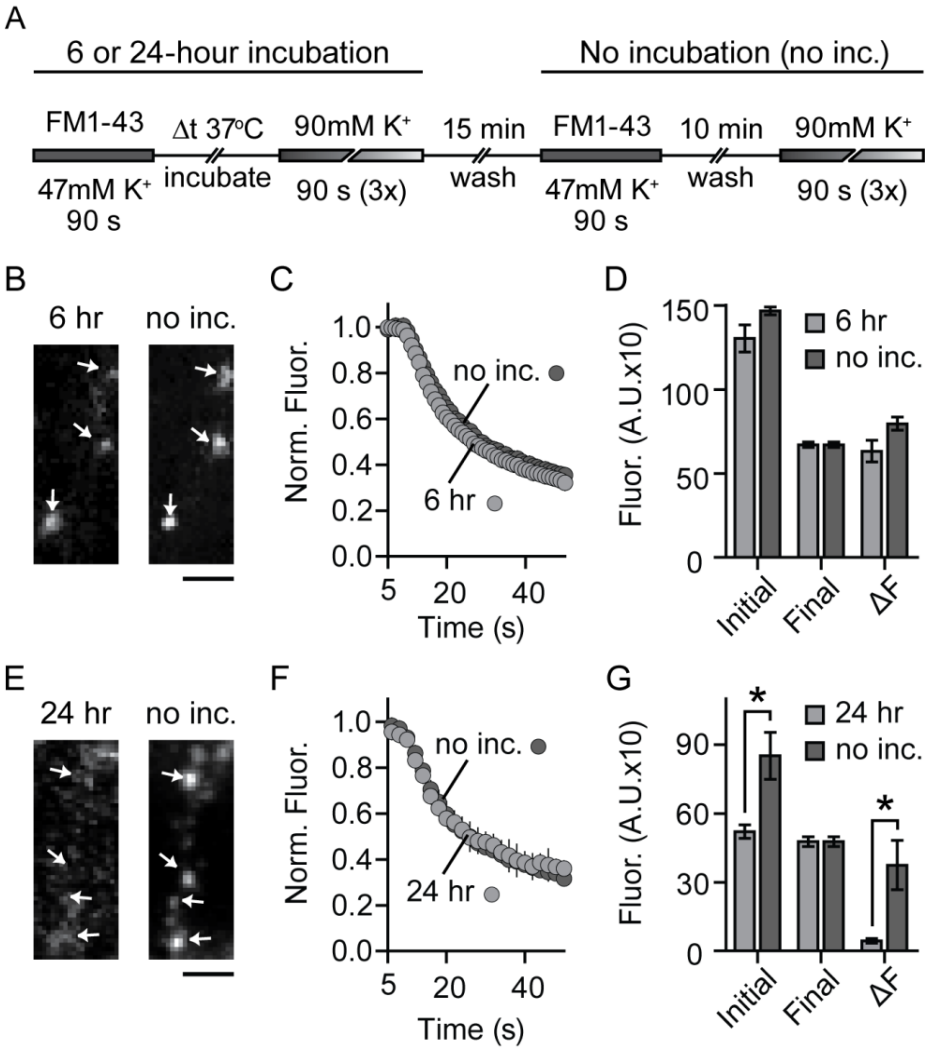

Figure 6.2.2.1 Recycling pool vesicles begin to fuse spontaneously after six hours at physiological temperatures.

(A) Diagram of the protocol for FM1-43 uptake and the release of dye after 6- or 24-hour incubation at 37°C in the absence of action potentials (using tetrodotoxin, TTX) (left) and the following uptake and release without incubation in the same synapses (right). (B-D) Six-hour incubation of recycling pool vesicles labeled with FM1-43. (B) Fluorescent images before dye release after incubating for 6 hours (left) and the following initial fluorescence in the same boutons after washing for only 10 minutes (right). (C) Summary plot of the average rate of fluorescence lost during stimulation depicting no change in the rate of dye release from boutons incubated 6 hours after FM1-43 uptake and the subsequent rate in the same synapses without incubating. (D) Quantity of the average fluorescence before (initial) and after (final) dye release along with amount of dye released (ΔF, initial minus final) showing a non-significant decrease in the

quantity of dye released after a 6-hour incubation (1.1-fold, p=0.12) compared to the amount of dye released from the recycling pool of the same synapse. The initial fluorescence values are also less but not significantly (1.3-fold, p=0.10).
(E-G) Incubation of FM1-43 labeled recycling pool vesicles for 24 hours in the absence of action potentials. (E) Sample fluorescent images before dye release in boutons labeled with FM1-43 after a 24-hour incubation (left) and the same synapses relabeled after washing for only 10 minutes (right). (F) Average rate of dye release from recycling pool vesicles labeled with FM1-43 24 hours before and the rate of dye release from the total recycling pool of vesicles labeled in the same synapses show no change in the kinetics of dye release from vesicles still containing FM1-43. (G) Chart summarizing the fluorescent values of boutons before and after dye release as well as the amount of dye available for release (ΔF) after a 24-hour incubation or after dye uptake in the same synapses showing a significant decrease in the amount of dye initially present after incubation (1.6-fold) compared to the capacity of those same synapses at the times of dye release. The total fluorescence lost (ΔF) is also significantly less after the prolonged incubation (8.3-fold). Error bars represent the SEM. (6 hr: n=3, 180 boutons total; 24 hr: n=3, 150 boutons)) (A.U. arbitrary fluorescence units, scale bar = 2μm; * p<0.02)

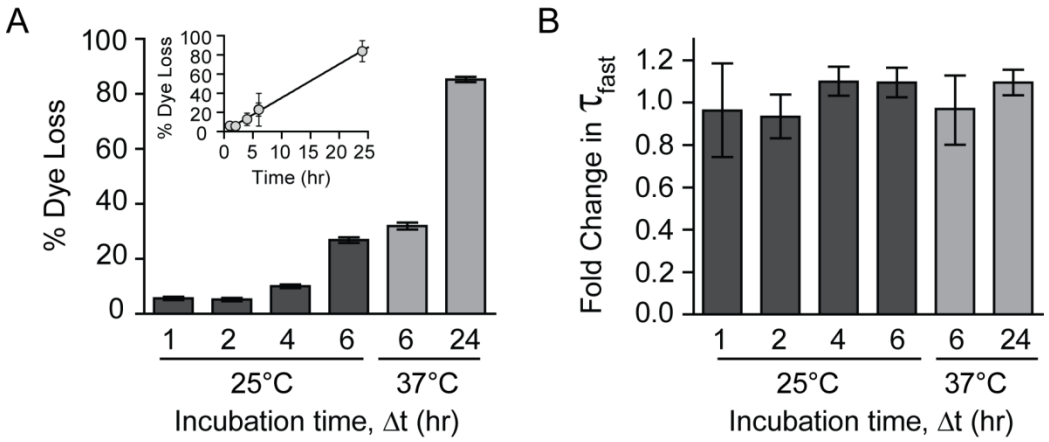

Figure 6.2.2.2 Recycling pool vesicles resist spontaneous fusion up to six hours and remain fusion competent up to twenty-four hours.

(A) Summary graph of the average percent spontaneous dye loss from the activity-dependent recycling pool during the periods of incubation (Δt) determined by comparing the amount of dye released from the recycling pool after completely releasing the FM1-43 available after incubation. Between one and six hours at 25°C, the average percent of spontaneous dye loss from labeled recycling pool vesicles is less than 20%. However after 6 and 24 hours at 37°C (grey bars), the average percent dye loss increases to 40 and 90%, respectively. Inset line graph represents the rate of % dye loss per time displaying a rate of 3.5% loss per hours (R^2 = 0.995). (B) Summary graph of the average fold change the rate of the fast component of fluorescence loss in vesicles still containing dye after

incubation compared to the rate of the rate of release from the total active recycling pool showing no significant change in the kinetics of dye release.
Error bars represent the SEM. (1 hr n=3 (180), 2 hr n=4 (275), 4 hr n=3 (300), 6 hr n=3 (180), 6 hr n=3 (180), 24 hr n=3 (150))

6.2.3 Ultrastructural investigation of spontaneous fusion of recycling pool and spontaneously fusing vesicles

The resistance to spontaneous fusion of recycling pool vesicles measured by FM1-43 imaging experiments make a strong case for a separate pool of spontaneously fusing vesicles. I wanted to look more closely at the difference between the spontaneous fusion of vesicles from these seemingly independent pools. To do this, I incubated dissociated hippocampal cultures in the presence of HRP in either high K^+ for 90 seconds or TTX for 15 minutes. After the high K^+ uptake of HRP, I washed away the HRP and either immediately fixed the neurons or incubated them for 6 hours at 37°C in the presence of TTX before fixing. For synapses incubated with HRP in the absence of action potentials, I fixed cultures immediately after washing away the HRP fixed or incubated these cultures for another 30 minutes prior to fixing. In both cases, after fixing, Xinran Liu captured electron micrograph images of synapses after applying DAB (which reacts with HRP and produces an electron dense substance within the HRP containing vesicles) (Fig. 6.2.3 A, D). Once imaged, I quantified the percent of HRP-labeled vesicles in each synapse and inferred the percent of vesicles that fused spontaneously by comparing incubated synapses to those washed immediately.

After the uptake of HRP in high K^+, approximately 80% of the HRP-positive recycling pools vesicles were present after the 6-hour incubation in TTX compared to those in non-incubated cultures (Fig. 6.2.3 B-C). This indicates that about 20% of HRP-positive recycling pool vesicles fuse spontaneously and release HRP over 6 hour. These results match well with the data obtained from the 6-hour incubation of FM1-43 labeled recycling pool vesicles (Figure 6.2.1, 6.2.2.1-2).

The 30-minute incubation of HRP containing spontaneous vesicles resulted in a 50% decrease in the number of HRP+ vesicles. While spontaneous fusion occurred from the recycling pool and from spontaneously fusing vesicles, the rate of fusion was significantly slower from the recycling pool compared to the vesicles labeled spontaneously. The spontaneously fusing vesicles could be from the recycling pool; however if all recycling vesicles can fuse spontaneously, then I would not see as much spontaneous loss from spontaneously-labeled vesicles due to exocytosis of other recycling pool vesicles. This suggests that vesicles fusing spontaneously prefer re-exocytosing in the absence of action potentials.

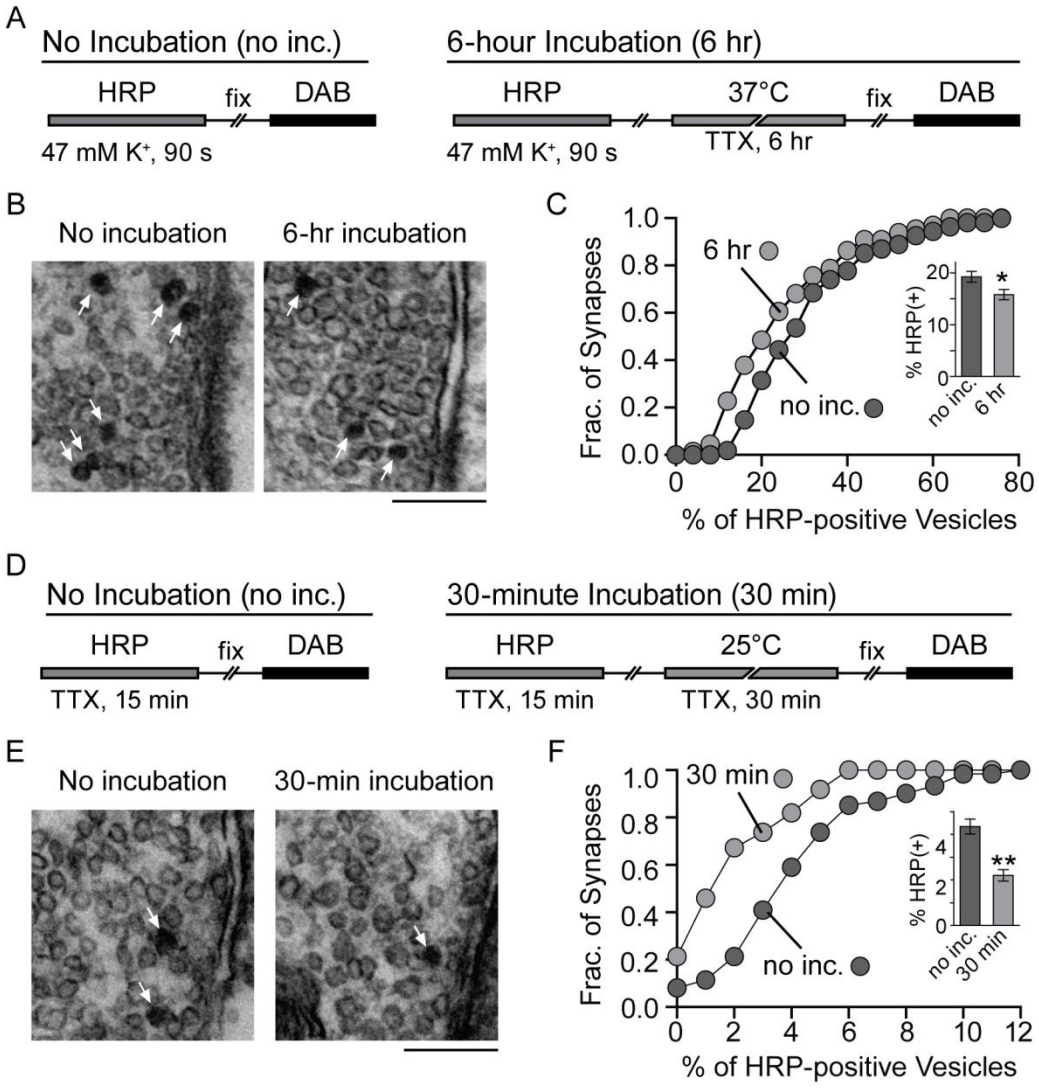

Figure 6.2.3 Ultrastructural analysis of spontaneous vesicle fusion from recycling pool and spontaneously fusing vesicles

(A-C) Quantization of spontaneous fusion of recycling pool vesicles over 6 hours at physiological temperature (A) Diagram depicting the experimental protocol: Briefly, dissociated hippocampal cultures were depolarized in the presence of HRP to label the recycling pool with HRP. Neurons were then washed and fixed or washed and incubated for 6 hours at 37°C before fixing. Vesicles containing HRP were then visualized by electron microscopy after reacting HRP with DAB creating and electron dense material in HRP-containing vesicles. (B) Representative electron micrograph images. (C) Cumulative histogram of the percent of HRP-positive (HRP+) vesicles per synapse in cultures maximally loaded with HRP with or without a 6-hour incubation. The average percent of HRP+ vesicles are represented in the inset graph. These plots depict an 18%

decrease in the percent of HRP+ vesicles per synapse in cultures incubated for 6 hours, which indicates that 18% of recycling pool vesicles fuse spontaneously over 6 hours. (no inc. n=56, 6 hr inc. n=57)
(D-F) Spontaneous fusion of spontaneously fusing vesicles over 30 minutes (A) Diagram of the experiment. Briefly, dissociated hippocampal cultures were incubated in HRP with TTX and either immediately washed and fixed or incubated for 30 minutes in TTX before fixing. Cultures were treated with DAB to react with HRP making an electron dense substance and then synapses were imaged by electron microscopy. (B) Representative images. (C) Cumulative histogram of the percent of HRP-positive (HRP+) vesicles per synapse in cultures containing spontaneously labeled with HRP and either incubated for 30 minutes or immediately washed before fixing. The inset plot depicts the average percent of HRP+ vesicles. These graphs depict a 50% loss in the percent of HRP+ vesicles per synapse in cultures incubated for 30 minutes before fixing. (no inc. n=61, 30 min inc. n=61)
Error bars represent the SEM. (*$p<0.02$, **$p<0.0001$; scale bar = 200 nm)

6.2.4 Prolonged treatment with folimycin selectively impairs spontaneous neurotransmission

Folimycin inhibits the reacidification of exocytosed vesicles preventing neurotransmitter refilling. To investigate whether spontaneously fusing vesicles participate in Ca^{2+}-dependent neurotransmission, I incubated primary dissociated hippocampal cultures with folimycin (10 nM in DMSO) or DMSO only for 1 hour in a 37°C incubator. I added tetrodotoxin (TTX) during the incubation to prevent spontaneous action potential firing, thus exposing only spontaneously fusing vesicles to the membrane-impermeable folimycin. After incubating and washing with either DMSO only or folimycin, I measured the charge of 1 second of spontaneous release as well as the charge recorded for responses after hypertonic sucrose (10 seconds) and field potential stimulated EPSCs (100ms). After exposing spontaneously fusing vesicles to folimycin for one hour, the charge of

both the first 10 seconds of the hypertonic sucrose response and 100 ms of the field stimulation evoked excitatory postsynaptic currents (EPSCs) decreased 4-fold compared to DMSO-treated cultures (Fig.6.2.4 B-E, H). The mEPSCs amplitude and frequency were 2- and 12-fold less in folimycin-treated neurons (respectively, data not shown) compared to treatment with DMSO alone, and the charge over one minute was decreased 20-fold (Fig. 15B-C, H). These results demonstrate that while hypertonic sucrose responses and field potential stimulated EPSCs attenuate after folimycin treatment, blocking neurotransmitter refilling in spontaneously fusing vesicles affects spontaneous neurotransmission more dramatically.

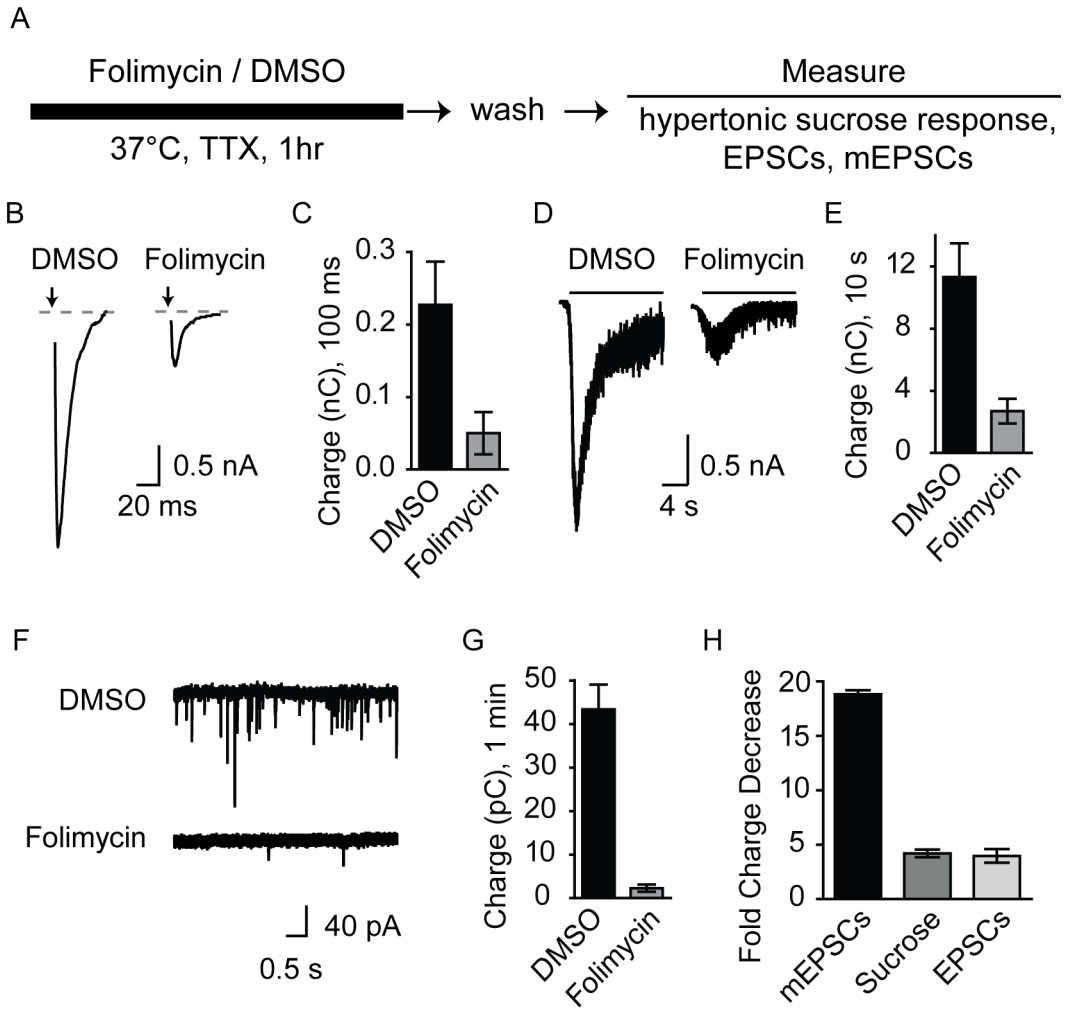

Figure 6.2.4 Prolonged treatment with vacuolar ATPase blocker folimycin selectively impairs spontaneous neurotransmission

(A) Diagram of the experimental procedure depicting the one hour incubation with folimycin in the absence of action potentials to block neurotransmitter refilling in spontaneously fusing vesicles.
(B-C) Hypertonic sucrose response recorded after DMSO or folimycin treatment (B) Representative traces (black bar represents the presence of sucrose solution). (C) Average charge of the first 10 s of the hypertonic sucrose response showing a 4-fold decrease in the charge of the responses after folimycin treatment compared to DMSO-treated neurons.
(D-E) EPSCs recorded after DMSO or folimycin treatment (D) Representative traces (black arrow represents the onset of stimulation). (E) Plot of the average charge of the first 100 ms of the EPSC after treatment depicting a 4-fold decrease in the charge in folimycin-treated neurons compared to neurons incubated with only DMSO.

(F-G) mEPSCs recorded after DMSO or folimycin treatment. (F) Representative traces (G) Summary chart of the average charge of mEPSC events over one minute showing a 20-fold decrease in the charge after folimycin treatment compared to DMSO-treated neurons.
(H) Average fold decreases in the charge showing an approximate 20-fold decrease in the mEPSC charge compared to only a 4-fold decrease in the hypertonic sucrose and EPSC charge after folimycin treatment.
Error bars represent the SEM. (n=5)

6.3 Summary

Of the total vesicles within a synapse only twenty to thirty percent of actively recycle. To determine if dormant vesicles replenish the active recycling pool over time or remain inactive, I observed the fate of these vesicles by tagging synaptic vesicles and examining them after between one to twenty-four hours after labeling them. Prolonged monitoring of the recycling synaptic vesicle pool revealed that this pool is stable for up to at least six hours and infrequently fuse spontaneously as indicated by HRP and FM dye experiments. This is inconsistent with the proposal that all vesicles are the same, because spontaneous vesicles recycle at a rate of 4 % per 15 min, while actively recycling vesicles fuse spontaneously at a rate four times slower. If all vesicles are the same then the recycling pool would experience a great deal more spontaneous fusion. Interestingly, after leaving synapses containing fluorescently labeled recycling pool vesicles for 24 hours, I observed a dramatic reduction in the amount of fluorescence present, indicating that about 90% of the recycling pool fused spontaneously during the incubation. In addition, the vesicles still containing dye

fused at the same rate as the active recycling pools at those synapses. From these results, I conclude that at rest the total recycling pool is stable and resists spontaneous fusion.

6.4 Methods

6.4.1 Cell culture

Dissociated hippocampal cultures were prepared from Sprague-Dawley rat pups at postnatal day 0-3(P0-P3) or using previously published protocol (Kavalali et al., 1999). All experiments were performed during 14–25 days in vitro (DIV)

6.4.2 Fluorescence imaging

Synaptic boutons were loaded with 8 μM FM1-43 (Molecular Probes, Eugene, OR) under conditions described in Results. The modified Tyrode's solution used in all experiments contained (in mM): 150 NaCl, 4 KCl, 2 $MgCl_2$, 10 glucose, 10 HEPES, and 2 $CaCl_2$, (pH 7.4, ≈ 310 mOsm). High K^+ solutions contained equimolar substitution of KCl (90 mM) for NaCl. All staining and washing protocols were performed with 10 μM 6-cyano-7-nitroquinoxaline-2,3-dione (CNQX) and 50 μM aminophosphonopentanoic acid (AP-5) to prevent recurrent activity. Maximal loading of the total recycling pool was performed by incubating cultures in a 47 mM K^+ solution (1:1 solution, modified Tyrode's solution: 90 mM K^+ Tyrode's solution) for 90 s, which labels all of the recycling vesicle pool in a given synapse (Harata et al., 2001). To load spontaneous vesicles, cultures were incubated in a modified Tyrode's solution containing 1 μM TTX, which inhibits action potentials induced by network activity inherent in the culture. In a typical experiment, high potassium challenge was applied at least three times (for 60-90 s each separated by 60 s intervals) to release all of the dye trapped in presynaptic terminals. Images were taken after 10-min washes in dye-free

solution in nominal Ca^{2+} to minimize spontaneous dye loss. In all experiments I selected isolated boutons (1 μm^2) from maximally labeled synaptic boutons for analysis and avoided apparent synaptic clusters (Kavalali et al., 1999b). All statistical analyses were performed using ANOVA using the number of coverslips as n unless stated otherwise. Experimental results are represented as mean ± SEM.

Room temperature experiments: Recycling vesicles were maximally filled with FM1-43 (16 µM) by incubating neurons in a high K^+ modified Tyrode's solution containing 47 mM K^+, 2 mM Ca^{2+} for 90 s. After washing with a nominal Ca^{2+}, dye-free Tyrode's solution for 1, 2, 4 or 6 hours, synaptic terminals challenged with a 90 mM K^+ Tyrode's solution three times for 60 s (each followed by a 60-s wash with Tyrode's solution). The cells were given a brief rest (10 min) and the same experiment was repeated, except the wash time after loading was reduced to 10 minutes.

Physiological temperature experiments: For experiments in which cells were incubated at 37°C, cells were loaded with FM1-43 in a sterile hood and incubated at 37°C in 5% CO_2/ 95% air for 6 or 24 hours in the original medium containing 1-5 µM TTX. After incubation, the fluorescence loss was measured during three rounds of 90 mM K^+ perfusion, and the monitoring FM1-43 and release experiment was repeated in the same synapses as described above. All solutions were sterile for the initial uptake of FM1-43. The field of view was selected during the wash, and fluorescence changes were recorded during the perfusion of 90mM K^+ for analysis. Images were obtained by a cooled, intensified digital CCD camera (Roper Scientific, Trenton, NJ) during illumination (1 Hz and 100 ms) at 480 nm via an optical switch (Sutter Instruments, Novato, CA). Images were acquired and analyzed using Metafluor Software (Universal Imaging, Downingtown, PA).

6.4.3 Electron microscopy

For high K^+ loading, cells were treated with 47 mM K^+ and HRP (20 mg/ml, Sigma) containing Tyrode's solution for 90 s. Coverslips were quickly rinsed and either fixed for 30 min with 2% glutaraldehyde in 0.1 M sodium phosphate buffer, pH 7.4 at 37°C, or incubated in the original medium containing 1 µM TTX for 6 hours before fixing. For spontaneous loading, cells were treated with 4 mM K^+ Tyrode's solution containing HRP (20 mg/ml, Sigma) and 1 µM TTX for 15 min. Coverslips were quickly rinsed and either fixed for 30 min with 2% glutaraldehyde in 0.1 M sodium phosphate buffer, pH 7.4 at 37°C, or incubated in 4 mM K^+ Tyrode's solution containing 1 µM TTX for 30 min for before fixing. For 3,3′-diaminobenzidine (DAB) reaction, coverslips were incubated in Tris-Cl buffer (100 mM, pH = 7.4) containing DAB (0.1%) and H_2O_2 (0.02%) for 15 min. They were then rinsed twice in buffer and incubated in 1% OsO_4 for 30 min at room temperature. After rinsing with distilled water, specimens were stained en bloc with 2% aqueous uranyl acetate for 15 min, dehydrated in ethanol, and embedded in Poly/Bed 812 for 24 hr. Sections (60 nm) were post-stained with uranyl acetate and lead citrate and viewed with a JEOL 1200 EX transmission microscope.

6.4.4 Electrophysiology

Folimycin (10 nM in DMSO, Calbiochem, La Jolla, CA) or an equal volume of DMSO only was added to the culture medium, and cultures were incubated in this solution at 37°C in 5% CO_2/95% air for 1 hour in the presence of 1 µM TTX. Following treatment, coverslips were transferred to a recording chamber and washed with modified Tyrode's solution for 5-10 minutes. Pyramidal cells were voltage clamped to –70 mV using whole-cell patch-clamp technique (electrode resistance 2-6 mΩ). Electrode solution contained (in mM): 115 Cs-$MeSO_3$, 10 CsCl, 5 NaCl, 10 HEPES, 0.6 EGTA, 20 TEA.Cl, 4 Mg-ATP, 0.3 Na_2GTP, and 10 QX-314 (Sigma, St Louis, MO, pH 7.35, 300 mOsm). An Axopatch 200B

amplifier and Clampex 9.0 software (Axon Instruments, Union City, CA) were used for acquiring the data. Recordings were filtered at 2 kHz and sampled at 5 kHz. For hypertonic sucrose recordings, a Tyrode's solution containing 500 mM sucrose and 1 µM TTX with 50 µM PTX was perfused over cultures for 30 seconds. EPSC measurements were performed using field stimulation with platinum electrodes at 20 mA for 1 ms per action potential in the Tyrode's solution containing 50 µM PTX. For spontaneous mEPSCs, recordings were performed in the modified Tyrode's solution containing 1 µM tetrodotoxin (TTX). All statistical comparisons were performed with two-tailed unpaired t test values are given as mean ± SEM.

CHAPTER 7: FREE RADICAL MODIFICATION OF SYNAPTIC VESICLES

7.1 Background

Are all vesicles the same? Is each vesicle competent to exocytose or are some vesicles better equipped? Techniques to isolate single synaptic vesicles do not currently exist. However the isolation of vesicles from many synapses is possible (Nagy et al., 1976, Huttner et al., 1983). Due to the inability to assay the compositions of individual vesicles, we cannot begin to understand the similarities or differences between vesicles within a single synapse. The field today commonly assumes that all vesicles are basically alike and interchangeable. The number of vesicles within a hippocampal synapse ranges from 50 to 200. Of these synaptic vesicles only 20-30% will participate in the release of neurotransmitter. Interestingly, the active synaptic vesicles appear to be separated into functionally separate groups, or pools. The synaptic vesicles participating in neurotransmission are the recycling pool. Of these, a small fraction preferentially fuses first, immediately after an action potential reaches the synapse and Ca^{2+} flows in. What drives the specific redirection of this readily releasable vesicle pool (RRP)?

Interestingly, a technique exists that prevents the fusion of lipid compartments with other membranes. This technique involves the introducing horse radish peroxidase (HRP) to the luminal domain of fusing lipid

compartments and then applying hydrogen peroxide (H_2O_2). The H_2O_2 passes through the membrane and reacts with HRP producing free radicals. The free radicals then attack surrounding molecules, changing their conformation and ultimately their ability to function properly. Using this technique, I attempted to modify synaptic vesicles and found that the formation of free radicals within vesicles not only fusing after several types of stimulations appear to differentially affect synaptic neurotransmission.

While I cannot directly prove the modification of vesicle components, the deficits in neurotransmission as well as the lack of this defect when a free radical absorbing antioxidant is present suggests that modifications do occur and are mediated by free radical formation. Therefore, from now on, I refer to the reaction of HRP and H_2O_2 as free radical formation or modification and assume that these free radicals do affect the composition of molecules within synaptic vesicles.

7.2 Results

7.2.1 Alterations in synaptic transmission after free radical formation in total recycling pool

To assess the effect of free radical formation on the vesicles of the recycling pool, I depolarized hippocampal neuron cultures with high K^+ in the presence of HRP for 90 seconds, to stimulate the fusion of recycling pool vesicles which then take up HRP during endocytosis. After thoroughly washing away HRP, I perfused

a H_2O_2 solution (0.02%) for 5 minutes followed by another 5 minute wash and patched pyramidal neurons to record mEPSCs and EPSCs (Fig. 7.2.1 A). If HRP is present within a vesicle, then H_2O_2 will react with the HRP to produce free radicals and modifying or inactivating proteins and/or lipids within the synaptic vesicle membrane.

After the high K^+ stimulated uptake of HRP and the following H_2O_2 perfusion, I observed a 2.7-fold increase in the average frequency of spontaneous neurotransmitter release (Fig.7.2.1B-C: Only HRP 2.1 ± 0.3 Hz, n=39; Only H_2O_2 2.1 ± 0.2 Hz, n=23; HRP+H_2O_2 5.8 ± 0.6 Hz, n=40, $p<<0.001$) without altering the amplitude of mEPSC events compared to cultures treated exactly the same except without HRP or without H_2O_2 (Fig.7.2.1B, D). Using the same comparison, I found the EPSC amplitudes decreased 4-fold (Fig. 7.2.1E-F: Only HRP 2.0 ± 0.1 nA, n=22; Only H_2O_2 2.3 ± 0.3 nA, n=13; HRP+H_2O_2 0.5 ± 0.1 nA, n=17; $p<<0.001$) with a significant increase in the rate of EPSC amplitude depression during a 1 Hz train of 100 field potential stimuli (AP) (Fig. 7.2.1 E, G). Thus this data demonstrates that the HRP and H_2O_2 treatment does affect the efficiency of the recycling vesicle, suggesting that free radicals are forming and affecting the efficiency of the vesicles containing them.

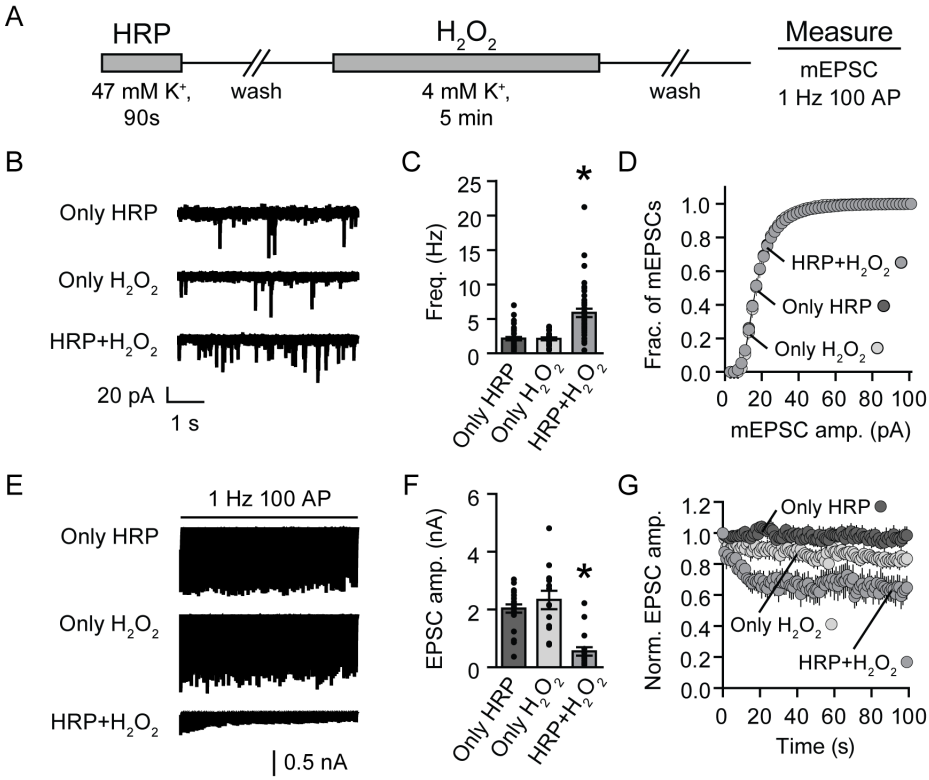

Figure 7.2.1 Reciprocal effect of chemical modification of recycling vesicles on spontaneous and Ca^{2+}-dependent fusing vesicles

(A) Diagram of the experiment: Hippocampal neurons were depolarized with a high K^+ buffer containing HRP for 90 s. HRP was washed out for 10 minutes, and H_2O_2 was perfused for 5 minutes then washed out for another 10 minutes. Neurons were patched and mEPSCs and EPSCs were recorded (HRP+H_2O_2). Control experiments (diagram not shown) were performed by omitting the HRP from the high K^+ buffer (Only HRP) or H_2O_2 from the 5 minute perfusion (Only H_2O_2).
(B-D) mEPSC frequency and amplitudes from control and treated neurons (B) Representative mEPSC recordings. (C) Plot summarizing the average frequency of mEPSCs before and after treatment. The average frequency increased 2.7-fold after chemical modification. (D) Distribution of mEPSC amplitudes showing no significant difference between groups. (Only HRP, n=39; Only H_2O_2, n=23; HRP+H_2O_2, n=40)
(E-G) EPSC amplitudes with and without treatment with both HRP and H_2O_2 (E) Representative traces of the first 40 ms of EPSCs recorded during 1 Hz train of 100 APs. (F) Summary graph of the average maximum EPSC amplitude showing an approximate 4-fold decrease in amplitude in treated neurons compared to controls. (G) Plot of EPSC amplitude per AP normalized to the first response. After treatment with both HRP and H_2O_2, EPSC amplitudes decreased faster compared to the rate of change in controls. (Only HRP, n=22; Only H_2O_2, n=13; HRP+H_2O_2, n=17)
Error bars represent the SEM. (* $p<<0.001$; One-way ANOVA)

7.2.2 The antioxidant, ascorbic acid, prevents the effects of free radical formation on synaptic transmission

While high K^+ uptake of HRP followed by H_2O_2 alters synaptic transmission, I wanted to assure that these defects resulted from free radical formation within the synaptic vesicles. To examine the free radical specificity, I introduced the antioxidant ascorbic acid into the vesicles alongside HRP so that ascorbic acid could absorb free radicals before they could do any damage. If free radicals are responsible for the defective neurotransmission, then the neutralization of the free radicals will prevent the synaptic deficits. To test this hypothesis, I depolarized synapses with a high K^+ buffer containing HRP and ascorbic acid then applied H_2O_2 to induce free radical formation within HRP containing vesicles. In neurons stimulated in the presence of both HRP and ascorbic acid, I found no changes in the frequency of mEPSCs as compared to HRP/ascorbic acid only and H_2O_2 only controls (Fig. 7.2.2 B-D: Only HRP 1.5 ± 0.5 Hz, n=12; Only H_2O_2 2.1 ± 0.4 Hz, n=7; HRP+ H_2O_2 2.1 ± 0.5 Hz, n=9; p=0.60). The maximum amplitudes of field potential-evoked EPSCs and the responses during a100 AP 1 Hz stimulus train remained unaltered compared to controls (Fig. 7.2.2 E-F: n=4;Only HRP, 2.3 ± 0.8 nA; Only H_2O_2, 3.2 ± 0.8 nA; HRP+H_2O_2, 3.3 ± 0.4 nA; p=0.62). These results suggest that the increased spontaneous fusion as well as deficits in field-potential stimulated EPSCs specifically require free radical action within the synaptic vesicle.

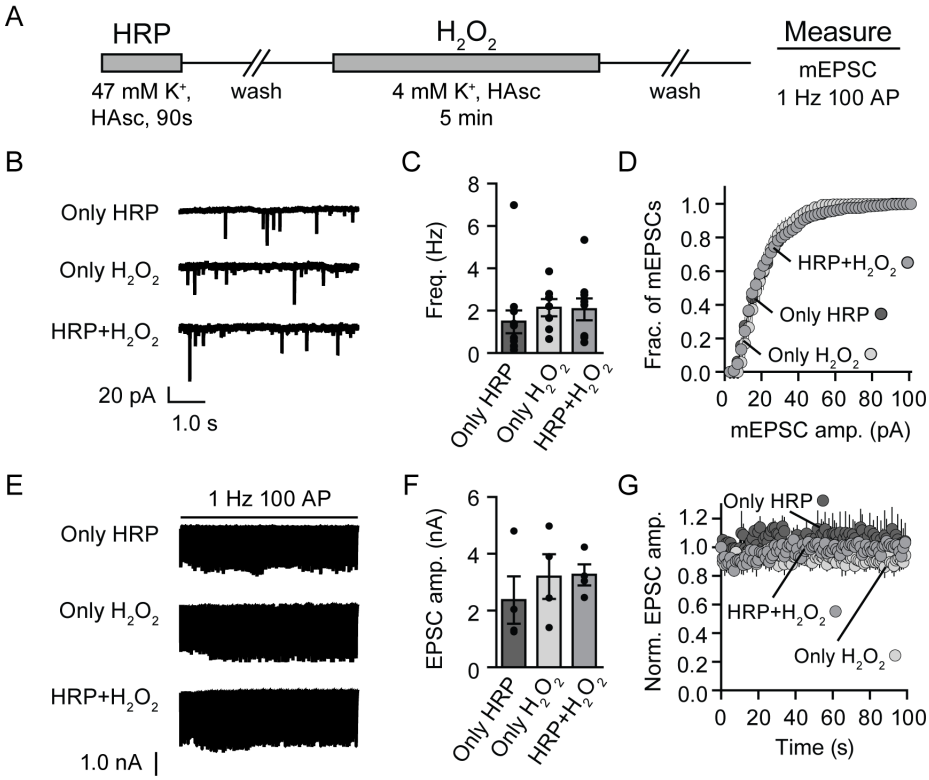

Figure 7.2.2 Free radical acceptor, ascorbic acid, blocks the defects in neurotransmission observed after H_2O_2 perfusion of synapses containing HRP labelled vesicles.

(A) Diagram of the experiment: Hippocampal neurons were depolarized with a high K^+ buffer containing HRP and ascorbic acid (HAsc) for 90 s. HRP was washed out for 10 minutes, and H_2O_2 was perfused for 5 minutes then washed out for another 10 minutes. Neurons were patched and mEPSCs and EPSCs were recorded (HRP+H_2O_2). Control experiments (diagram not shown) were performed by omitting the HRP from the high K^+ buffer (Only HRP) or H_2O_2 from the 5-minute perfusion (Only H_2O_2)
(B-D) mEPSC frequency and amplitudes before and after treatment (B) Representative mEPSC recordings (C) Plot summarizing the average frequency of mEPSCs showing that the average frequency did not differ between groups. (D) Distribution of mEPSC amplitudes showing no significant difference between groups. (Only HRP, n=12; Only H_2O_2, n=7; HRP+H_2O_2, n=9)
(E-G) EPSC amplitudes of control and experimental treatments (E) Representative traces of the first 40 ms of EPSCs recorded during a 1 Hz train of 100 APs. (F) Summary graph of the average maximum EPSC amplitude showing no change in amplitude after treatment. (G) Plot of EPSC amplitude per AP normalized to the first response. After HRP uptake with HAsc and H_2O_2 perfusion, the rate of change of EPSC amplitudes was unchanged compared to control treatments. (n=4)
Error bars represent the SEM.

7.2.3 Free radical modification of vesicles fusing during 1 and 20 Hz trains of 100 AP fusing

After demonstrating a free radical-mediated modification of neurotransmitter release, I wanted to try the same experiment with only a portion of the recycling pool. If all of the vesicles within a synapse are the same, then the alterations of a few recycling vesicles could potentially have no affect what so ever due to the other vesicles ability to fuse in their stead; however, if the choice of which vesicle fuses depends on the proximity to the synapse, then it would be logical to assume that the effects would be random. On the other hand, if some vesicles are more equipped to fuse, then the effects of their modifications would be consistent. By stimulating neurons with field potentials in the presence of a high concentration of HRP (20 mg/ml), I labeled portions of the recycling pool and then applied H_2O_2. To more precisely understand the effects of these modifications, I patched the neurons before stimulating the uptake of HRP to measure the original synaptic transmission. I then stimulated the uptake with field potential stimuli (at either 1 or 20 Hz for 100 AP), washed away the HRP, and perfused H_2O_2. I then measured the postsynaptic currents again and compared them to their original properties (Figure 7.2.3). For each HRP uptake protocol I performed before and after experiments using the same protocols without HRP or without H_2O_2, and neither the length of the experiment or either treatment (with

HRP only or H_2O_2 only) caused any noticeable differences between the before and after recordings (data not shown)

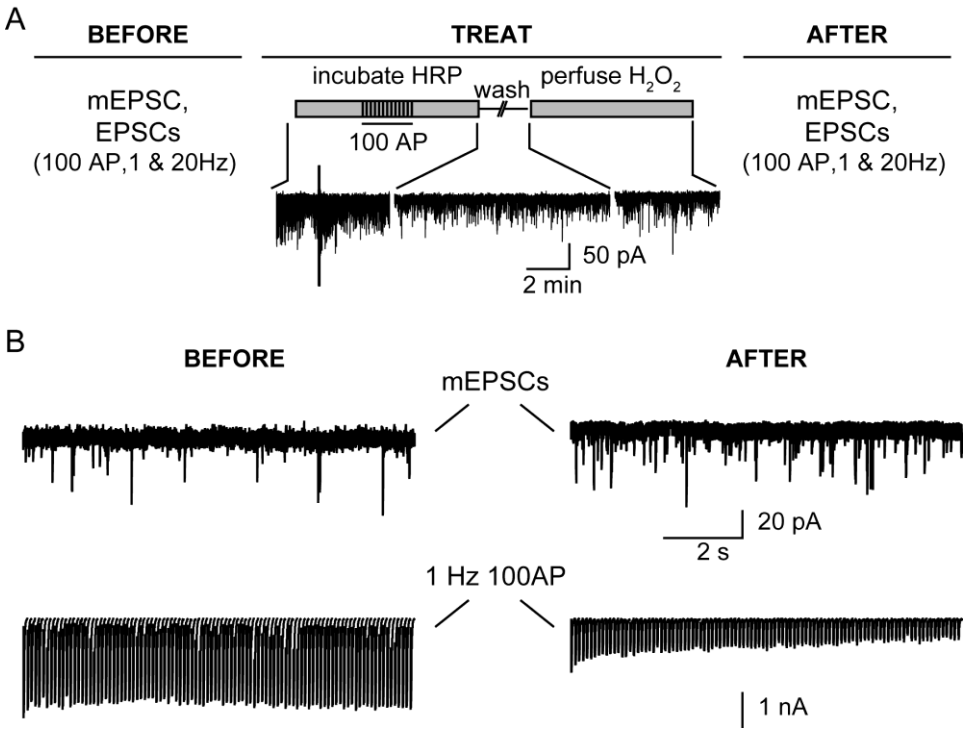

Figure 7.2.3 Field potential stimulated uptake of HRP: Data traces from one experiment

(A) Diagram of the experiment: Before treating, the hippocampal neuron was patched, and mEPSCs and EPSCs were recorded (Before). HRP was perfused and the neuron was stimulated with a 20 Hz train of 100 AP (5 s). After incubating for another 2 minutes, HRP was washed out for 10 minutes. H_2O_2 was perfused for 5 minutes and washed out for another 10 minutes. Then mEPSCs and EPSCs were recorded again from the same neuron (After).
(B-D) TOP: Sample traces of mEPSC recordings before and after the treatment.
BOTTOM: Representative traces of the first 40 ms of EPSCs recorded during 1 Hz train of 100 APs.

7.2.3.1 Free radical modification of vesicles fusing at 20 Hz not only decreases EPSC amplitudes but also enhances spontaneous neurotransmission.

To modify a smaller portion of the recycling pool, I stimulated neurons with 100 field potential stimuli at a frequency of 20 Hz in the presence of HRP after first patching and recording the original spontaneous and evoked neurotransmitter release. This stimulation paradigm evokes the fusion of many but not all recycling pool vesicles. After HRP uptake, I perfused H_2O_2 and again recorded the synaptic transmission (Fig. 7.2.3.1A). Compared to the frequency before HRP uptake, I found the frequency of mEPSCs increased 2.7-fold (Fig. 7.2.3.1 B-C: Before HRP, 2.3 ± 0.5 Hz; After H_2O_2, 6.1 ± 1.2 Hz; n=4; $p<0.04$) after H_2O_2 treatment, while the amplitudes of the events remained unaltered (Fig. 7.2.3.1 B, D). The amplitudes of the first EPSC decreased after modification (2.2-fold; Fig.7.2.3.1 E-F: Before HRP, 2.9 ± 0.4 nA; After H_2O_2, 1.3 ± 0.1 nA; n=4; $p<0.04$) and the rate of EPSC depression increased significantly after the 25^{th} stimulus of the 1Hz train (Fig. 7.2.3.1 E, G; $p<0.05$)

Consistent with the effects of modifying the entire recycling pool (Fig. 7.2.1), alterations in both the spontaneous and evoked neurotransmission occurred and I found no variation of these effects from cell to cell. In this experiment, the spontaneous fusion increased on the order of the change seen in neurons after treatment of the entire recycling pool (each 2.7-fold). However, the intensity of

the EPSC amplitude decrease was half that of the more intense modification, indicating that the vesicles fusing during the 20 Hz stimulation with HRP consist of a large enough part of the recycling pool to enhance spontaneous neurotransmission after modification but not big enough to mimic the magnitude of EPSC attenuation.

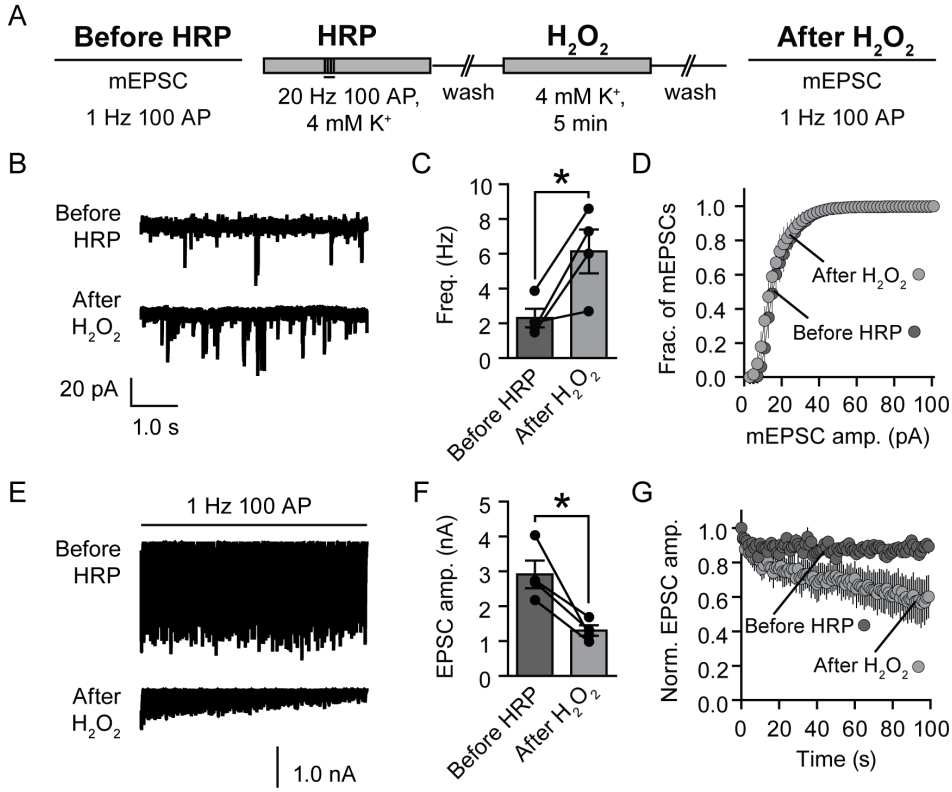

Figure 7.2.3.1 Chemical modification of vesicles fusing at a high frequency stimulation decreases Ca^{2+}--dependent neurotransmission and enhances spontaneously fusion.

(A) Diagram of the experiment: A hippocampal neuron was first patched, and mEPSCs and EPSCs were recorded (Before HRP). HRP was perfused and the neurons were stimulated with a 20 Hz train of 100 AP (5 s). After incubating for another 2 minutes, HRP was washed out for 10 minutes. H_2O_2 was perfused for 5 minutes and washed out for another 10 minutes. Then mEPSCs and EPSCs were recorded again from the same neuron (After H_2O_2).

(B-D) mEPSC frequency and amplitudes before and after treatment (B) Representative mEPSC recordings before HRP and after H_2O_2 (C) Plot summarizing the average frequency of mEPSCs before and after treatment (values from the same neurons are connected). The average frequency increased 2.7-fold after chemical modification. (D) Distribution of mEPSC amplitudes showing no significant difference between groups. (E-G) EPSC amplitudes before HRP and after H_2O_2 (E) Representative traces of the first 40 ms of EPSCs recorded during 1 Hz train of 100 APs. (F) Summary graph of the average maximum EPSC amplitude showing a 2.2-fold decrease in amplitude after treatment (values from the same neurons are connected). (G) Plot of EPSC amplitude per AP normalized to the first response before HRP and after H_2O_2. After HsO_2, EPSC amplitudes decreased faster compared to the rate of amplitude change before HRP. Error bars represent the SEM. (n=4; * $p < 0.04$; paired t-test)

7.2.3.2 Free radical modification of vesicles fusing at 1 Hz attenuates EPSC amplitudes without affecting spontaneous neurotransmission

To observe the effect of modifying an even smaller pool of vesicles, I reduced the stimulation frequency in the presence of HRP from 20 Hz to 1 Hz maintaining the same number of stimuli. After recording the original mEPSC and EPSCs from a neuron, I stimulated the uptake of HRP into a portion of the recycling pool by applying 100 field potential stimuli at a 1 Hz frequency in the presence of HRP. Then I perfused H_2O_2 (0.02%) for 5 minutes after washing away the HRP. I rinsed away the H_2O_2 and measured the mEPSCs and EPSCs (Fig. 7.2.3.2A). I compared the measurements observed before HRP uptake (Before HRP) to the measurements after H_2O_2 perfusion (After H_2O_2). After the H_2O_2 treatment, I found the frequency and amplitude of the mEPSC events unchanged compared to before HRP (Fig. 7.2.3.2 B-D: Before HRP, 1.7 ± 0.6 Hz; After H_2O_2, 1.1 ± 0.3 Hz; n=5; p=0.27). However, the initial EPSC amplitude of

the 1 Hz 100 AP train decreased by 1.5-fold after the HRP and H_2O_2 treatment (Fig. 7.2.3.2 E-F: Before HRP, 3.1 ± 0.2 nA; After H_2O_2, 2.1 ± 0.3 nA; n=5; $p<<0.001$). I also observed no change in the dynamics of EPSC amplitude changes during the 1 Hz train (Fig. 7.2.3.2 E, G).

These results display a consistent attenuation in the EPSC amplitudes indicates that the vesicles fusing during the 1 Hz stimulation with HRP contribute to the overall output of neurotransmitter; however, the lack of change in the EPSCs amplitudes during the 100-AP stimulation indicates that the remaining vesicles can maintain the attenuated release. Possibly, the maintenance of this decreased EPSC magnitude suggests that the modified vesicles participate continually at this frequency.

Interestingly, the spontaneous fusion rate did not increase as seen after modifying the entire recycling pool, which suggests that either the portion of vesicles modified in this experiment do not begin to fuse spontaneously or that the vesicles do fuse spontaneously but are too few to result in a visible increase. Another consideration is that the vesicles fusing spontaneously may contribute to spontaneous neurotransmission normally, thus not affecting the rate.

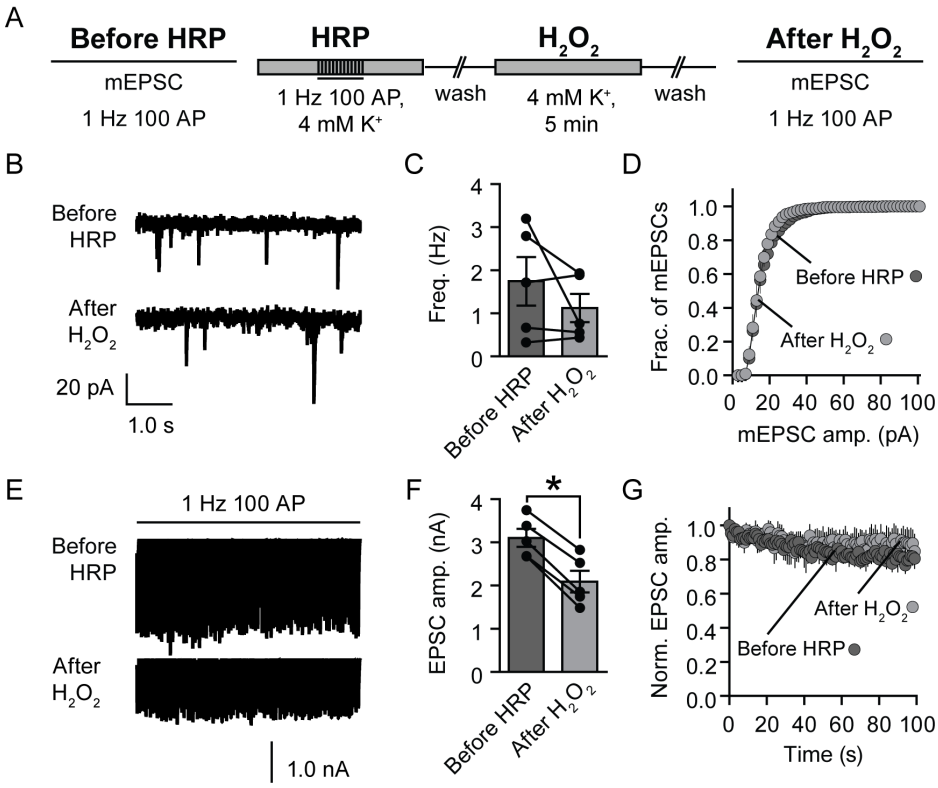

Figure 7.2.3.2 Free radical modification of vesicles fusing at 1 Hz enhances spontaneous neurotransmission without affecting EPSC amplitudes

(A) Diagram of the experiment: A hippocampal neuron was first patched, and mEPSCs and EPSCs were recorded (Before HRP). HRP was perfused and the neurons were stimulated with a 1 Hz train of 100 AP (1 min 40 s). After incubating for another 2 minutes, HRP was washed out for 10 minutes. H_2O_2 was perfused for 5 minutes and washed out for another 10 minutes. Then mEPSCs and EPSCs were recorded again from the same neuron (After H_2O_2).
(B-D) mEPSC frequency and amplitudes before and after treatment (B) Representative mEPSC recordings before HRP and after H_2O_2 (C) Plot summarizing the average frequency of mEPSCs before and after treatment (values from the same neurons are connected). The average frequency did not significantly change after treatment. (D) Distribution of mEPSC amplitudes showing no significant difference between groups.
(E-G) EPSC amplitudes before HRP and after H_2O_2 (E) Representative traces of the first 40 ms of EPSCs recorded during 1 Hz train of 100 APs. (F) Summary graph of the average maximum EPSC amplitude showing a 1.5-fold decrease in amplitude after treatment (values from the same neurons are connected). (G) Plot of EPSC amplitude per AP normalized to the first response before HRP and after H_2O_2. After H_2O_2, the rate of decrease in EPSC amplitude was unchanged when compared to the rate of change before HRP.
Error bars represent the SEM. (n=5; * $p << 0.001$; paired t-test).

7.2.4 Free-radical modification of spontaneously fusing vesicles enhances spontaneous fusion without affecting EPSC amplitudes.

Each of the prior experiments attempted to modify the composition of vesicle by stimulating their exocytosis. Any alteration in vesicles of the recycling pool led to the defects in neurotransmitter release. To determine changes after free radical formation within spontaneously fusing vesicles, I recorded the normal mEPSCs and EPSC amplitudes over 100 AP at 1 Hz, then modified spontaneously fusing vesicles and measured these parameters again. To modify the vesicles, I incubated neurons with HRP in the absence of action potentials for the same period as the action potential stimulated uptake experiments (5 min 40 s), then I applied H_2O_2 after removing HRP and again washed. The mEPSCs frequency increased after modification compared to the rate of events before HRP application (Fig. 7.2.4 B-C; 2.2-fold; Before HRP, 3.3 ± 0.7 Hz; After H_2O_2, 7.2 ± 1.5 Hz; n=5; $p< 0.04$) without affecting the amplitude distribution of the events (Fig.7.2.4 D). Conversely, I found no changes in the initial EPSC amplitudes (Fig. 7.2.4 E-F; Before HRP, 2.7 ± 0.4 nA; After H_2O_2, 2.4 ± 0.4 nA; n=5; p=0.34) or the amplitudes during the next 99 APs compared to the responses recorded from the same neuron before modification (Fig. 7.2.4 E, G). This suggests that spontaneously fusing vesicles are not necessary for the efficiency of synaptic transmission during low frequency stimulation.

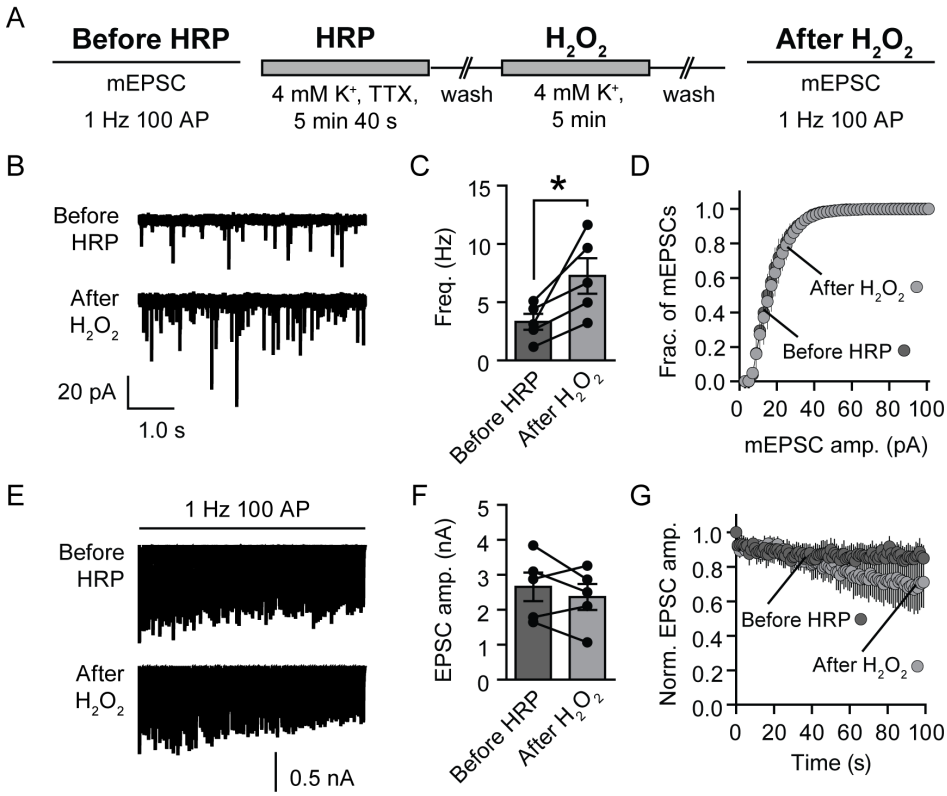

Figure 7.2.4 Chemical modification of spontaneously fusing vesicles enhances spontaneous fusion without effecting Ca^{2+}-dependent neurotransmission.

(A) Diagram of the experiment: A hippocampal neuron was first patched, and mEPSCs and EPSCs were recorded (Before HRP). HRP was perfused with TTX and incubated for 5 minutes and 40 s. HRP was washed out for 10 minutes, and then $H_2O_2$was perfused for 5 minutes and again washed out for 10 minutes. Then mEPSCs and EPSCs were recorded again from the same neuron (After H_2O_2).

(B-D) mEPSC frequency and amplitudes before and after treatment (B) Representative mEPSC recordings before HRP and after H_2O_2 (C) Plot summarizing the average frequency of mEPSCs before and after treatment (values from the same neurons are connected). The average frequency increased 2.2-fold after treatment. (D) Distribution of mEPSC amplitudes showing no significant difference between groups.

(E-G) EPSC amplitudes before HRP and after H_2O_2 (E) Representative traces of the first 40 ms of EPSCs recorded during 1 Hz train of 100 APs. (F) Summary graph of the average maximum EPSC amplitude showing no change in amplitude after treatment (values from the same neurons are connected). (G) Plot of EPSC amplitude per AP normalized to the first response before HRP and after H_2O_2. After H_2O_2, the rate of decrease in EPSC amplitude was unchanged when compared to the rate of change before HRP.

Error bars represent the SEM. (n=5; * $p < 0.04$; paired t-test)

7.2.5 Vesicle recycling after chemical modification

To further understand the possible effects of free radical modification on SVs, I monitored the reavailability of subsets of recycling vesicles after altering their composition. After modification, the excitatory postsynaptic input decreased indicating a deficit in presynaptic neurotransmitter release. To explore the reason for this change, I modified vesicles containing a fluorescent marker and monitored the fusibility of those synaptic vesicles within individual synapses. The release of the fluorescent dye FM1-43 from modified vesicles revealed that these vesicles can fuse with the synaptic membrane although at a slower rate.

To examine the reavailability of modified synaptic vesicles, I incubated hippocampal neuron cultures with FM1-43 and HRP then applied 100 field potentials at either 1 or 20 Hz. Then I washed away the excess HRP and FM1-43 and applied H_2O_2 to create free radicals within the labeled vesicles (Fig. 7.2.5.1A, 2A; FM+HRP). After removing the H_2O_2, I monitored the synaptic bouton fluorescence during several rounds of field potential stimulation and determined the amount and rate of dye loss. By initially measuring the FM1-43 uptake and release before modifying synaptic vesicles, I could compare the modified synaptic properties to the original, non-modified synapses.

Synapses stimulated at 1 Hz for 100 s in the presence of both FM1-43 and HRP and then perfused with H_2O_2 (Fig 7.2.5.1 A), I measured the release of the dye taken up before free radical formation and found a non-significant decrease in

the total amount of dye lost ($p=0.19$) and in the initial fluorescence ($p= 0.07$) compared to the original FM1-43 experiment (Fig 7.2.5.1D-E). The rate of the dye lost during the first round of release, however, was slower (Fig. 7.2.5.1 F-G: FM 4.1±0.4 s; FM+HRP 9.7±1.8 s; $n=4$; $p<0.03$), indicating that the same quantity of dye was released but it was delayed. The rate of FM1-43 loss also slowed from vesicles labeled with 20 Hz 100 AP (Fig. 7.2.5.2 A-C: FM 3.6±0.5 s; FM+HRP 10.0±2.1 s; $p<0.04$); however, I observed an insignificant decrease in the initial fluorescence ($p=0.10$) and total FM1-43 lost ($p=0.08$) (Fig 7.2.5.2 A, D).

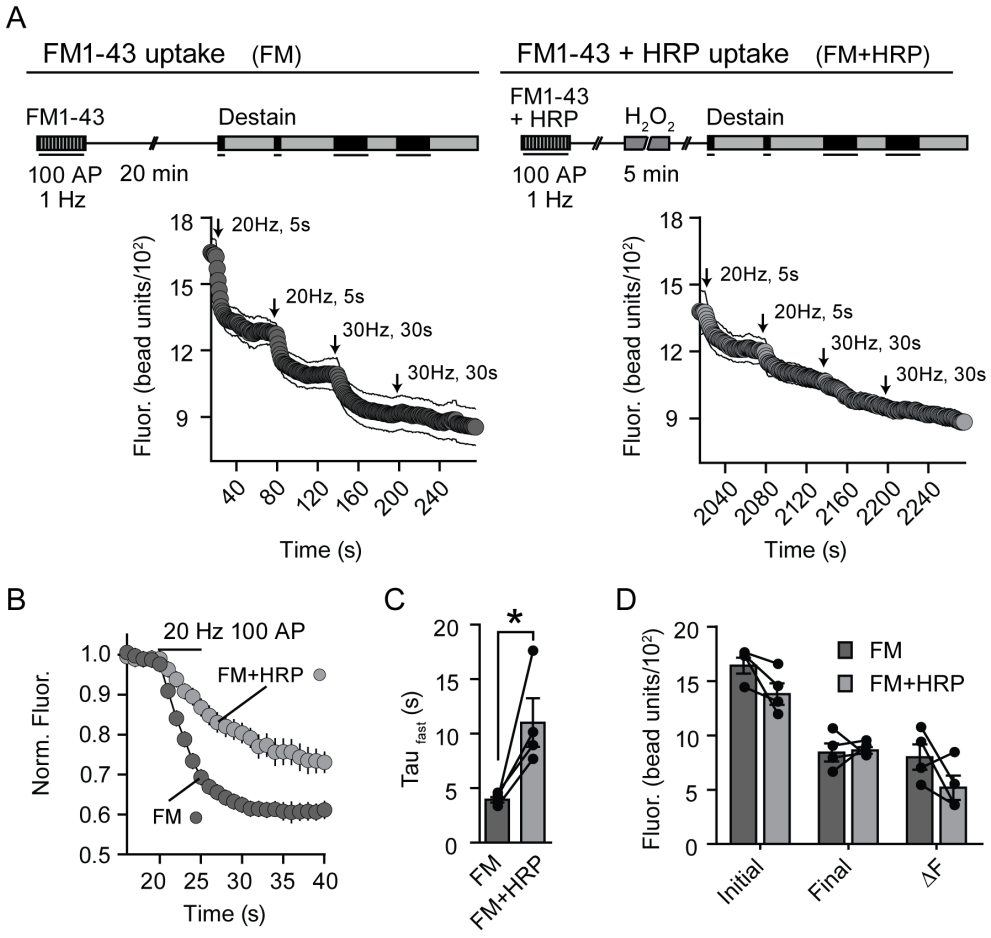

Figure 7.2.5.1 Reavailability of modified synaptic vesicles which fuse during 1 Hz 100 AP stimulation

(A) TOP: Depiction of the initial FM1-43 uptake and release (FM) followed by the simultaneous uptake of HRP and FM1-43 and release after H_2O_2 perfusion (FM + HRP) in the same synapses. BOTTOM: The average fluorescence values during the release of FM1-43 after each uptake protocol. Note that the summary plot lines up with the diagram above.
(B) Summary plot of the normalized average loss of fluorescence measured during the initial 20 Hz 5s stimulation depicting slower kinetics of FM1-43 release after modification of dye containing vesicles. (C) Graph depicting the average rate constant for the first 20Hz 5 s stimulation showing a significant increase in the rate constant of dye loss. (D) Chart summarizing the average fluorescence values per coverslips showing an insignificant downward trend in both the initial fluorescence intensity and the total fluorescence lost indicating a possible increase in the spontaneous fusion of the labeled vesicles during the wash. No n final fluorescence values after modification no significant

change in the initial or final fluorescence (also see panel B) as well as in the total amount of FM1-43 released by the end of the experiment (ΔF) after chemical modification of FM1-43 containing vesicles compared to the values before HRP.
Error bars represent the SEM. (n=4, *p<0.03, two-tailed paired t test)

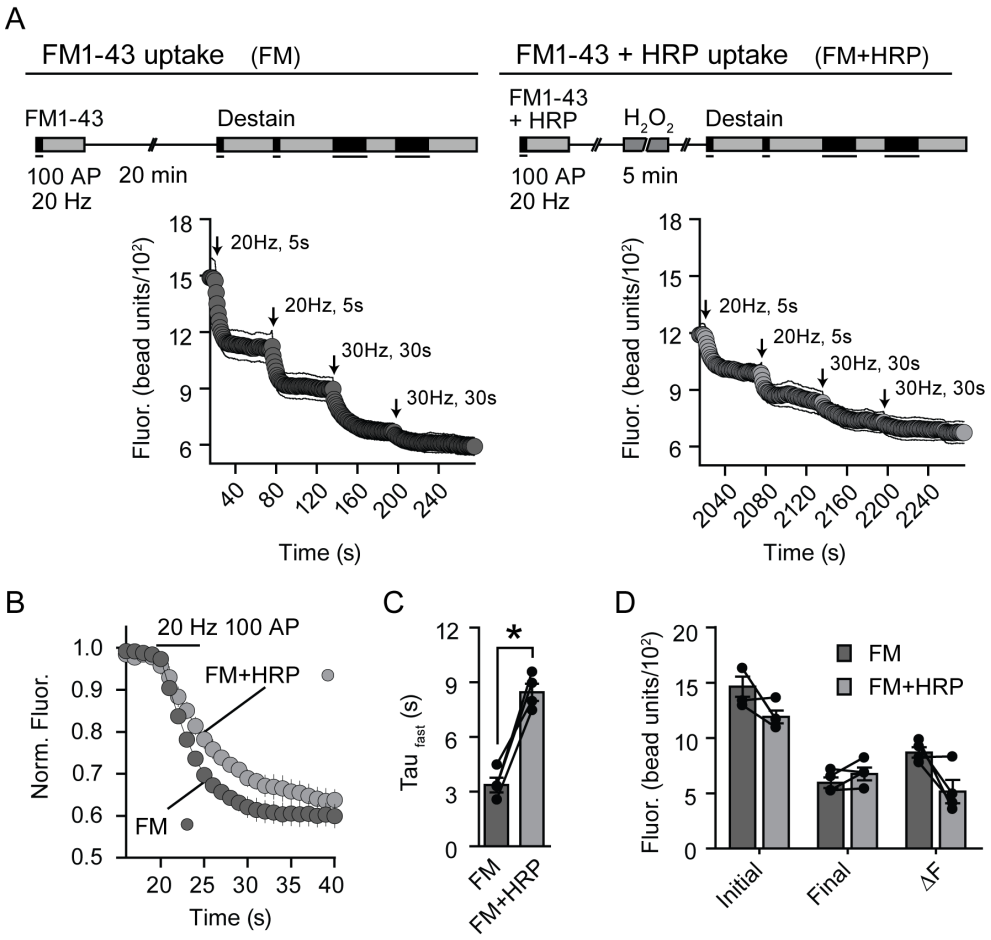

Figure 7.2.5.2 Reavailability of modified synaptic vesicles which fuse during 20 Hz 100 AP stimulation

(A) TOP: Diagram of the initial FM1-43 uptake and release (FM) followed by the simultaneous uptake of HRP and FM1-43 and release after H_2O_2 perfusion (FM + HRP) in the same synapses. BOTTOM: The average fluorescence values during the release of FM1-43 after each uptake protocol. Note that the summary plot lines up with the diagram above.
(B) Summary plot of the normalized average loss of fluorescence measured during the initial 20 Hz 5s stimulation depicting slower kinetics of FM1-43 release after modification of dye containing vesicles. (C) Graph depicting the average rate constant for

the first 20Hz 5 s stimulation showing a significant increase in the rate of dye loss. (D) Chart summarizing the average fluorescence values per coverslips showing no significant change in the initial or final fluorescence (also see panel B) as well as in the total amount of FM1-43 released by the end of the experiment (ΔF) after chemical modification of FM1-43 containing vesicles compared to the values before HRP. Note: The initial and total fluorescence loss decrease appear to experience a decrease after modification. Error bars represent the SEM. (n=4, *$p<0.05$, two-tailed paired t test)

7.3 Summary

These experiments demonstrate that alterations in synaptic vesicle membranes affect synaptic transmission. Free radical-dependent modification of the total pool of recycling vesicles hindered action potential stimulated neurotransmitter release while augmenting the frequency of spontaneous vesicle fusion events. This modification does not completely block all evoked fusion, indicating that some vesicles are still competent to fuse. The opposing increase in spontaneous fusion implies that some mechanism within the membrane of recycling pool or spontaneously fusing vesicles restrain spontaneous and free radical modification interrupts this interaction.

Partial modification of the recycling pool had similar effects on synaptic transmission, the magnitude of which depended on the stimulation frequency used to take up HRP. Stimulating with a 20 Hz 100 action potential train mobilizes many of the recycling vesicles, while 1 Hz stimulation is milder resulting in the fusion of fewer recycling pool vesicles. So not surprisingly, modification of the larger portion of vesicles decreased the magnitude of EPSCs to a greater extent than the 1Hz protocol. Moreover, the modifications of the 20 Hz vesicles

enhanced spontaneous fusion to the same degree as complete recycling pool modification, while altered 1 Hz vesicles did not contribute to any change in spontaneous fusion. This possibly suggests the following: (1) Stronger stimulation results in more full collapse of fusing vesicles increasing accessibility of the vesicle to fill with HRP; (2) Ca^{2+} concentration increases within the synapse after strong stimulation thus increasing spontaneous fusion and their exposure to HRP.

Also of note, the availability of synaptic vesicles becomes slower after modification. When I stimulated the HRP uptake with either high K^+ or 20 Hz 100 AP stimulation, the rate of EPSC depression increased during a mild 1 Hz 100 AP train compared to the controls. This implies a decrease not only in the initial numbers of vesicles fusing but also a loss in the availability during repeated stimulation. Conversely, I found no defect in 1 Hz depression after modifying vesicles which fused during the 1 Hz HRP uptake, suggesting that the vesicles responding to repetitive stimulation are most likely non-modified vesicle.

Moreover, fluorescent tracking revealed that modified vesicles are not completely inactivated. By stimulating cultures using two field potential stimulus trains in the presence of both FM1-43 and HRP and then perfusing H_2O_2, I found that vesicles modified with free radical formation were still fusion competent ; however, the rate of this fusion at each synapse significantly decreased compared to their original release rates. This is could be a function of slower vesicle recruitment to the active zone and/or the fusion of non-modified vesicles during

the stimulation. Interestingly, the rate of dye loss before modification was no different between vesicles labeled by 1 Hz or 20 Hz stimulation; however, after modification, the vesicles fusing at 1 Hz experience a more dramatic decrease in the dye release rate. Considering this difference in vesicle reuse and the sustained release at 1 Hz, small modified portions of the recycling pool may have to compete with non-modified vesicles resulting in fewer opportunities for the altered vesicles to exocytose. In contrast, modification of a larger portion of the recycling pool might decrease this competition due to fewer competent vesicles at the active zone.

And finally, I exposed neurons to HRP spontaneously and applied H_2O_2 to create free radicals within the HRP containing vesicles, and I observed an increase in spontaneous fusion that matched the fold increases after modification of recycling pool and 20 Hz-fusing vesicles. This demonstrates that regulation with in the membrane of spontaneously fusing vesicles may exist.

Although these experiments prove to provoke more questions than they answer, free radical formation within synaptic vesicles does affect their fusion competency. Therefore, this technique provides a mechanism by which we can start to distinguish molecular requirements for specific synaptic vesicle function.

7.4 Methods

7.4.1 Cell culture

The hippocampi were dissected and dissociated from postnatal day 0-3 (P0-3) Sprague-Dawley rats as previously described in (Kavalali et al., 1999). Dissociated cells were plated on zero thickness 12-mm glass coverslips and stored at 37°C with 5% CO_2 in a humidified incubator.

7.4.2 Free radical formation in synaptic vesicles using HRP and H_2O_2

To form free radicals in vesicles, cultures were stimulated using the following paradigms in the presence of HRP, then washed and perfused with H_2O_2 (0.02% in modified Tyrode's solution containing 1 μM TTX and 50 μM picrotoxin (PTX)) for 5 or 10 minutes. To assess synaptic neurotransmission, both mEPSCs and EPSCs stimulated by 1 and 20 Hz trains of 100 stimuli (referred to as AP) were recorded using whole-cell voltage patch clamp. In all experiments except for the high K^+ HRP uptake experiments, recordings were taken from patched neurons before HRP uptake and after H_2O_2 perfusion. Thus each recording is paired (Before HRP to After H_2O_2). Experiments excluding the H_2O_2 or the HRP were performed as controls for all experiments (HRP only or H_2O_2 only, respectively) for these experiments.

High K^+ uptake of HRP: Cultures were incubated with HRP (5 mg/ml, Sigma) in a 47 mM K^+ solution (1:1 solution, modified Tyrode's solution: 90 mM K^+ Tyrode's solution) for 2 minutes. To simultaneously

Action potential uptake of HRP: Neurons were patched, and both mEPSCs and EPSC responses from 1 Hz and 20 Hz trains of 100 action potentials (AP) were recorded. After determining the basal synaptic properties of the neuron, the coverslip was perfused with HRP (20 mg/ml) in a modified Tyrode's solution and incubated for two minutes. The neurons were then stimulated with 100 action

potentials at a frequency of 1 or 20 Hz and incubated in the solution for and extra two minutes (delay) to allow fused SV to endocytose.

Spontaneous uptake of HRP: Cultures were incubated with HRP (20 mg/ml) for 5 minutes and 40 seconds (time equivalent to the time HRP is present in the AP experiments) in a modified Tyrode's solution containing 1 μM TTX (to which inhibit action potential-dependent vesicle fusion).

7.4.3 Electrophysiology

A modified Tyrode's solution was used for all experiments (except where noted otherwise) that contained (in mM): 145 NaCl, 4 KCl, 2 $MgCl_2 \bullet (6H_2O)$, 10 glucose, 10 HEPES, 2 $CaCl_2$ (pH 7.4, osmolarity 300 mOsM). Pyramidal neurons were whole-cell voltage clamped at –70 mV with borosilicate glass electrodes (3-5 MΩ). Electrode solutions contained (in mM): 105 Cs-methanesulphonate, 10 CsCl, 5 NaCl, 10 HEPES, 20 TEA.Cl hydrate, 4 Mg-ATP, 0.3 GTP, 0.6 EGTA, 10 QX-314 (pH 7.3, osmolarity 290 mOsM). To measure excitatory postsynaptic current (EPSC) amplitudes, neurons were washed with a modified Tyrode's solution containing 50 μM PTX and 50 μM AP5 (DL-2-Amino-5-phosphonovaleric acid, NMDA receptor blocker), and field potentials were induced with a 0.1-ms pulse of 10 mA of current through a bipolar platinum electrode. Spontaneous neurotransmitter release was measured by recording miniature EPSC (mEPSC) frequency and amplitudes in a modified Tyrode's solution containing 1 μM TTX, 50 μM PTX and 50 μM AP5.

7.4.4 Fluorescent detection of synaptic vesicle recycling

To measure the original properties of FM1-43 uptake and release before free radical formation, cultures were stimulated with 100 AP at a 1 or 20 Hz frequency in the presence of 8 μM FM1-43(Molecular Probes, Eugene, OR). The dye was washed out with the perfusion of a dye-free Tyrode's solution for 20 minutes. FM1-43 within endocytosed vesicles was released by stimulating the cultures with

two rounds of 100 AP at 20 Hz followed by two rounds of 450 AP at 30 Hz. After washing for 10 minutes, the same boutons were stimulated using the same paradigm in the presence of FM1-43(8 µM) and HRP (20 mg/ml). Images were taken during the release of FM1-43. In all experiments I selected isolated boutons (1 μm^2) from the original experiment (non-modified boutons) for analysis and avoided apparent synaptic clusters (Kavalali et al., 1999b). All statistical analyses were performed using the paired t-test with the number of coverslips as n. Experimental results are represented as mean ± SEM.

7.4.5 Statistical analysis

All statistics for pairwise comparisons were calculated using a two-tailed paired t test. Statistics for experiments comparing more than two variables were performed using one-way ANOVA. To determine the significance of mEPSC amplitude distributions, the Kolmogorov-Smirnov test (K-S test, $p>0.0001$) was used.

CHAPTER 8: CONCLUSION

8.1 Vesicle Identity

Most vesicles within a synapse are dormant. The rest participate in synaptic neurotransmitter release; however, within this group of actively recycling vesicles, a small percent appear to preferentially exocytose first. Moreover, all synapses experience spontaneous neurotransmitter release and may originate from the random exocytosis of vesicles prepared to fuse immediately upon Ca^{2+} influx; however, these spontaneously fusing vesicles prefer to fuse spontaneously. The functional separation argues that the compositions the synaptic vesicle membranes are somehow unique between pools.

By following the actively recycling pool, I observed that actively recycling vesicles maintained active for up to 24 hours. While still active, recycling pool vesicles containing a fluorescent marker lost about 3.5 % of the dye spontaneously per hour. On the other hand, spontaneously fusing vesicles re-fused spontaneously at a rate at least four times faster. This suggests that some vesicles within the synapse frequently fuse spontaneously, while recycling pool vesicles rarely do. In addition, free radical formation within recycling pool vesicles revealed that altered synaptic vesicle integrity differentially affected the properties of spontaneous and action potential-dependent vesicle fusion. Free radical-dependent changes within synaptic vesicles resulted in the inhibition of

evoked exocytosis while increasing the frequency of spontaneous fusion, implying a fundamental difference between the two types of neurotransmission.

8.2 Modification of synaptic transmission: role of sphingosine and cholesterol

Membrane lipids such as phosphoinositides, sphingosine and cholesterol are each found in synapses and often located together. Sphingosine and cholesterol are commonly found together in dense domains involved in protein interactions and signaling processes.

8.2.1Synaptic transmission after increasing sphingosine

Experiments performed by Bazbek Davletov group implicated sphingosine as a key regulator of the synaptic vesicle SNARE protein synaptobrevin. They found that sphingosine as well as some derivatives of sphingosine positively regulated synaptobrevin resulting in enhanced SNARE complex formation and that the addition of sphingosine to neuromuscular junctions facilitated their response to hypertonic sucrose responses. I further examined the effects of increased sphingosine within CNS neurons of synaptobrevin-2-deficient mice and heterozygous littermates. The addition of sphingosine to these neurons enhanced responses to both hypertonic sucrose and field potential stimulation in a synaptobrevin-dependent manner. Another positive regulator of SNARE formation, sphinganine increased evoked neurotransmission in wild-type rat hippocampal neurons, while an ineffective modulator C_2-dihydroceramide did

not. Ultimately, the addition of sphingosine appears to act as a positive regulator of synaptobrevin activity resulting in the increased efficacy of synaptic vesicle fusion.

8.2.2 Implications of decreased neuronal cholesterol

While prior data implicates cholesterol in the efficacy of endocytosis and evoked exocytosis, cholesterol also acts to inhibit spontaneous vesicle fusion (Zamir and Charlton, 2006, Wasser et al., 2007). In hippocampal neurons, decreasing cholesterol by acute depletion with methyl-β-cyclodextrin, inhibition of synthesis or by using cultured neurons from mice deficient in cholesterol trafficking results in a significant increase in the rate of spontaneous vesicle fusion and a substantial decrease in evoked vesicle fusion. Cholesterol addition reversed each of these effects. After acute depletion of cholesterol with MCD, the potentiated spontaneous frequency persisted for up to 20 minutes, and the number of vesicles that took up HRP spontaneously increased compared to non-depleted synapses. The increase in spontaneous uptake of HRP and the continued high level of spontaneous release observed after cholesterol removal suggest that the enhanced spontaneous fusion is coupled to an increase in endocytosis indicating an overall alteration in the recycling of spontaneous vesicles rather than an increase spontaneous fusion alone after acute MCD-mediated cholesterol removal.

Cholesterol contributes to membrane dynamics, particularly the regulation of membrane fluidity and microdomains involved in protein interactions. In the central nervous system, cholesterol synthesis is primarily *de novo* and tightly regulated (Spady and Dietschy, 1983, Dietschy et al., 1993). At the synapse, cholesterol depletion experiments implicate cholesterol in the regulation of the efficiency of Ca^{2+}-dependent exocytosis by mediating SNARE protein localization at the synapse (Chamberlain et al., 2001, Lang et al., 2001, Salaun et al., 2004, Churchward et al., 2005, Jia et al., 2006) and the retrieval of exocytosed membrane through clathrin-dependent pathways (Rodal et al., 1999, Subtil et al., 1999).

Synaptic neurotransmission in Niemann-Pick type C1 (NPC1)-deficient neuronal cultures mimicked the observations seen after acute cholesterol decreases. These NPC1-deficient neurons have a defect in cholesterol trafficking which traps cholesterol in the late endosome/lysosome and results in decreased concentration of cholesterol at the synapse. Along with the attenuation of evoked responses, both NPC1-deficient neurons in slice or culture displayed a higher frequency of spontaneous vesicle fusion compared to the wild-type littermates.

This finding suggests that the presence of cholesterol increases the efficiency Ca^{2+}-dependent fusion while inhibiting spontaneous fusion. Interestingly, vesicular cholesterol oxidation (instead of complete extraction) also resulted in an increase in spontaneous fusion frequency. The oxidation of

cholesterol does not effect the fluidity of the membrane (Lau and Das, 1995) , however alterations in cholesterol-dependent protein interactions could occur suggesting a protein-mediated inhibition of spontaneous fusion regulated by the presence of cholesterol. Impairments in synaptic transmission, especially the large increase in spontaneous neurotransmission, might well form the potential basis for the neurological symptoms and neurodegeneration seen in patients with Niemann-Pick disease.

8.2.3 NPC1 pathology and possible links to synaptic defects in NPC1-deficient neurons

Under physiological as well as pathophysiological circumstances spontaneous fusion events can set the concentration of ambient levels of neurotransmitter within the synaptic cleft and in the extracellular environment. In the brain, enhanced spontaneous release can be deleterious. First, it may simply cause tonic excitation of target neurons. In the brain, unregulated release of excitatory neurotransmitters can lead to neuronal damage and death. Excitotoxicity is the common name for the type of neuronal death induced by increased glutamate in the synaptic cleft (Whetsell and Shapira, 1993). Several pathophysiologies implicated in excitotoxic cell death are Alzheimer's and Huntington's diseases along with ischemia and epilepsy (Lo et al., 2003) (Nishizawa, 2001, Hynd et al., 2004) Second, it may cause vesicle depletion

presynaptically and impair synaptic function in the long term. Because spontaneous neurotransmitter release appears to be both harmful if absent or too much, then regulation mechanisms are necessary to control the fine-tuning of this type of fusion. Furthermore, if spontaneously fusing vesicles have unique requirements for fusion, then differential pathways of regulation for synchronous and random release could exist.

Changes in the cholesterol content of neurons lead to an increased release of neurotransmitter spontaneously. I found that this change generally accompanied a decrease in the efficiency of synchronous Ca^{2+} triggered vesicle fusion. Implications for each of these could contribute to the pathology of the NPC1 disease. Patients afflicted with mutations in the NPC1 gene experience a wide range of symptoms and ages of onset (< 1 month to >20 years). The most common age of diagnosis is between childhood and adolescence; in addition, these young people tend not to live past their teenage years and many die much earlier (Vanier and Millat, 2003). The enhanced excitatory spontaneous neurotransmitter release as well as attenuated responses to action potentials in NPC1-deficient neurons could be linked to some of the neurological symptoms of patients afflicted with this disease, such as neurodegeneration, seizures, dementia and psychosis. The increased excitatory input might result in uncontrolled activation of NPC1 patients' neuronal circuitry resulting in seizures or mania. Both increased activation and higher concentrations of excitatory neurotransmitter

would result in enhanced influx of Ca^{2+} through NMDA receptors, a specialized postsynaptic receptor implicated in long-term memory storage. This can lead to cell death due to harmful downstream reactions activated by high levels of Ca^{2+} and even defects in learning or memory retention due desensitization of memory storage. Purkinje cell death in the cerebellum is most common in NPC1-deficient brains, which correlates to the onset of ataxia. Cerebellar circuits require precise regulation of inhibition and excitation for control of motor movements, and the misfiring or death of Purkinje cells would ultimately result in motor coordination defects. However, most of the brain is highly malleable, and so early on neurons might be able to compensate for over excitation; however, with age or increased synaptic dysfunction some neurons might not be able to compensate. This could explain the seemingly increased occurrence of psychosis and dementia in older patients with the NPC1 disease. The decreased action potential-dependent neurotransmitter release could also result in a decreased fidelity of communication with target neurons, possibly resulting in problems with learning, memory recall or even normal behavior. Considering the possible connections to the pathology, synaptic transmission in NPC1-deficient neurons deserves further examination, preferably in more intact systems to gain insight into the physiological implications of mutations in the NPC1 gene.

8.3 Summary

Each aspect of my research coincidentally addressed the theory that vesicles have an individual identity. While addition of sphingosine appeared to only increase vesicle fusion, my study of cholesterol modification revealed a differential effect of decreased cholesterol concentration on actively recycling and spontaneously fusing vesicles. When I tracked the dynamics of recycling vesicles after extended incubations in the absence of action potentials, I found that the recycling pool was still active and resisted spontaneous fusion up to at least six hours; while spontaneous fusion of spontaneously fusing vesicles was much faster. This argues against the idea that spontaneously fusing vesicles originate from the recycling pool. In addition, after exposing recycling pool vesicles to free radicals, I found a differential change in spontaneous and evoked neurotransmission. Taken together, the fusion of action potential-dependent and-independent vesicles appears to be regulated by different mechanisms.

REFERENCES

Alberts AW, Chen J, Kuron G, Hunt V, Huff J, Hoffman C, Rothrock J, Lopez M, Joshua H, Harris E, Patchett A, Monaghan R, Currie S, Stapley E, Albers-Schonberg G, Hensens O, Hirshfield J, Hoogsteen K, Liesch J, Springer J (1980) Mevinolin: a highly potent competitive inhibitor of hydroxymethylglutaryl-coenzyme A reductase and a cholesterol-lowering agent. Proc Natl Acad Sci U S A 77:3957-3961.

Bankaitis VA, Morris AJ (2003) Lipids and the exocytotic machinery of eukaryotic cells. Curr Opin Cell Biol 15:389-395.

Bouron A (2001) Modulation of spontaneous quantal release of neurotransmitters in the hippocampus. Prog Neurobiol 63:613-635.

Brown MS, Goldstein JL (1980) Multivalent feedback regulation of HMG CoA reductase, a control mechanism coordinating isoprenoid synthesis and cell growth. J Lipid Res 21:505-517.

Caccin P, Rossetto O, Rigoni M, Johnson E, Schiavo G, Montecucco C (2003) VAMP/synaptobrevin cleavage by tetanus and botulinum neurotoxins is strongly enhanced by acidic liposomes. FEBS Lett 542:132-136.

Carstea ED, Morris JA, Coleman KG, Loftus SK, Zhang D, Cummings C, Gu J, Rosenfeld MA, Pavan WJ, Krizman DB, Nagle J, Polymeropoulos MH, Sturley SL, Ioannou YA, Higgins ME, Comly M, Cooney A, Brown A, Kaneski CR, Blanchette-Mackie EJ, Dwyer NK, Neufeld EB, Chang TY, Liscum L, Strauss JF, 3rd, Ohno K, Zeigler M, Carmi R, Sokol J, Markie D, O'Neill RR, van Diggelen OP, Elleder M, Patterson MC, Brady RO, Vanier MT, Pentchev PG, Tagle DA (1997) Niemann-Pick C1 disease gene: homology to mediators of cholesterol homeostasis. Science 277:228-231.

Chamberlain LH, Burgoyne RD, Gould GW (2001) SNARE proteins are highly enriched in lipid rafts in PC12 cells: implications for the spatial control of exocytosis. Proc Natl Acad Sci U S A 98:5619-5624.

Churchward MA, Rogasevskaia T, Hofgen J, Bau J, Coorssen JR (2005) Cholesterol facilitates the native mechanism of Ca2+-triggered membrane fusion. J Cell Sci 118:4833-4848.

Colmeus C, Gomez S, Molgo J, Thesleff S (1982) Discrepancies between spontaneous and evoked synaptic potentials at normal, regenerating and botulinum toxin poisoned mammalian neuromuscular junctions. Proc R Soc Lond B Biol Sci 215:63-74.

Cremona O, Di Paolo G, Wenk MR, Luthi A, Kim WT, Takei K, Daniell L, Nemoto Y, Shears SB, Flavell RA, McCormick DA, De Camilli P (1999) Essential role of phosphoinositide metabolism in synaptic vesicle recycling. Cell 99:179-188.

Davies JP, Ioannou YA (2000) Topological analysis of Niemann-Pick C1 protein reveals that the membrane orientation of the putative sterol-sensing domain is identical to those of 3-hydroxy-3-methylglutaryl-CoA reductase and sterol regulatory element binding protein cleavage-activating protein. J Biol Chem 275:24367-24374.

Deak F, Schoch S, Liu X, Sudhof TC, Kavalali ET (2004) Synaptobrevin is essential for fast synaptic-vesicle endocytosis. Nat Cell Biol 6:1102-1108.

Deutsch JW, Kelly RB (1981) Lipids of synaptic vesicles: relevance to the mechanism of membrane fusion. Biochemistry 20:378-385.

Dietschy JM, Turley SD, Spady DK (1993) Role of liver in the maintenance of cholesterol and low density lipoprotein homeostasis in different animal species, including humans. J Lipid Res 34:1637-1659.

Dittman JS, Regehr WG (1996) Contributions of calcium-dependent and calcium-independent mechanisms to presynaptic inhibition at a cerebellar synapse. J Neurosci 16:1623-1633.

Edelmann L, Hanson PI, Chapman ER, Jahn R (1995) Synaptobrevin binding to synaptophysin: a potential mechanism for controlling the exocytotic fusion machine. Embo J 14:224-231.

Fredholm BB, Chen JF, Cunha RA, Svenningsson P, Vaugeois JM (2005) Adenosine and brain function. Int Rev Neurobiol 63:191-270.

Gil C, Soler-Jover A, Blasi J, Aguilera J (2005) Synaptic proteins and SNARE complexes are localized in lipid rafts from rat brain synaptosomes. Biochem Biophys Res Commun 329:117-124.

Gimpl G, Burger K, Fahrenholz F (1997) Cholesterol as modulator of receptor function. Biochemistry 36:10959-10974.

Glitsch M (2006) Selective inhibition of spontaneous but not Ca2+ -dependent release machinery by presynaptic group II mGluRs in rat cerebellar slices. J Neurophysiol 96:86-96.

Goldstein JL, Brown MS (1990) Regulation of the mevalonate pathway. Nature 343:425-430.

Goritz C, Mauch DH, Pfrieger FW (2005) Multiple mechanisms mediate cholesterol-induced synaptogenesis in a CNS neuron. Mol Cell Neurosci 29:190-201.

Goslin K, Asmussen H, Banker G (1998) Rat Hippocampal Neurons in Low-Density Culture. In: Culturing Nerve Cells(Banker, G. and Goslin, K., eds), pp 339-370 London: A Bradford Book.

Groemer TW, Klingauf J (2007) Synaptic vesicles recycling spontaneously and during activity belong to the same vesicle pool. Nat Neurosci 10:145-147.

Harata N, Pyle JL, Aravanis AM, Mozhayeva M, Kavalali ET, Tsien RW (2001) Limited numbers of recycling vesicles in small CNS nerve terminals: implications for neural signaling and vesicular cycling. Trends Neurosci 24:637-643.

Hering H, Lin CC, Sheng M (2003) Lipid rafts in the maintenance of synapses, dendritic spines, and surface AMPA receptor stability. J Neurosci 23:3262-3271.

Hu K, Carroll J, Fedorovich S, Rickman C, Sukhodub A, Davletov B (2002) Vesicular restriction of synaptobrevin suggests a role for calcium in membrane fusion. Nature 415:646-650.

Humeau Y, Vitale N, Chasserot-Golaz S, Dupont J-L, Du G, Frohman MA, Bader M-F, Poulain B (2001) A role for phospholipase D1 in neurotransmitter release. PNAS 98:15300-15305.

Huttner WB, Schiebler W, Greengard P, De Camilli P (1983) Synapsin I (protein I), a nerve terminal-specific phosphoprotein. III. Its association with synaptic vesicles

studied in a highly purified synaptic vesicle preparation. J Cell Biol 96:1374-1388.
Hynd MR, Scott HL, Dodd PR (2004) Glutamate-mediated excitotoxicity and neurodegeneration in Alzheimer's disease. Neurochem Int 45:583-595.
Istvan ES, Palnitkar M, Buchanan SK, Deisenhofer J (2000) Crystal structure of the catalytic portion of human HMG-CoA reductase: insights into regulation of activity and catalysis. Embo J 19:819-830.
Jahn R, Lang T, Sudhof TC (2003) Membrane fusion. Cell 112:519-533.
Jahn R, Scheller RH (2006) SNAREs--engines for membrane fusion. Nat Rev Mol Cell Biol 7:631-643.
Jia J, Lamer S, Schuemann M, Schmidt M, Krause E, Haucke V (2006) Quantitative proteomic analysis of detergent-resistant membranes from chemical synapses: Evidence for cholesterol as spatial organizer of synaptic vesicle cycling. Mol Cell Proteomics.
Karten B, Campenot RB, Vance DE, Vance JE (2005) The Niemann-Pick C1 protein in recycling endosomes of pre-synaptic nerve terminals. J Lipid Res.
Karten B, Campenot RB, Vance DE, Vance JE (2006) The Niemann-Pick C1 protein in recycling endosomes of presynaptic nerve terminals. J Lipid Res 47:504-514.
Karten B, Vance DE, Campenot RB, Vance JE (2002) Cholesterol accumulates in cell bodies, but is decreased in distal axons, of Niemann-Pick C1-deficient neurons. Journal of neurochemistry 83:1154-1163.
Karten B, Vance DE, Campenot RB, Vance JE (2003) Trafficking of cholesterol from cell bodies to distal axons in Niemann Pick C1-deficient neurons. The Journal of biological chemistry 278:4168-4175.
Kavalali ET, Klingauf J, Tsien RW (1999) Activity-dependent regulation of synaptic clustering in a hippocampal culture system. Proc Natl Acad Sci U S A 96:12893-12900.
Klein U, Gimpl G, Fahrenholz F (1995) Alteration of the myometrial plasma membrane cholesterol content with beta-cyclodextrin modulates the binding affinity of the oxytocin receptor. Biochemistry 34:13784-13793.
Kobayashi T, Beuchat MH, Lindsay M, Frias S, Palmiter RD, Sakuraba H, Parton RG, Gruenberg J (1999) Late endosomal membranes rich in lysobisphosphatidic acid regulate cholesterol transport. Nat Cell Biol 1:113-118.
Lang T, Bruns D, Wenzel D, Riedel D, Holroyd P, Thiele C, Jahn R (2001) SNAREs are concentrated in cholesterol-dependent clusters that define docking and fusion sites for exocytosis. Embo J 20:2202-2213.
Lau WF, Das NP (1995) In vitro modulation of rat adipocyte ghost membrane fluidity by cholesterol oxysterols. Experientia 51:731-737.
Lee AG (2004) How lipids affect the activities of integral membrane proteins. Biochim Biophys Acta 1666:62-87.
Lesa GM, Palfreyman M, Hall DH, Clandinin MT, Rudolph C, Jorgensen EM, Schiavo G (2003) Long chain polyunsaturated fatty acids are required for efficient neurotransmission in C. elegans. J Cell Sci 116:4965-4975.
Li H, Repa JJ, Valasek MA, Beltroy EP, Turley SD, German DC, Dietschy JM (2005) Molecular, anatomical, and biochemical events associated with

neurodegeneration in mice with Niemann-Pick type C disease. J Neuropathol Exp Neurol 64:323-333.
Lo EH, Dalkara T, Moskowitz MA (2003) Mechanisms, challenges and opportunities in stroke. Nat Rev Neurosci 4:399-415.
Loftus SK, Morris JA, Carstea ED, Gu JZ, Cummings C, Brown A, Ellison J, Ohno K, Rosenfeld MA, Tagle DA, Pentchev PG, Pavan WJ (1997) Murine model of Niemann-Pick C disease: mutation in a cholesterol homeostasis gene. Science 277:232-235.
Lou X, Scheuss V, Schneggenburger R (2005) Allosteric modulation of the presynaptic Ca2+ sensor for vesicle fusion. Nature 435:497-501.
Mauch DH, Nagler K, Schumacher S, Goritz C, Muller EC, Otto A, Pfrieger FW (2001) CNS synaptogenesis promoted by glia-derived cholesterol. Science 294:1354-1357.
Mozhayeva MG, Sara Y, Liu X, Kavalali ET (2002) Development of vesicle pools during maturation of hippocampal synapses. J Neurosci 22:654-665.
Mukherjee S, Maxfield FR (2004) Lipid and cholesterol trafficking in NPC. Biochim Biophys Acta 1685:28-37.
Murthy VN, Stevens CF (1999) Reversal of synaptic vesicle docking at central synapses. Nat Neurosci 2:503-507.
Nagy A, Baker RR, Morris SJ, Whittaker VP (1976) The preparation and characterization of synaptic vesicles of high purity. Brain Res 109:285-309.
Nishizawa Y (2001) Glutamate release and neuronal damage in ischemia. Life Sci 69:369-381.
Omkumar RV, Darnay BG, Rodwell VW (1994) Modulation of Syrian hamster 3-hydroxy-3-methylglutaryl-CoA reductase activity by phosphorylation. Role of serine 871. J Biol Chem 269:6810-6814.
Pfrieger FW (2003) Role of cholesterol in synapse formation and function. Biochim Biophys Acta 1610:271-280.
Prange O, Murphy TH (1999) Correlation of miniature synaptic activity and evoked release probability in cultures of cortical neurons. J Neurosci 19:6427-6438.
Prasad A, Fischer WA, Maue RA, Henderson LP (2000) Regional and developmental expression of the Npc1 mRNA in the mouse brain. Journal of neurochemistry 75:1250-1257.
Pucadyil TJ, Chattopadhyay A (2005) Cholesterol modulates the antagonist-binding function of hippocampal serotonin1A receptors. Biochim Biophys Acta 1714:35-42.
Quetglas S, Leveque C, Miquelis R, Sato K, Seagar M (2000) Ca2+-dependent regulation of synaptic SNARE complex assembly via a calmodulin- and phospholipid-binding domain of synaptobrevin. Proc Natl Acad Sci U S A 97:9695-9700.
Rigoni M, Caccin P, Gschmeissner S, Koster G, Postle AD, Rossetto O, Schiavo G, Montecucco C (2005) Equivalent effects of snake PLA2 neurotoxins and lysophospholipid-fatty acid mixtures. Science 310:1678-1680.
Rodal SK, Skretting G, Garred O, Vilhardt F, van Deurs B, Sandvig K (1999) Extraction of cholesterol with methyl-beta-cyclodextrin perturbs formation of clathrin-coated endocytic vesicles. Mol Biol Cell 10:961-974.

Rohrbough J, Broadie K (2005) Lipid regulation of the synaptic vesicle cycle. Nat Rev Neurosci 6:139-150.
Rohrbough J, Rushton E, Palanker L, Woodruff E, Matthies HJ, Acharya U, Acharya JK, Broadie K (2004) Ceramidase regulates synaptic vesicle exocytosis and trafficking. J Neurosci 24:7789-7803.
Rosenmund C, Stevens CF (1996) Definition of the readily releasable pool of vesicles at hippocampal synapses. Neuron 16:1197-1207.
Salaun C, Gould GW, Chamberlain LH (2005) Lipid raft association of SNARE proteins regulates exocytosis in PC12 cells. J Biol Chem 280:19449-19453.
Salaun C, James DJ, Chamberlain LH (2004) Lipid rafts and the regulation of exocytosis. Traffic 5:255-264.
Sara Y, Virmani T, Deak F, Liu X, Kavalali ET (2005) An isolated pool of vesicles recycles at rest and drives spontaneous neurotransmission. Neuron 45:563-573.
Schikorski T, Stevens CF (2001) Morphological correlates of functionally defined synaptic vesicle populations. Nat Neurosci 4:391-395.
Schneggenburger R, Meyer AC, Neher E (1999) Released fraction and total size of a pool of immediately available transmitter quanta at a calyx synapse. Neuron 23:399-409.
Schoch S, Deak F, Konigstorfer A, Mozhayeva M, Sara Y, Sudhof TC, Kavalali ET (2001) SNARE function analyzed in synaptobrevin/VAMP knockout mice. Science 294:1117-1122.
Simons M, Keller P, De Strooper B, Beyreuther K, Dotti CG, Simons K (1998) Cholesterol depletion inhibits the generation of beta-amyloid in hippocampal neurons. Proc Natl Acad Sci U S A 95:6460-6464.
Sollner TH (2003) Regulated exocytosis and SNARE function (Review). Mol Membr Biol 20:209-220.
Spady DK, Dietschy JM (1983) Sterol synthesis in vivo in 18 tissues of the squirrel monkey, guinea pig, rabbit, hamster, and rat. J Lipid Res 24:303-315.
Subtil A, Gaidarov I, Kobylarz K, Lampson MA, Keen JH, McGraw TE (1999) Acute cholesterol depletion inhibits clathrin-coated pit budding. Proc Natl Acad Sci U S A 96:6775-6780.
Sudhof TC (2000) The synaptic vesicle cycle revisited. Neuron 28:317-320.
Sudhof TC (2004) The synaptic vesicle cycle. Annu Rev Neurosci 27:509-547.
Sutton RB, Fasshauer D, Jahn R, Brunger AT (1998) Crystal structure of a SNARE complex involved in synaptic exocytosis at 2.4 A resolution. Nature 395:347-353.
Thiele C, Hannah MJ, Fahrenholz F, Huttner WB (2000) Cholesterol binds to synaptophysin and is required for biogenesis of synaptic vesicles. Nat Cell Biol 2:42-49.
Van der Kloot W, Naves LA (1996) Localizing quantal currents along frog neuromuscular junctions. J Physiol 497:189-198.
Vanier MT, Millat G (2003) Niemann-Pick disease type C. Clin Genet 64:269-281.
Verhage M, Maia AS, Plomp JJ, Brussaard AB, Heeroma JH, Vermeer H, Toonen RF, Hammer RE, van den Berg TK, Missler M, Geuze HJ, Sudhof TC (2000)

Synaptic assembly of the brain in the absence of neurotransmitter secretion. Science 287:864-869.

Wasser CR, Ertunc M, Liu X, Kavalali ET (2007) Cholesterol-dependent balance between evoked and spontaneous synaptic vesicle recycling. J Physiol 579:413-429.

Wenk MR, De Camilli P (2004) Protein-lipid interactions and phosphoinositide metabolism in membrane traffic: insights from vesicle recycling in nerve terminals. Proc Natl Acad Sci U S A 101:8262-8269.

Whetsell WO, Jr., Shapira NA (1993) Neuroexcitation, excitotoxicity and human neurological disease. Laboratory investigation; a journal of technical methods and pathology 68:372-387.

Wu LG, Borst JG (1999) The reduced release probability of releasable vesicles during recovery from short-term synaptic depression. Neuron 23:821-832.

Xia F, Gao X, Kwan E, Lam PP, Chan L, Sy K, Sheu L, Wheeler MB, Gaisano HY, Tsushima RG (2004) Disruption of pancreatic beta-cell lipid rafts modifies Kv2.1 channel gating and insulin exocytosis. J Biol Chem 279:24685-24691.

Yelamanchili SV, Reisinger C, Becher A, Sikorra S, Bigalke H, Binz T, Ahnert-Hilger G (2005) The C-terminal transmembrane region of synaptobrevin binds synaptophysin from adult synaptic vesicles. European journal of cell biology 84:467-475.

Zamir O, Charlton MP (2006) Cholesterol and synaptic transmitter release at crayfish neuromuscular junctions. J Physiol 571:83-99.

Zenisek D, Steyer JA, Almers W (2000) Transport, capture and exocytosis of single synaptic vesicles at active zones. Nature 406:849-854.